PRINCIPALS OF MALDI TOF

Josef Havel

havel@chemi.muni.cz

Department of Chemistry
Department of Physical Electronics, Faculty of Science, Masaryk University, Kotlářská 2, 611 37 Brno, Czech Republic
CEPLANT, R&D Center for Low-Cost Plasma and Nanotechnology Surface Modifications, Masaryk University, Kotlářská 2, 61137 Brno, Czech Republic

ULL, La Laguna, Seminary of GRANT MAT2014-57465-R, Ministry of Economy and Competiveness, Spain, 13th October 2015

Joseph John THOMSON

(1856 - 1940)

Cambridge University
Cambridge, Great Britain

The Nobel Prize in Physics 1906
"in recognition of the great merits of his theoretical and experimental investigations on the conduction of electricity by gases"

The Nobel Foundation

first mass spectrometer

Mass spectrum of neon with masses 20 and 22 u measured by J. J. Thomson (1913) using his parabola mass spectrograph

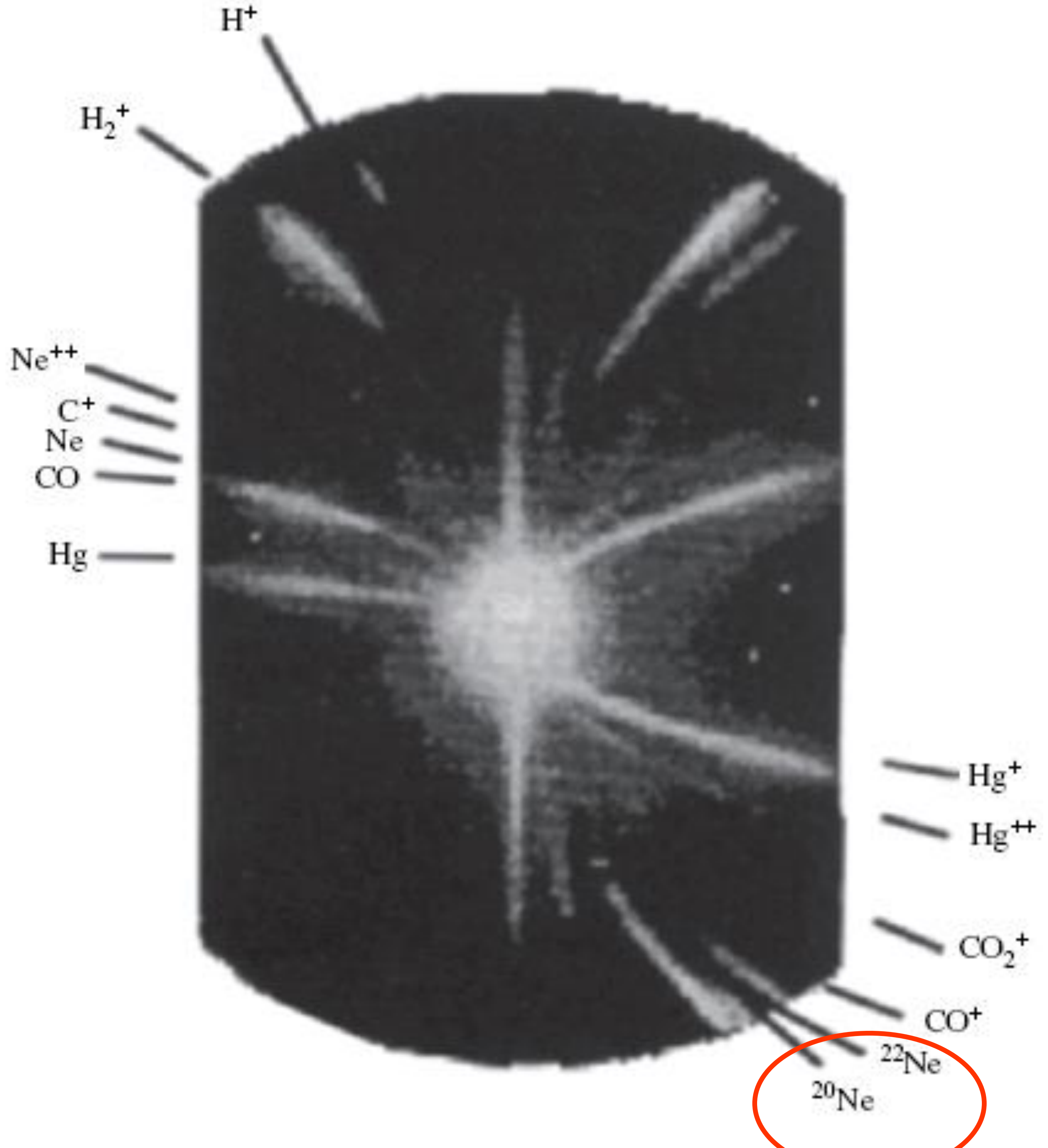

Francis William ASTON

(1877 - 1945)

Cambridge University
Cambridge, Great Britain

The Nobel Prize in Chemistry 1922

"for his discovery, by means of his mass spectrograph,

of isotopes, in a large number of non-radioactive elements,

and for his enunciation of the whole-number rule"

The Nobel Foundation

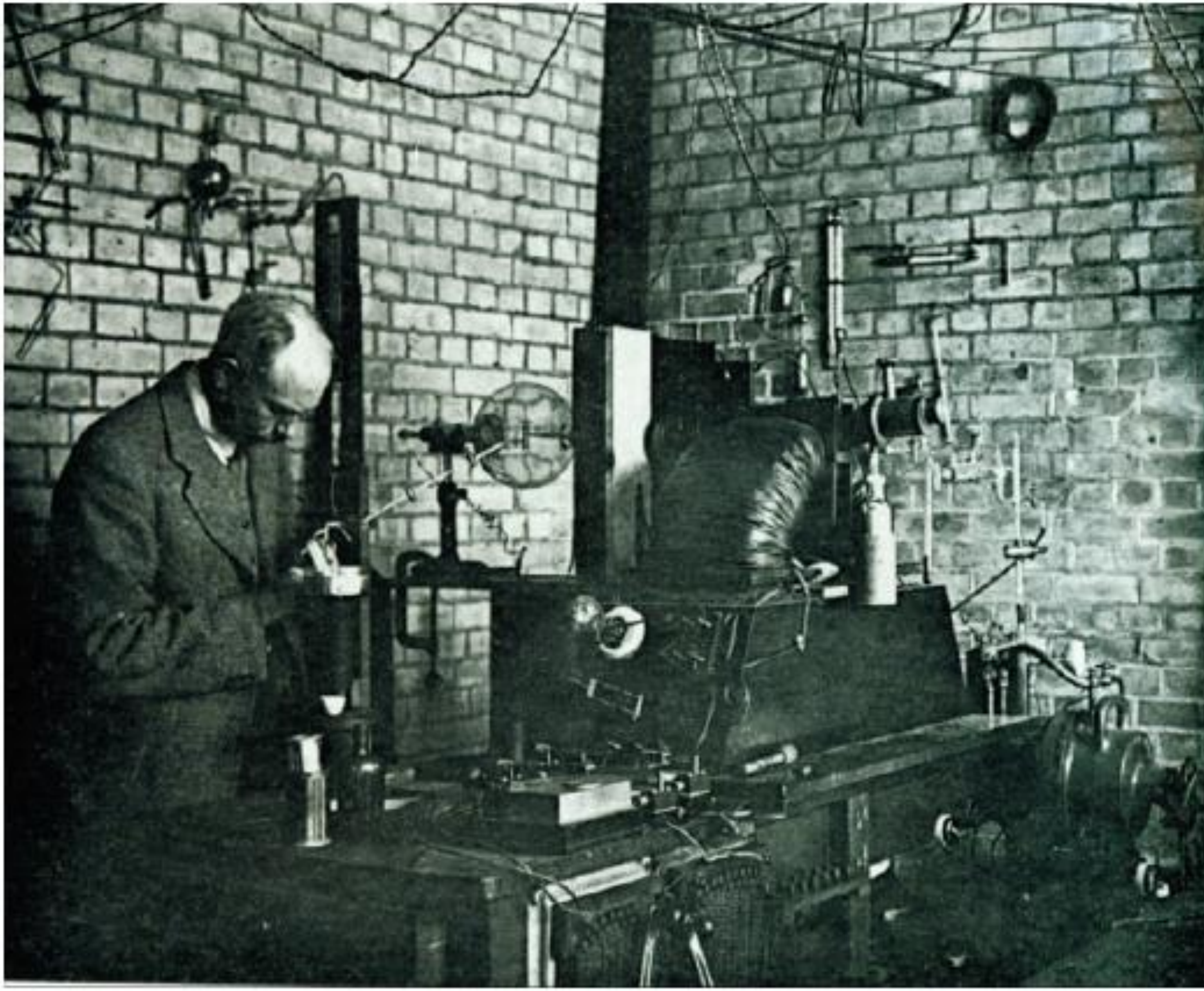

Figure 1.11 F.W. Aston with second mass spectrograph (1922).

Wolfgang Paul

(1913 - 1993)

University of Bonn
Bonn, Germany

The Nobel Prize in Physics 1989
"for the development of the ion trap technique"

The Nobel Foundation

A quite different type of mass spectrometer – the first 180 magnetic sector field mass spectrometer (see Figure 1.7), with directional focusing of ions for isotope analysis, was constructed by Dempster, independently of other instrumental developments in mass spectrometry, in 1918.

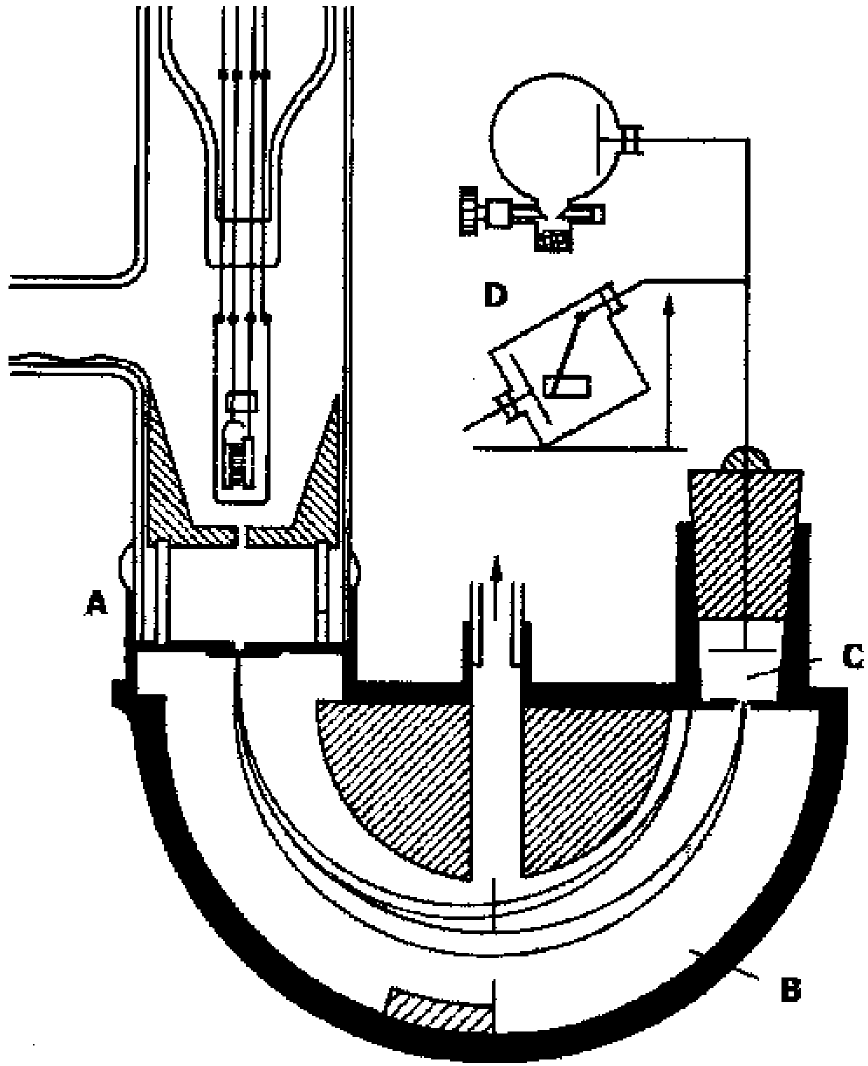

A – ion source; B – electromagnet; C – Faraday cup; D – electrometer

Basic investigations in mass spectrometry, continue to influence instrumental developments.

The first application in ion cyclotron resonance mass spectrometry (ICR-MS) was described by

Sommer, Thomas and Hipple in 1949.

The instrumental development of

a **quadrupole ion trap**,

which can trap and analyze ions separated by their m/z ratio using a 3D quadrupole radio-frequency electric field, was initiated by **Paul** and coworkers in the fifties.

In 1974, Comarisov and Marshall developed

Fourier transform ion cyclotron resonance mass spectrometry (FTICR-MS).

This technique allows mass spectrometric measurements at ultrahigh mass resolution R = 100 000–1000 000, which is higher than that of any other type of mass spectrometer and has the highest mass accuracy at attomole detection limits.

Ultrahigh mass resolution R = 100 000–1000 000, which is higher than that of any other type of mass spectrometer and has the highest mass accuracy at attomole detection limits.

However,
NEEDS for Mass Spectrometry of HIGH MASS BIOMOLECULES

were growing and
SOFT MS approaches were searched for ....

Two recently developed mass spectrometric techniques have had a major impact on the analysis of large biomolecules:

matrix-assisted laser desorption/ionization mass spectrometry (MALDI-MS)

and

electrospray ionization mass spectrometry (ESI-MS).

SOFT IONISATION

Fenn and Tanaka (together with **2002**

Wüthrich) received the Nobel Prize

for chemistry in 2002 in recognition of their contribution to the characterization of biomolecular macromolecules and to mass spectrometry and nuclear resonance spectroscopy (NMR).

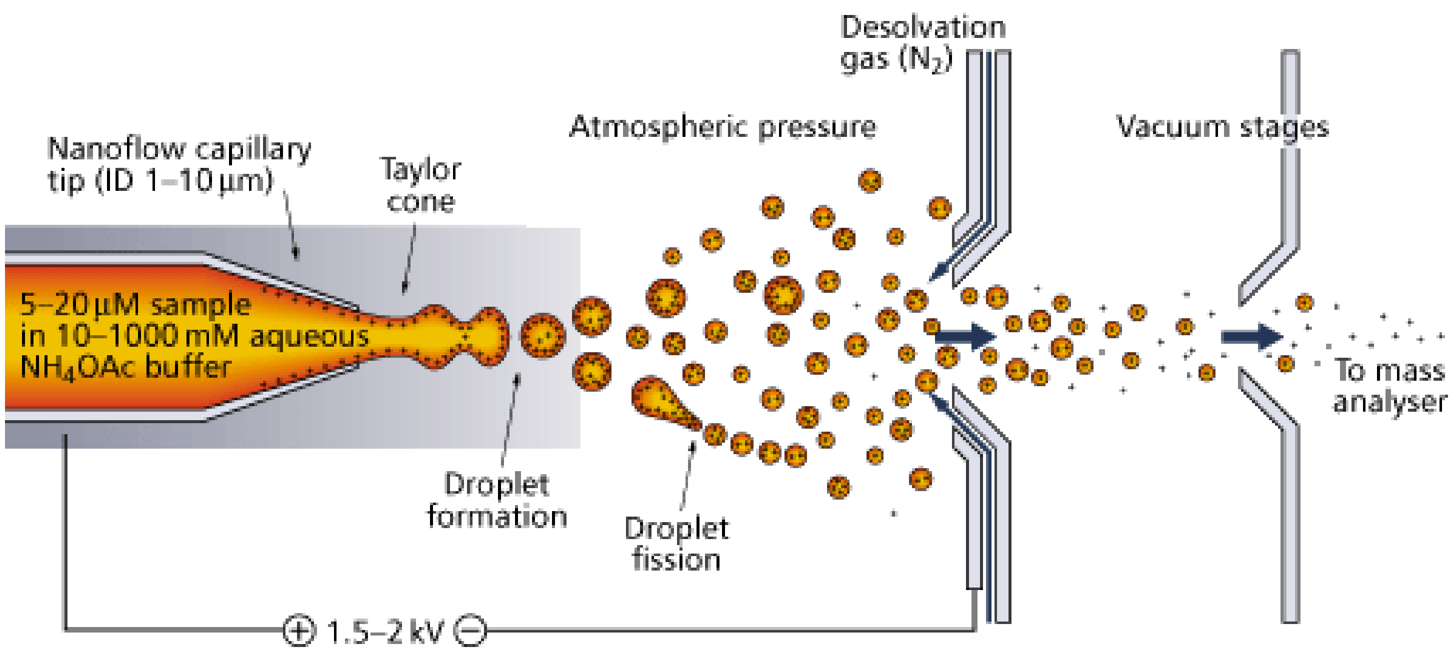

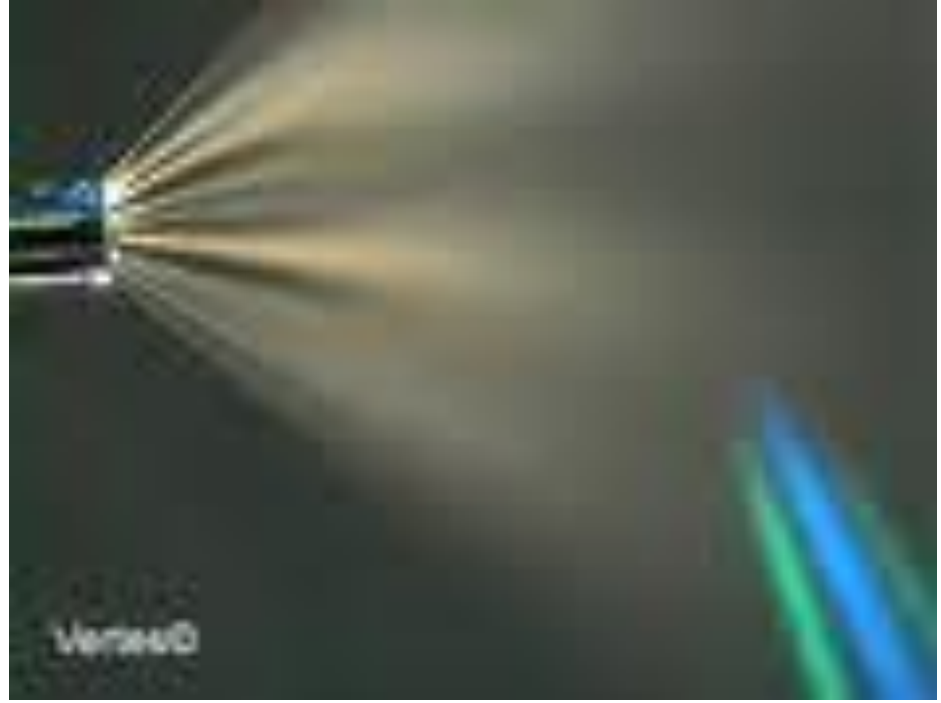

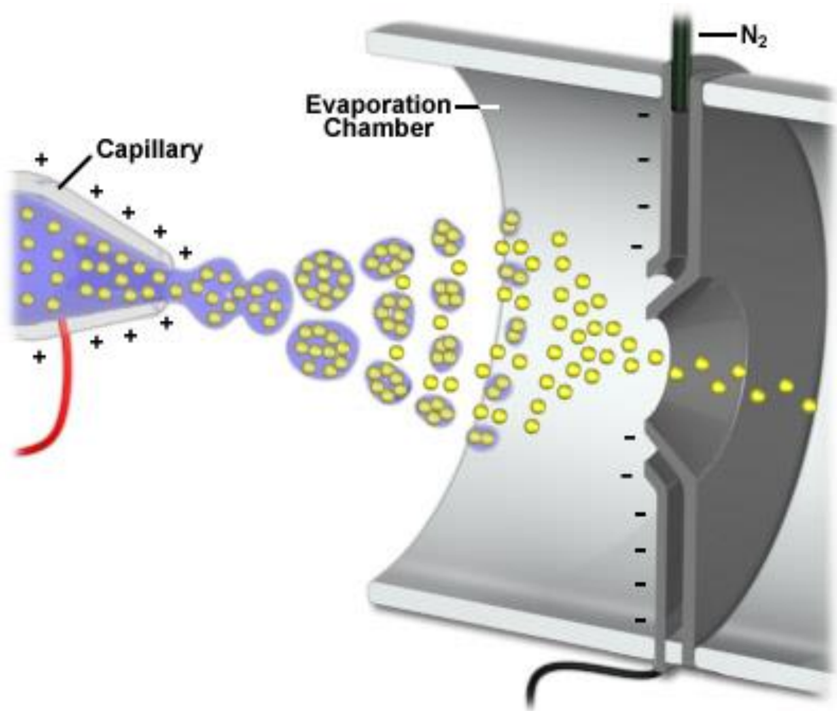

ELECTROSPRAY
Nobel Prize
for chemistry in 2002

K. Tanaka

MALDI
Nobel Prize
for chemistry in 2002

MALDI TOF MS

Matrix **A**ssisted

Laser **D**esorption **I**onisation

Time **O**f **F**light

Mass **S**pectrometry

MALDI

1.Laser Desorption Ionisation LDI

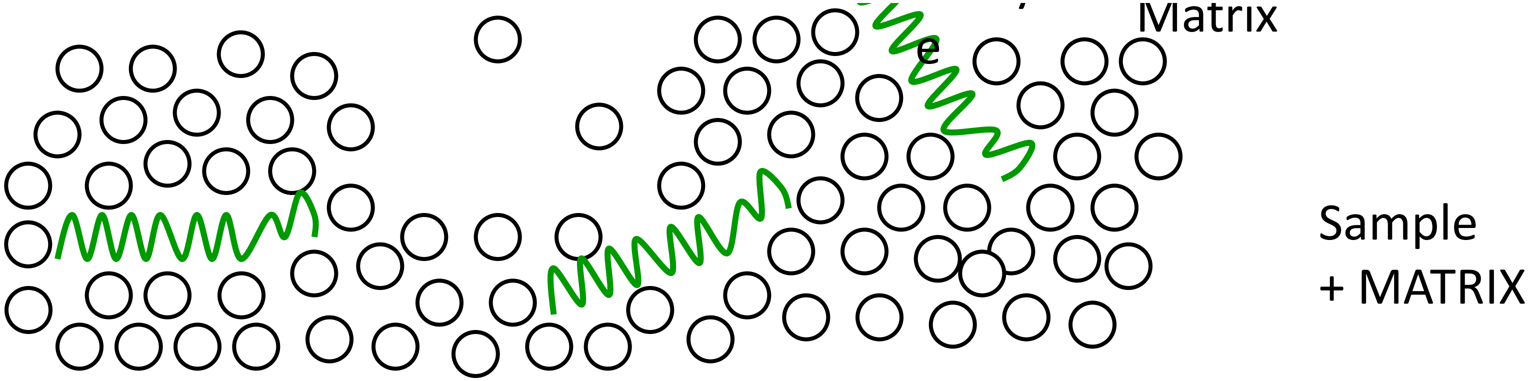

MALDI

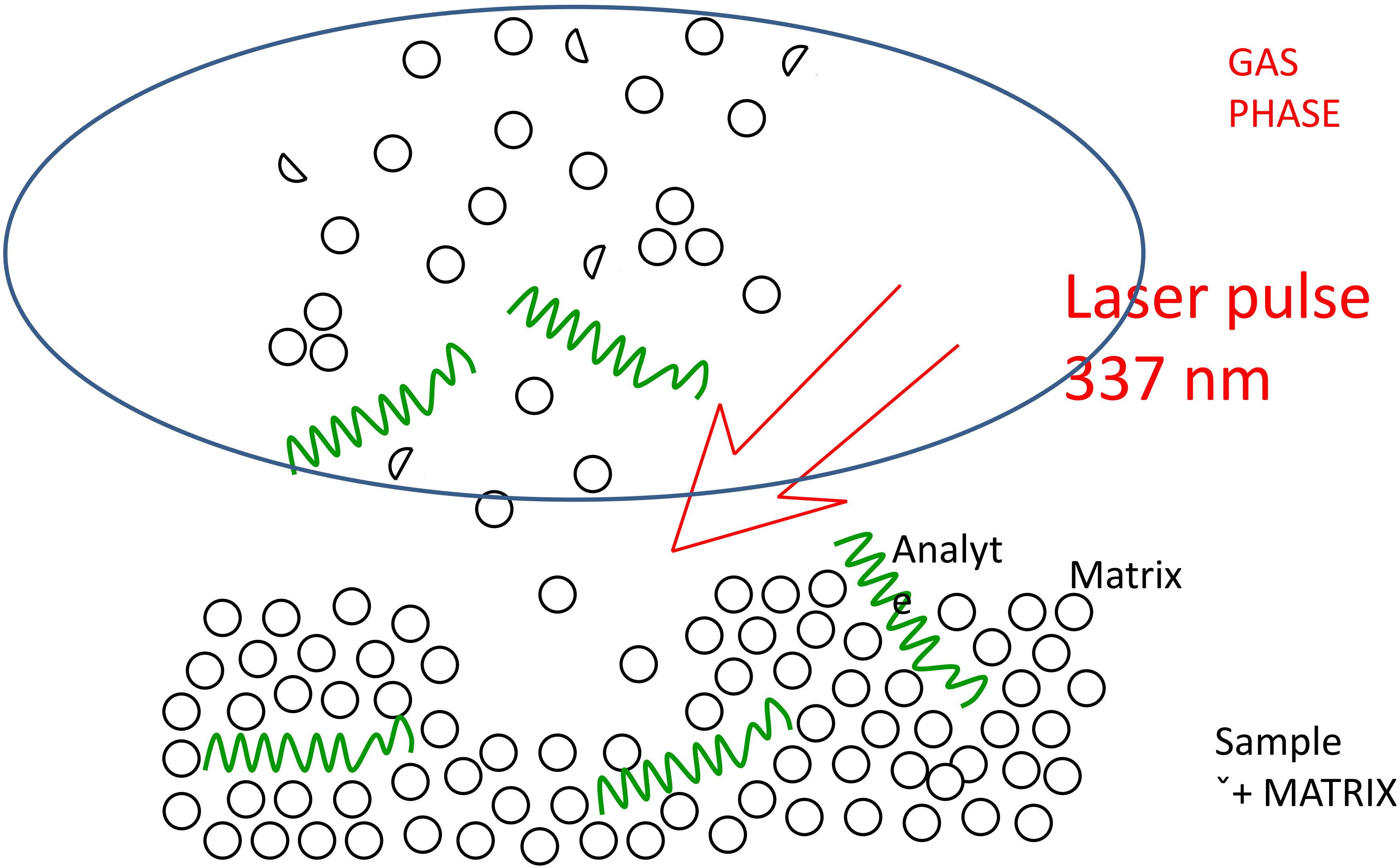

IONISATION

The matrix absorbs the laser energy and from analyte M the ions are formed

for example [M+H]+ in the case of an added proton,

[M+Na]+ in the case of an added sodium ion,

or [M-H]- in the case of a removed proton.

Awarded Order of Culture at the Imperial Palace on November 3rd, 2002

Profs KARAS and HILLENKAMP, Germany : co-discovered MALDI

Matrix **A**ssisted **L**aser **D**esorption **I**onisation

Time **O**f **F**light **M**ass **S**pectrometry

[1] Karas M., Hillenkamp F., *Anal. Chem. 1988, 60, 2299-2301.*

[2] Tanaka K., Waki H., Ido Y., Akita S., Yoshida Y., Yoshida T., *Rapid Commun. Mass Spectrom. 1988, 8, 151-53.*

Matrix-assisted laser desorption/ionization mass spectrometry (MALDI-MS)

+TOF

PEPTIDES, PROTEINS

PROTEOMICS

BIOMOLECULES

TISSUE IMAGINING

1. LASER DESORPTION IONISATION

2. DELAYED EXTRACTION

3. TOF DETECTION

4. REFLECTRON

1. LASER desorption ionisation

1. IONISATION

DELAYED EXTRACTION

TIME OF FLIGHT DETECTOR

REFLECTRON

High productivity: 384 samples/target

Matrices used for MALDI:

MALDI

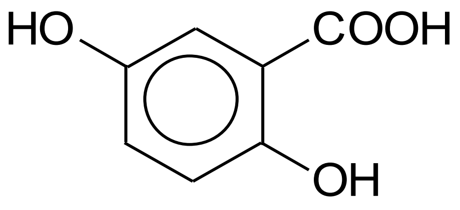

Dihydroxybenzoic Acid (154,1)

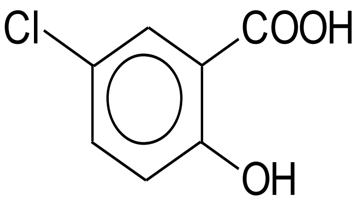

5-chlorsalicylic Acid
(172,6)

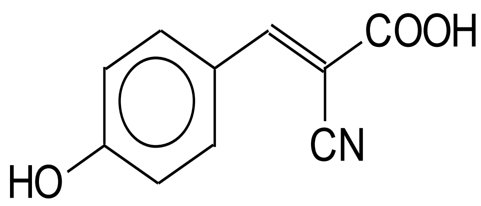

α-Cyano-4-hydroxycinnamic Acid (189,17)

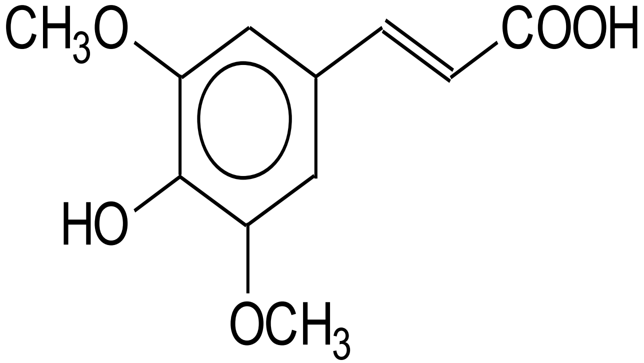

Sinapinic acid
(224,21)

Axima Kratos - CFR Shimadzu Mass Spectrometer

Nitrogen laser 337 nm,

pulse duration 3 ns

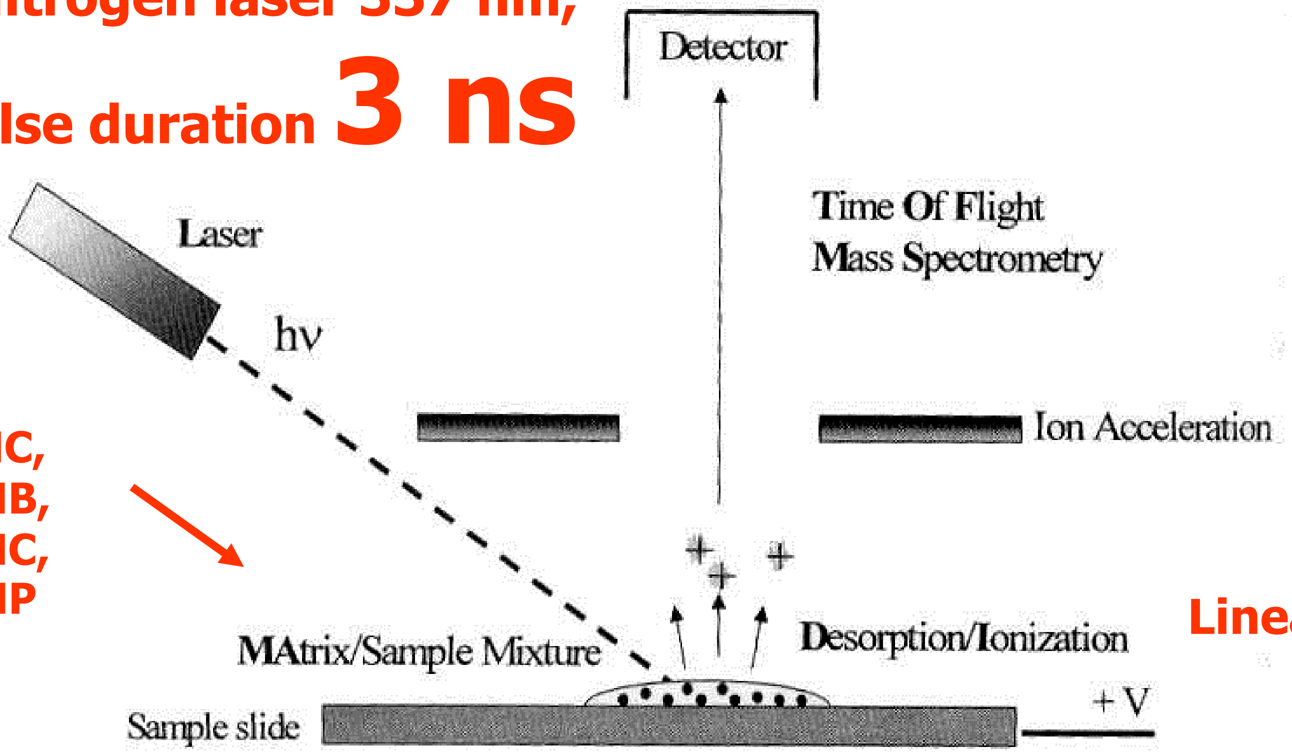

CHC, DHB, DHC, OHP

Linear positive mode

Principals of LDI and MALDI

1. **Ultra short laser pulse**, typically $t \sim 3$ ns (LDI, MALDI), max. μs.

Molecules are vaporized BEFORE decomposition.

2. **Energy** is **absorbed** mostly by **matrix** (M), not by analyte.

ε(matrix) >> ε(analyte), c(matrix) >> c(analyte)

Matrix $\rightarrow$ MH^+, M^+, M*, fragments, ions of fragments.

Analyte, dispersed in matrix, is vaporized together with matrix.

The problem: Peaks are inherently broad in MALDI-TOF spectra (poor mass resolution).

The cause: Ions of the same mass coming from the target have different speeds. This is due to uneven energy distribution when the ions are formed by the laser pulse.

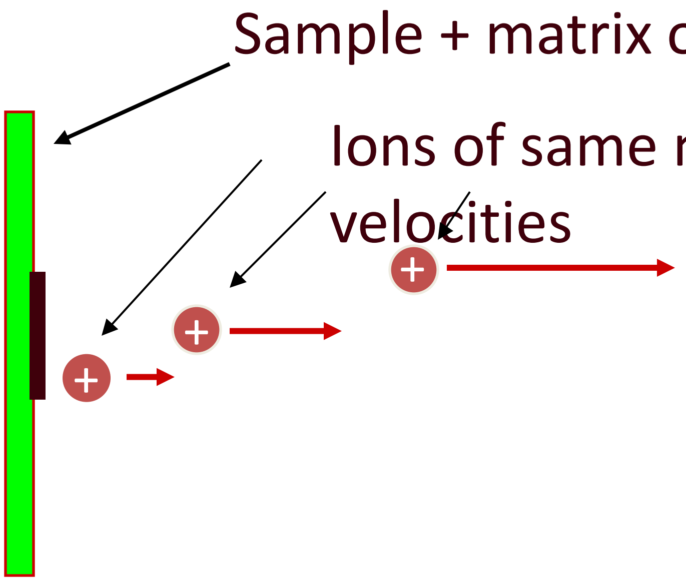

DELAYED EXTRACTION

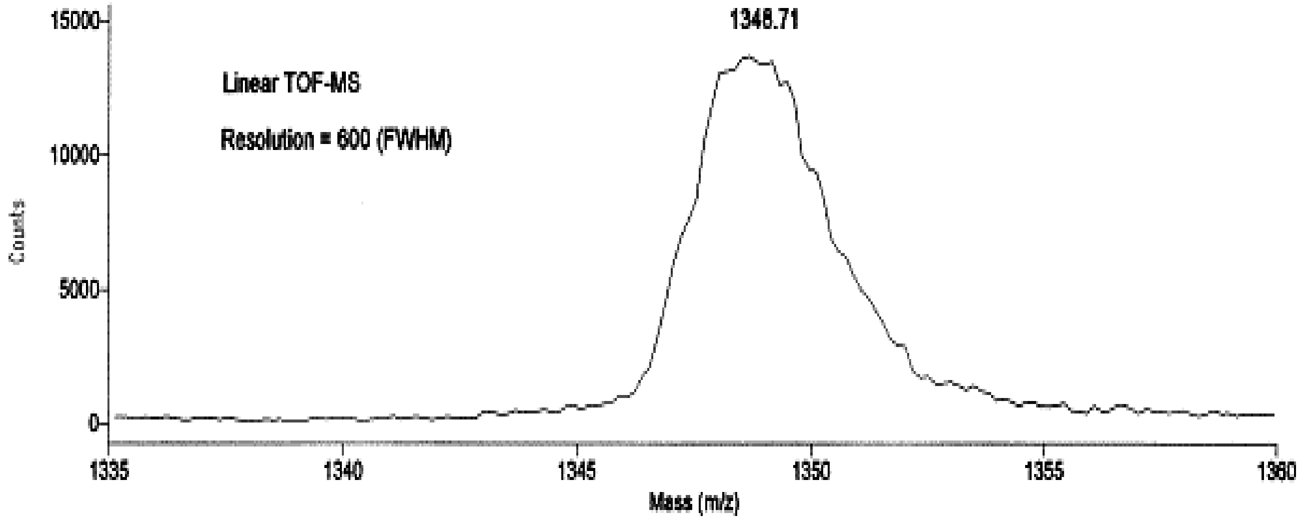

Can we compensate for the initial energy spread of ions of the same mass to produce narrower peaks?

Delayed Extraction

Reflector TOF Mass Analyzer

2. DELAYED EXTRACTION

Delayed Extraction (DE) improves performance

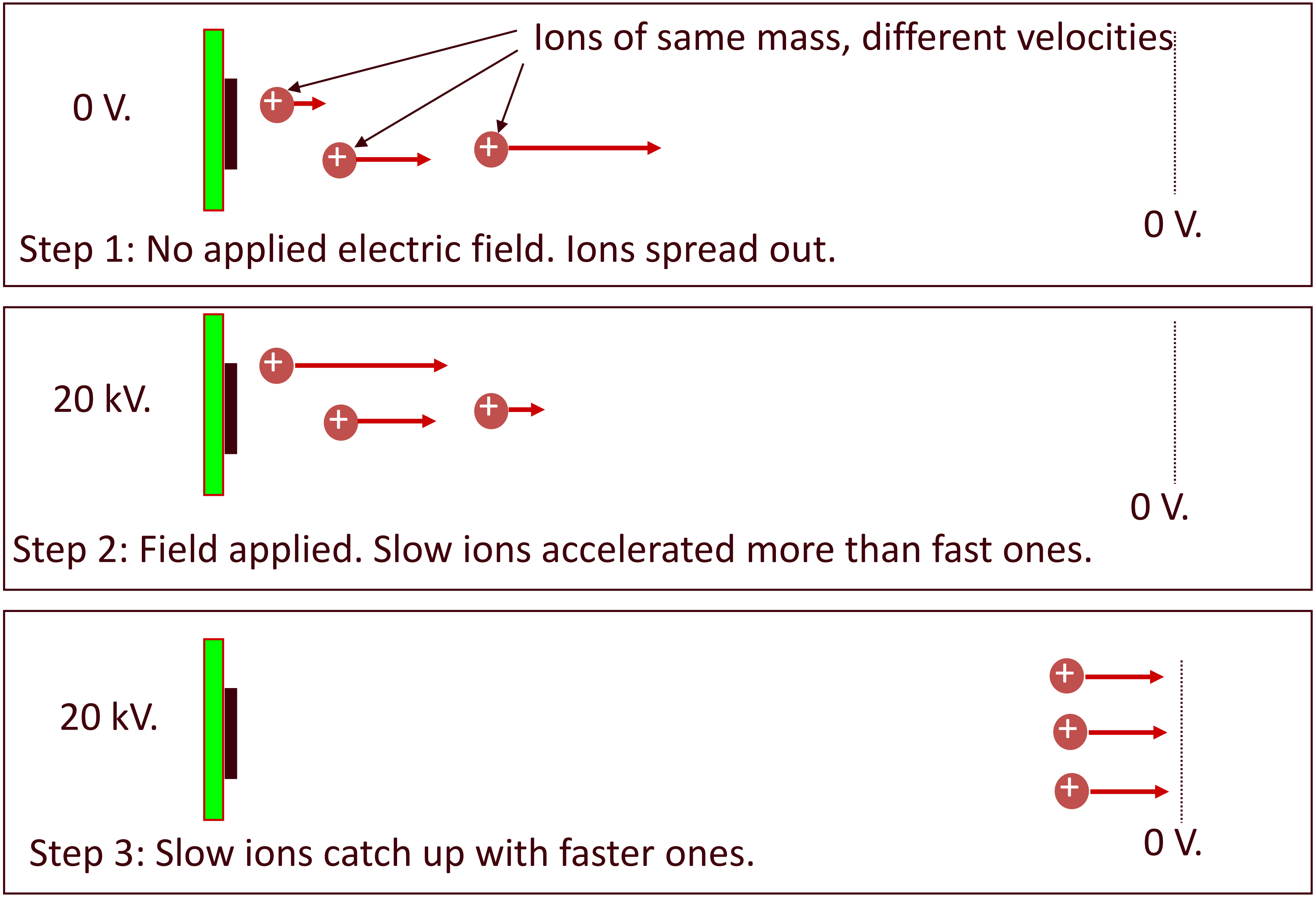

3. DELAYED EXTRACTION

A "delayd extraction".

This is basically **a time delay** between ion generation and allowing the ions to go into the flight tube.

This, in a way, cools the ions and **narrows their initial kinetic energy distribution**, so they start with more uniform kinetic energies improving resolution.

DELAYED EXTRACTION

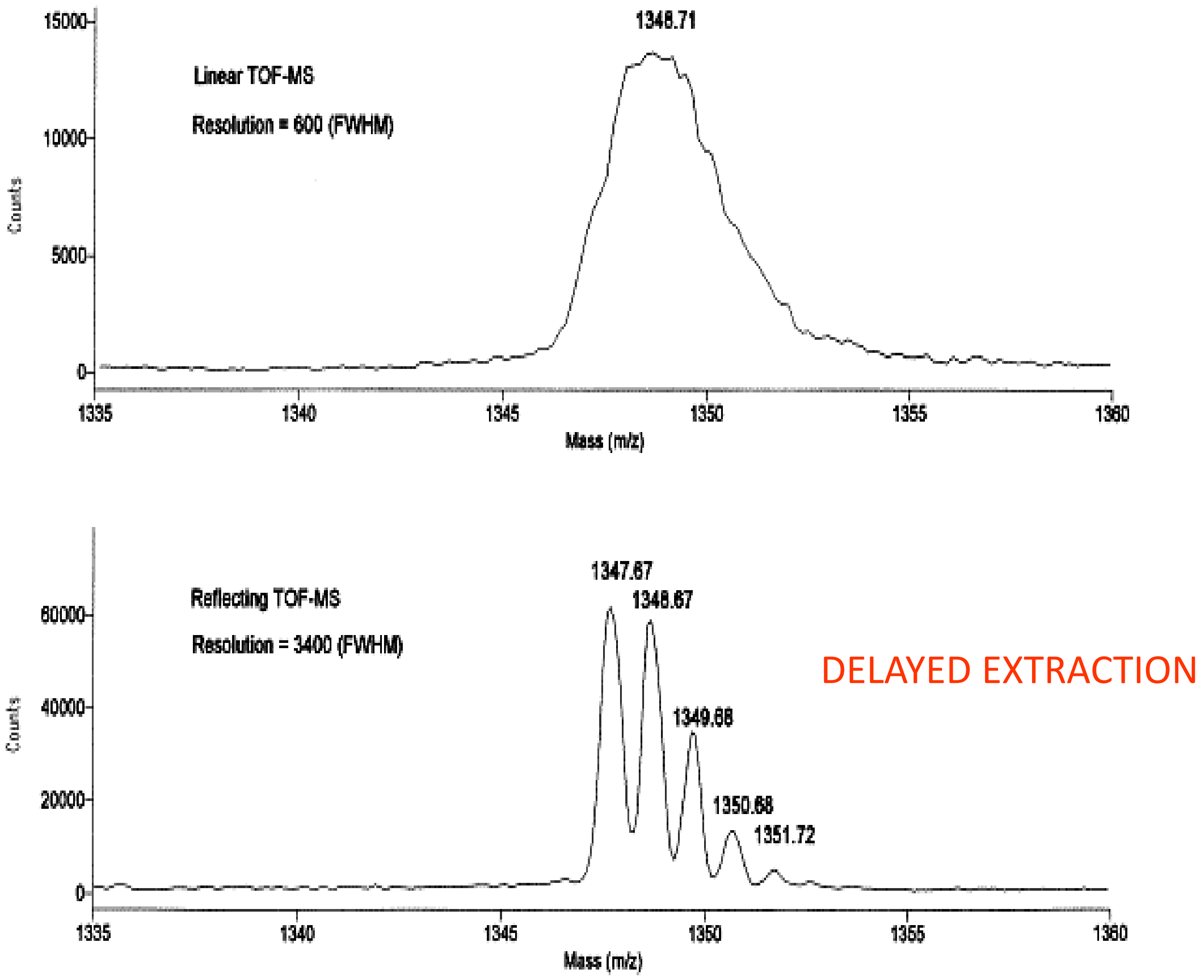

TIME OF FLIGHT TOF

The mass-to-charge ratio of an ion is proportional to the square of its drift time (**T**ime **O**f **F**light)

$$\frac{m}{z} = \frac{2t^2K}{L^2}$$

t	=	Drift time
L	=	Drift length
m	=	Mass
K	=	Kinetic energy of ion
z	=	Number of charges on ion

5. REFLECTRON

MALDI TOF MS

- Moderní hmotnostně spektrometrická metoda

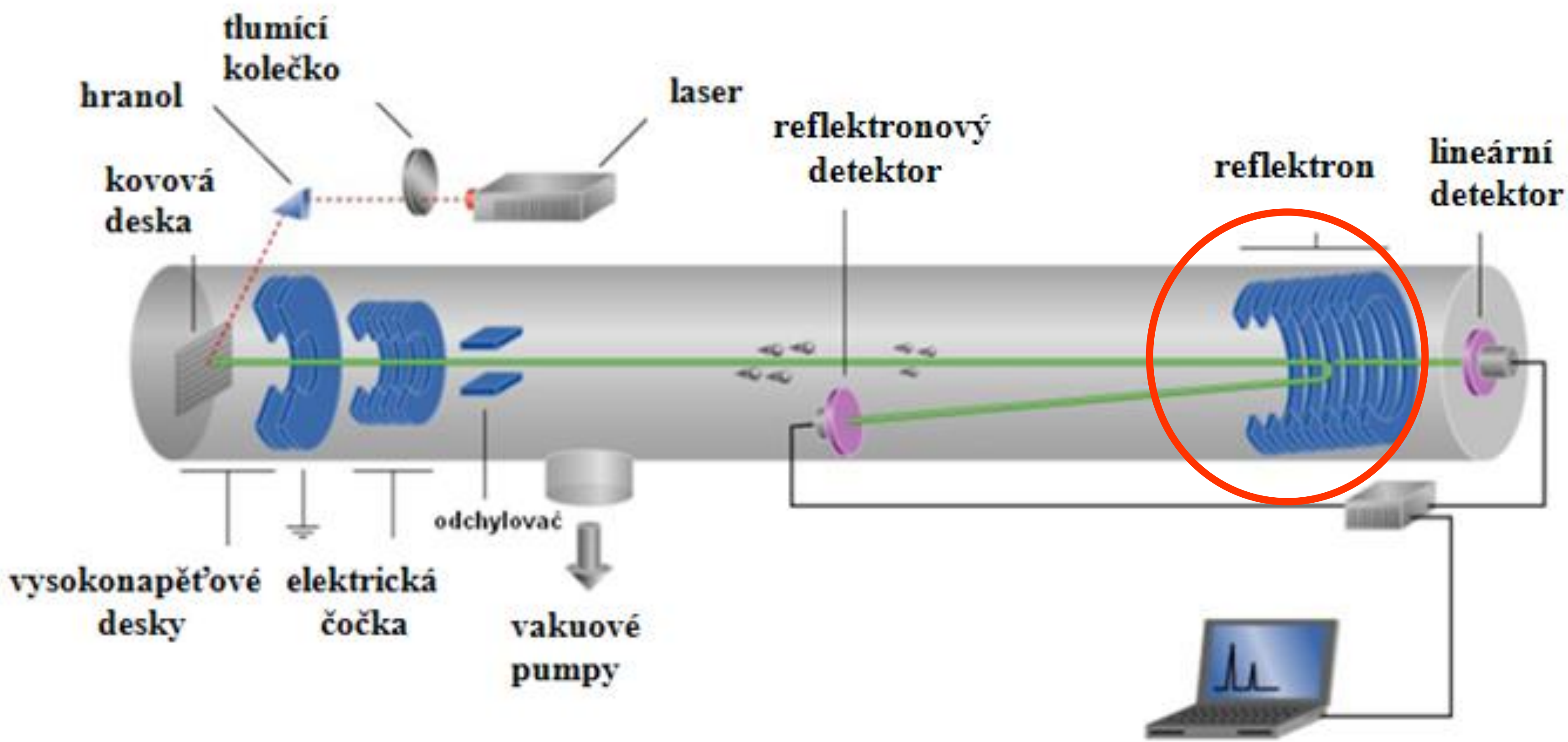

Schéma přístroje MALDI TOF

What is a reflector TOF analyzer?

A single stage gridded ion mirror that subjects the ions to a uniform repulsive electric field to reflect them.

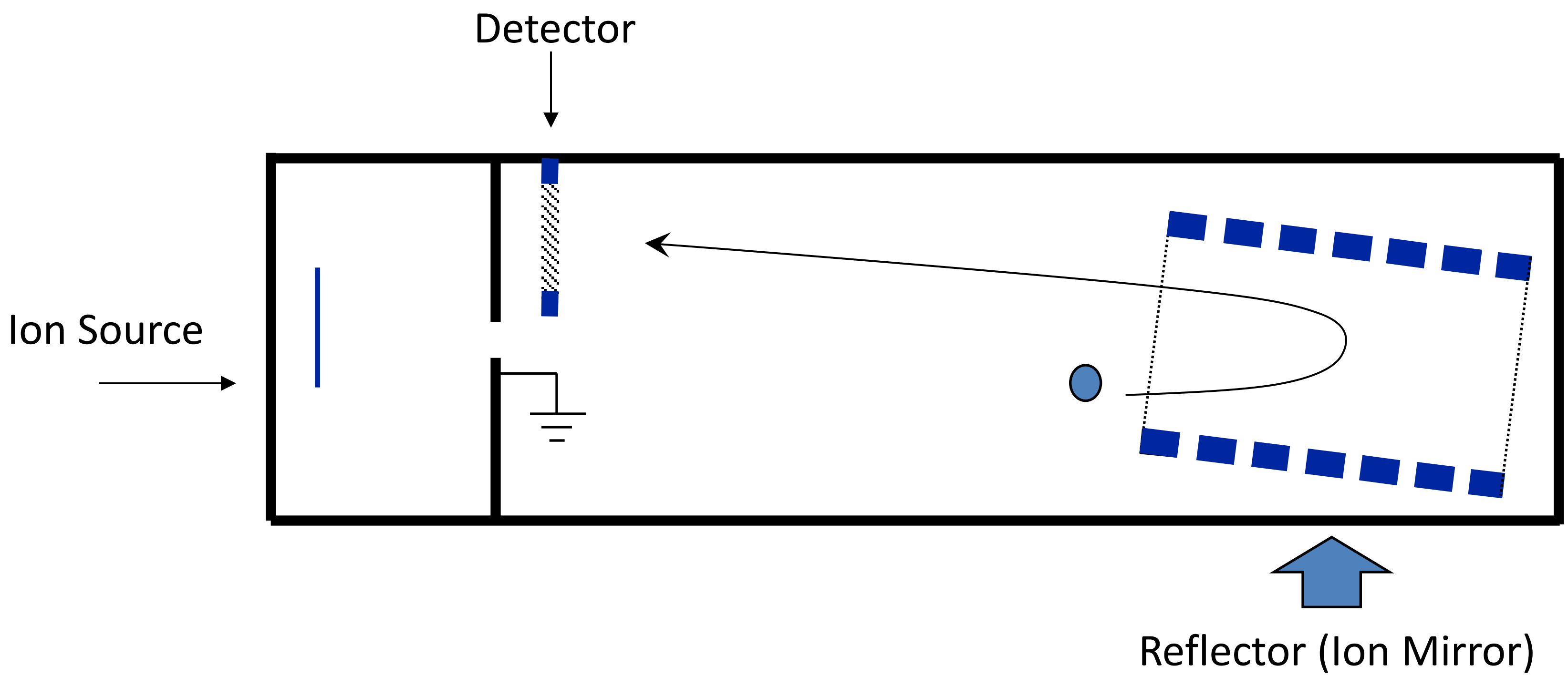

The reflector or ion mirror compensates for the initial energy spread of ions of the same mass coming from the ion source, and improves resolution.

A reflector focuses ions to give better mass resolution

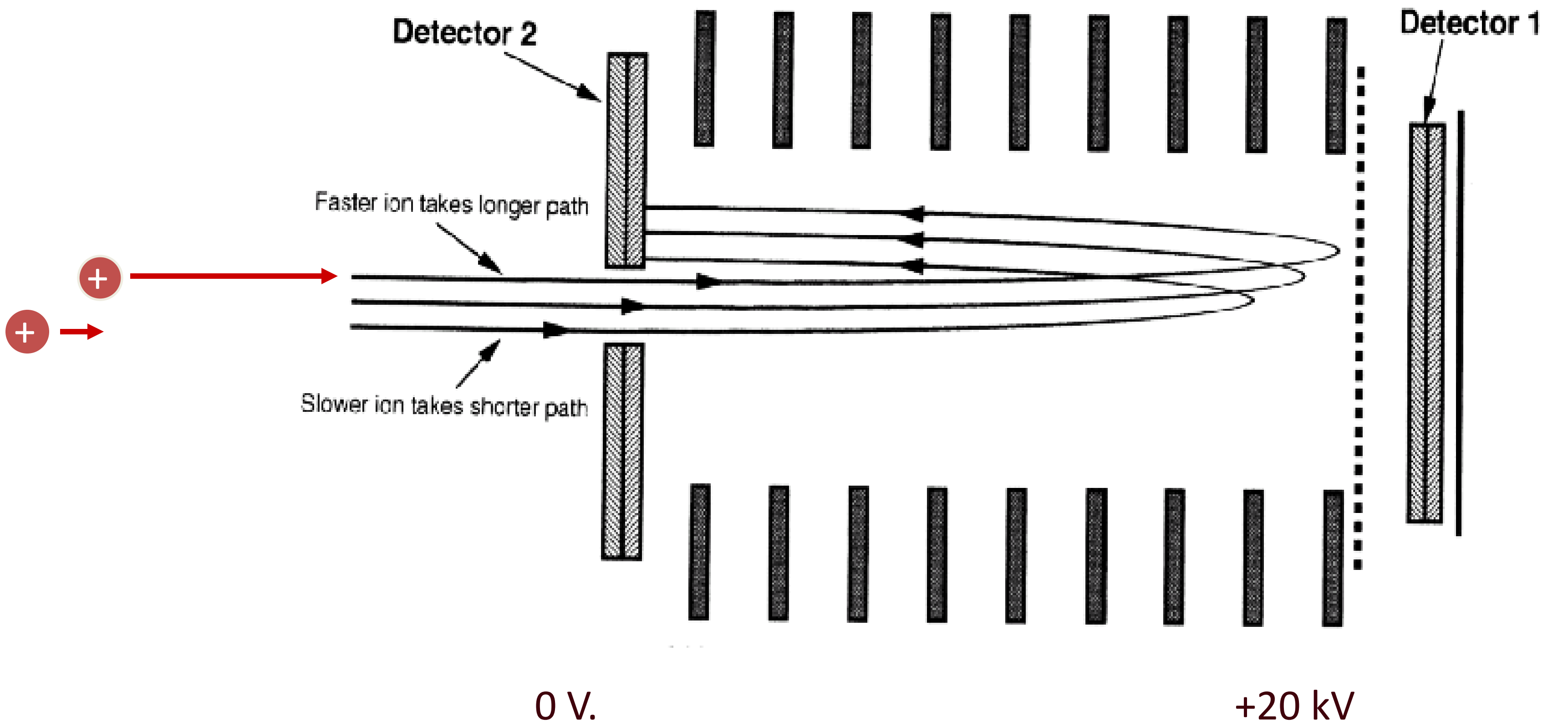

Reflector

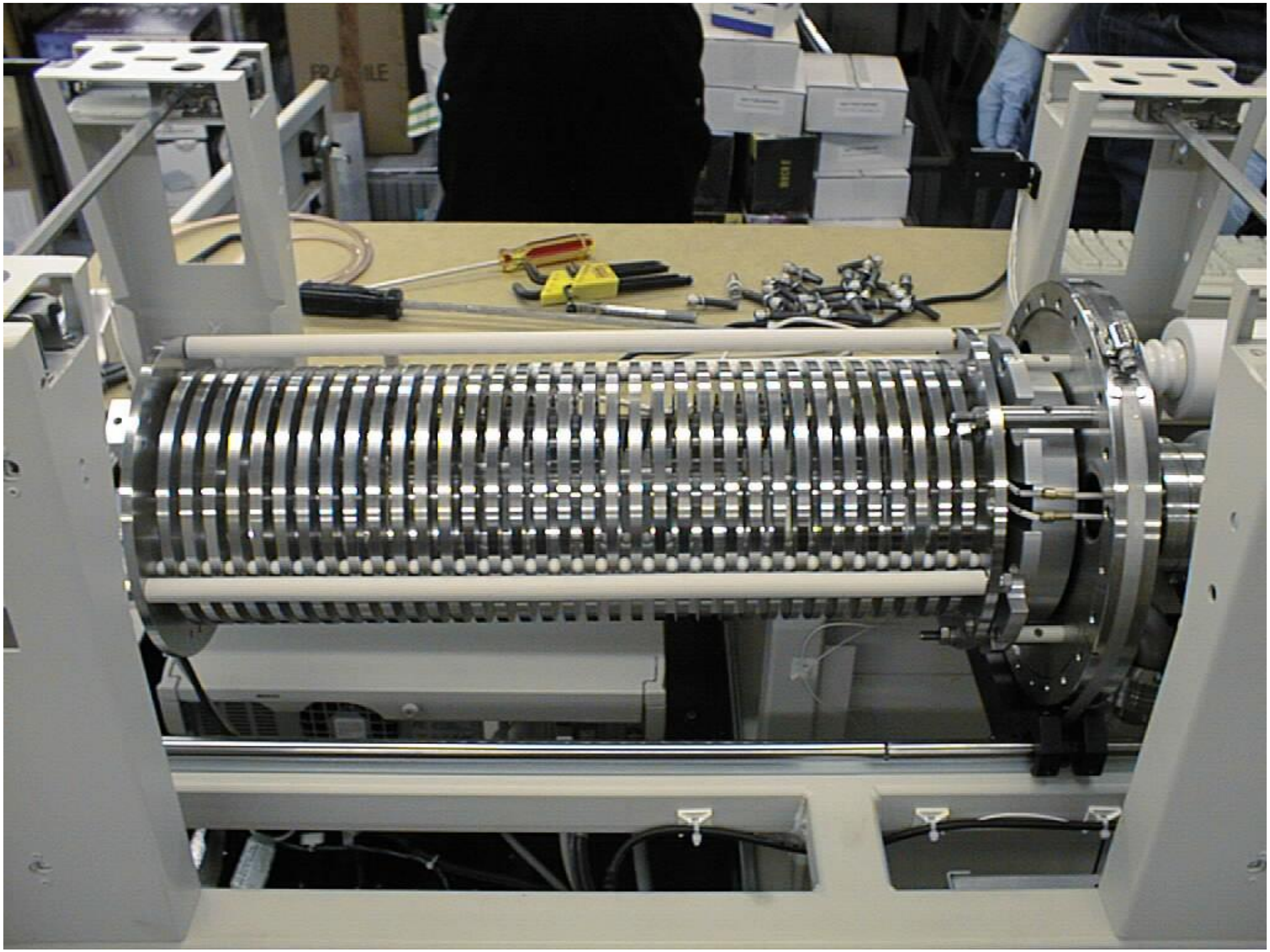

Resolution & mass accuracy on mellitin

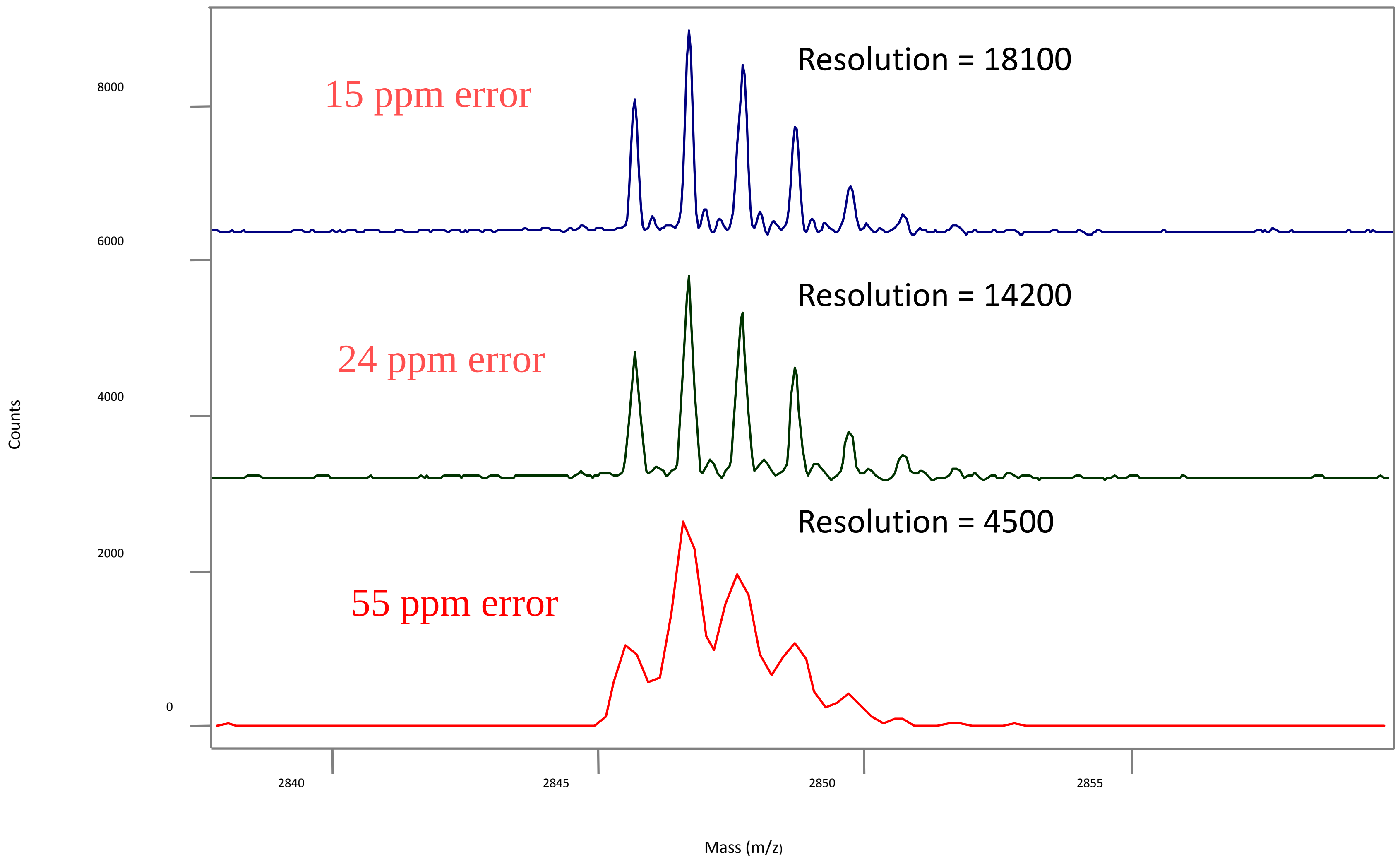

Sensitivity and resolution: MALDI MS peptide (< fmol)

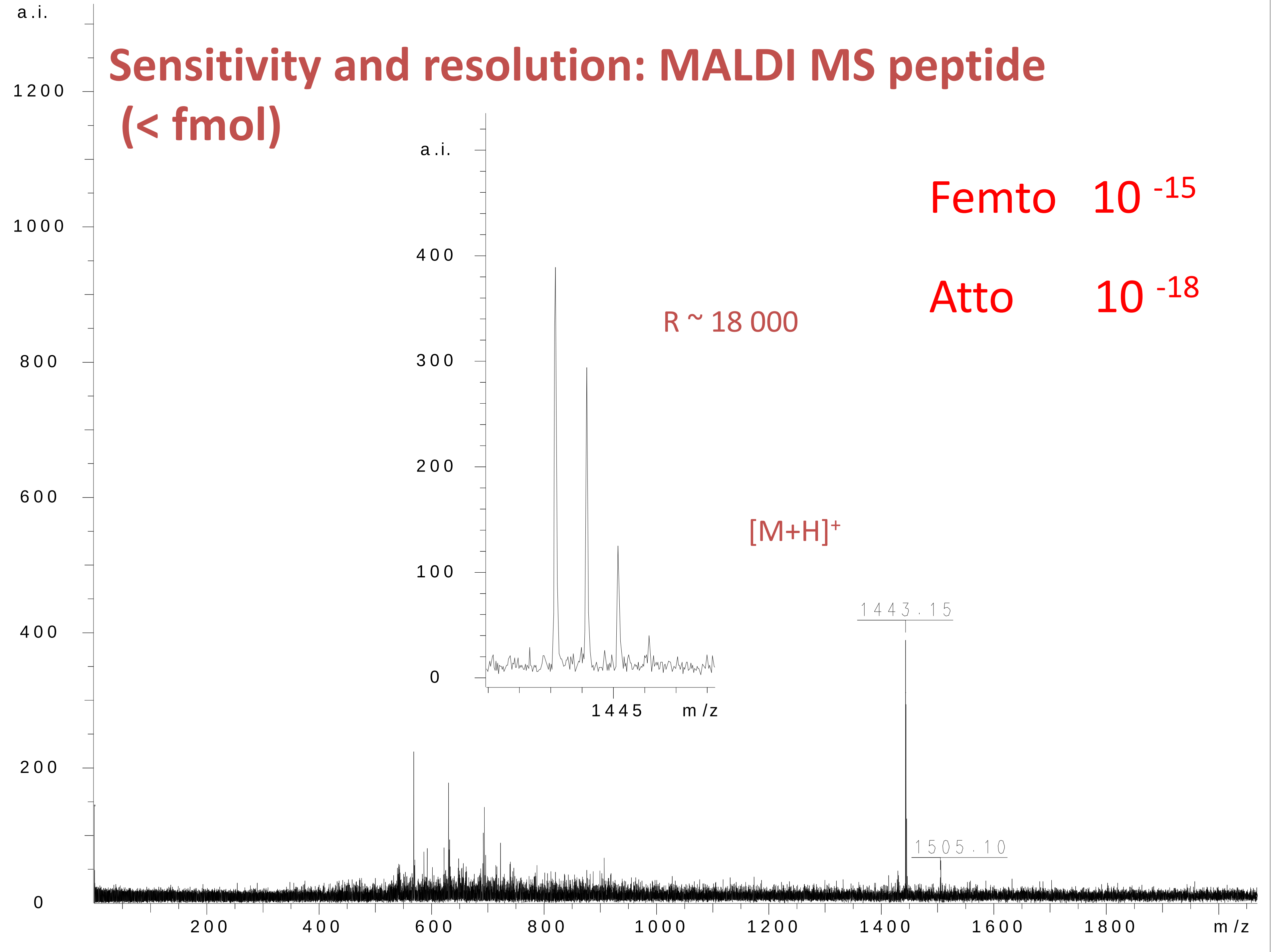

Matrix-assisted laser desorption/ionization mass spectrometry (MALDI-MS)

+TOF

PEPTIDES, PROTEINS

PROTEOMICS

BIOMOLECULES

TISSUE IMAGING

INORGANIC MATERIALS?


AXIMA-CFR
KRATOS
ANALYTICAL


AXIMA

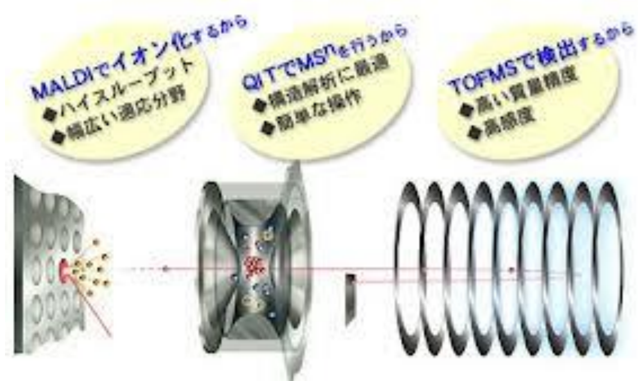
MALDIでイオン化するから
◆ハイスループット
◆幅広い適応分野
QITでMSⁿを行うから
◆構造解析に最適
◆簡単な操作
TOFMSで検出するから
◆高い質量精度
◆高感度

INORGANIC COMPOUNDS

MATERIALS

NANO-MATERIALS

SURFACES

Laser ablation synthesis

Examples:

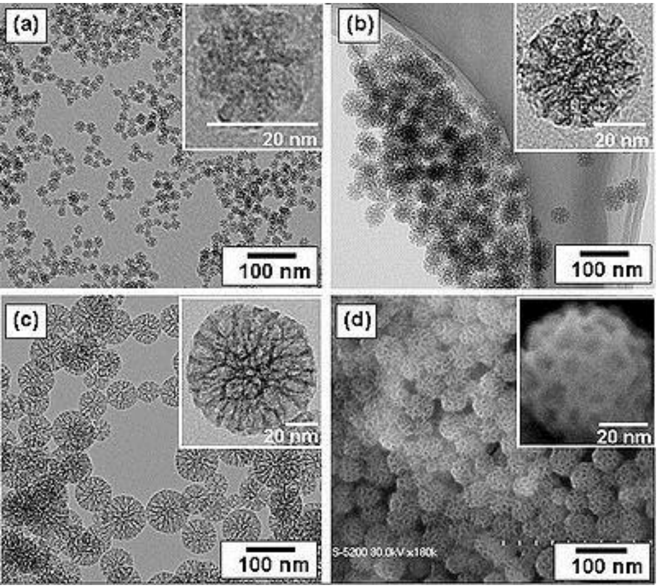

Nanoparticles

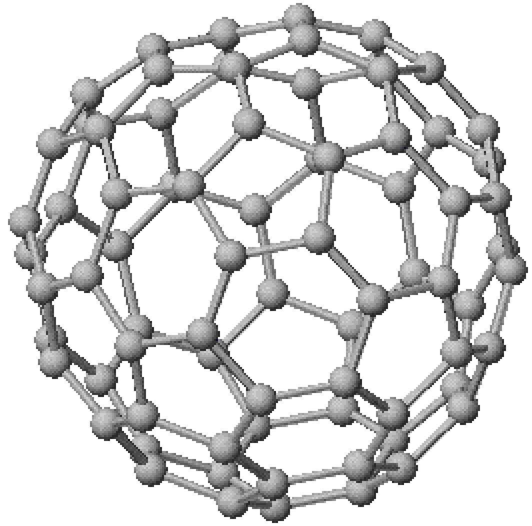

Fullerene

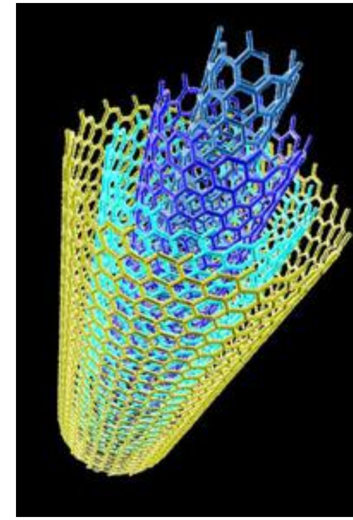

Nanotubes

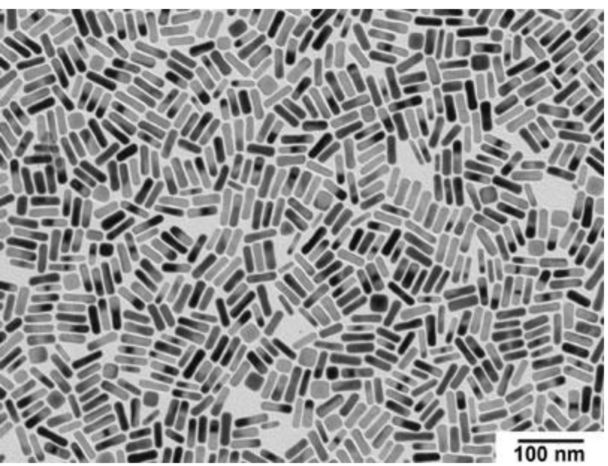

Nanorods

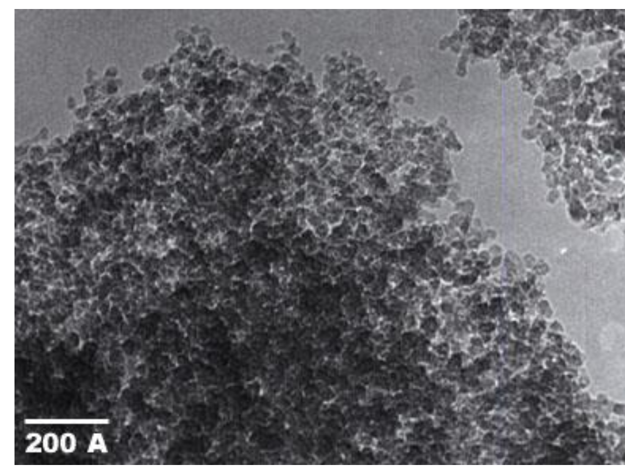

Nanodiamonds

Nanomaterials

Silver or silver nanoparticles: a hazardous threat to the environment and human health?

Silver clusters

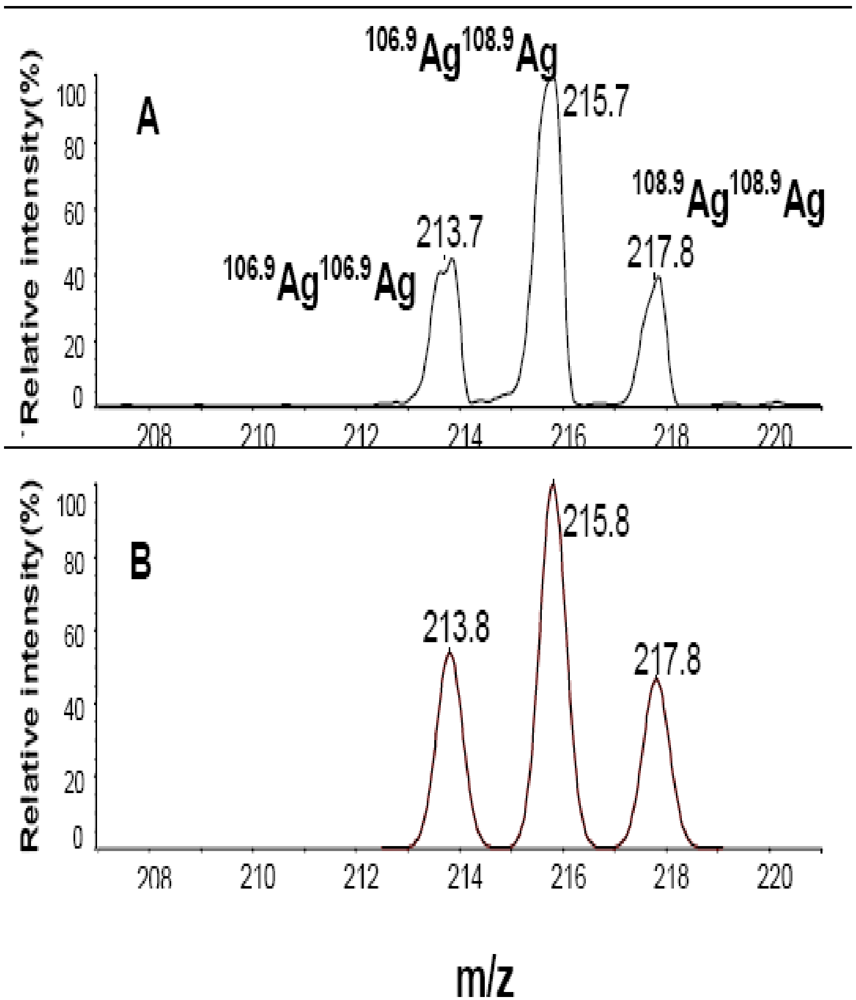

Ag_2 cluster

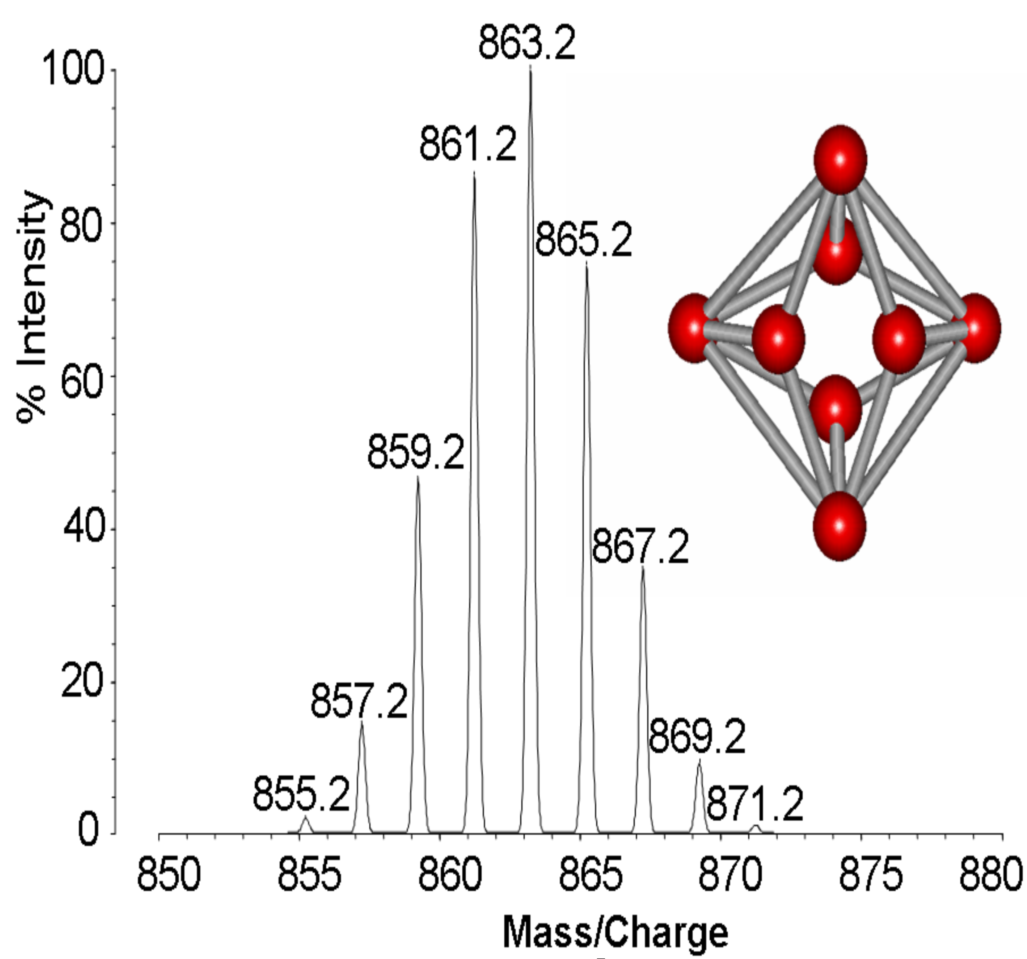

Ag_8 cluster

N. R. Panyala, E. M. Pena/Mendez,et al. Silver or silver nanoparticles: a hazardous threat to the environment and human health? *J. Appl. Biomed.* **2008**, 6,117.

NANO GOLD

Structure of selected Nano-gold clusters

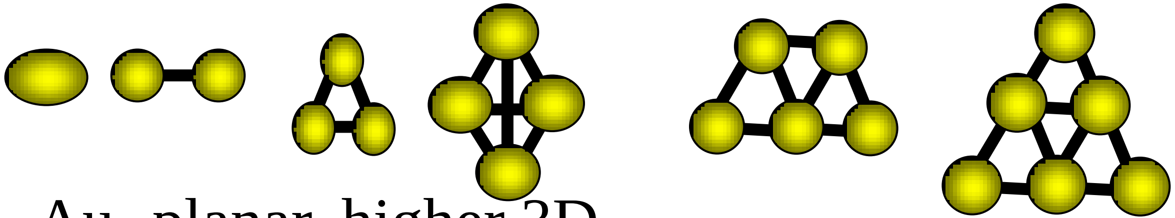

Au_1-Au_6 clusters

- Au_1-Au_8 planar, higher 3D

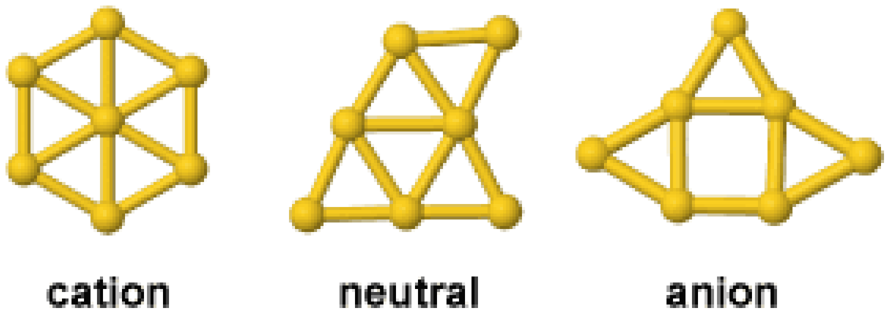

Structure of clusters e.g. like Au_7 is different for cation, neutral and anion

- Structures of some higher gold clusters:

Au_{16}

GOLD FULLERENE !!!!!

Bulusu, S., Li, Xi., Wang, L.S., Zeng, X.C. (2006) Evidence of hollow golden cages. *PNAS*, 103: 8326-8330.

Titanium carbide, TiC

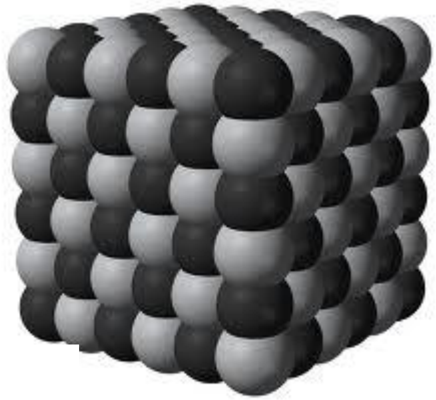

Titanium Carbide –DLC composite MAGNETRONE SPUTTERING

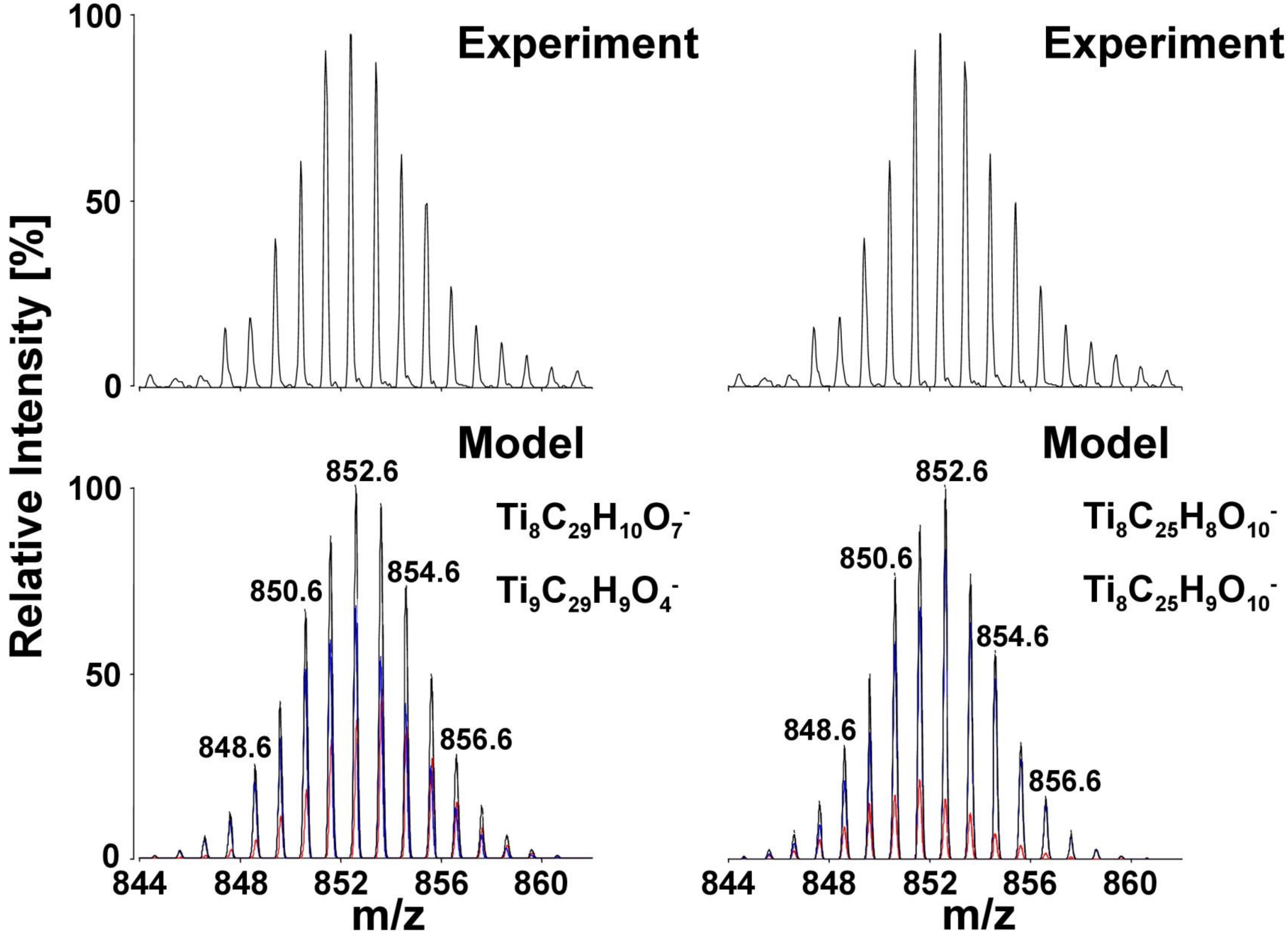

. Laser desorption ionisation quadrupole ion trap time-of-flight mass spectrometry of titanium-carbon thin films. Rapid Commun. Mass Spectrom, 2013, 27, 1-7.

SURFACE ANALYSIS

and

CLEANING via PLASMA TREATMENT

A. Pamreddy, D. Skácelová, M. Haničinec, P. Sťahel, M. Stupavská, M. Černák a J. Havel. Plasma cleaning and activation of silicon surface in Dielectric Coplanar Surface Barrier Discharge. *Surf. Coat. Technol.*, 2013, 236, 326-331.

FIGURE X

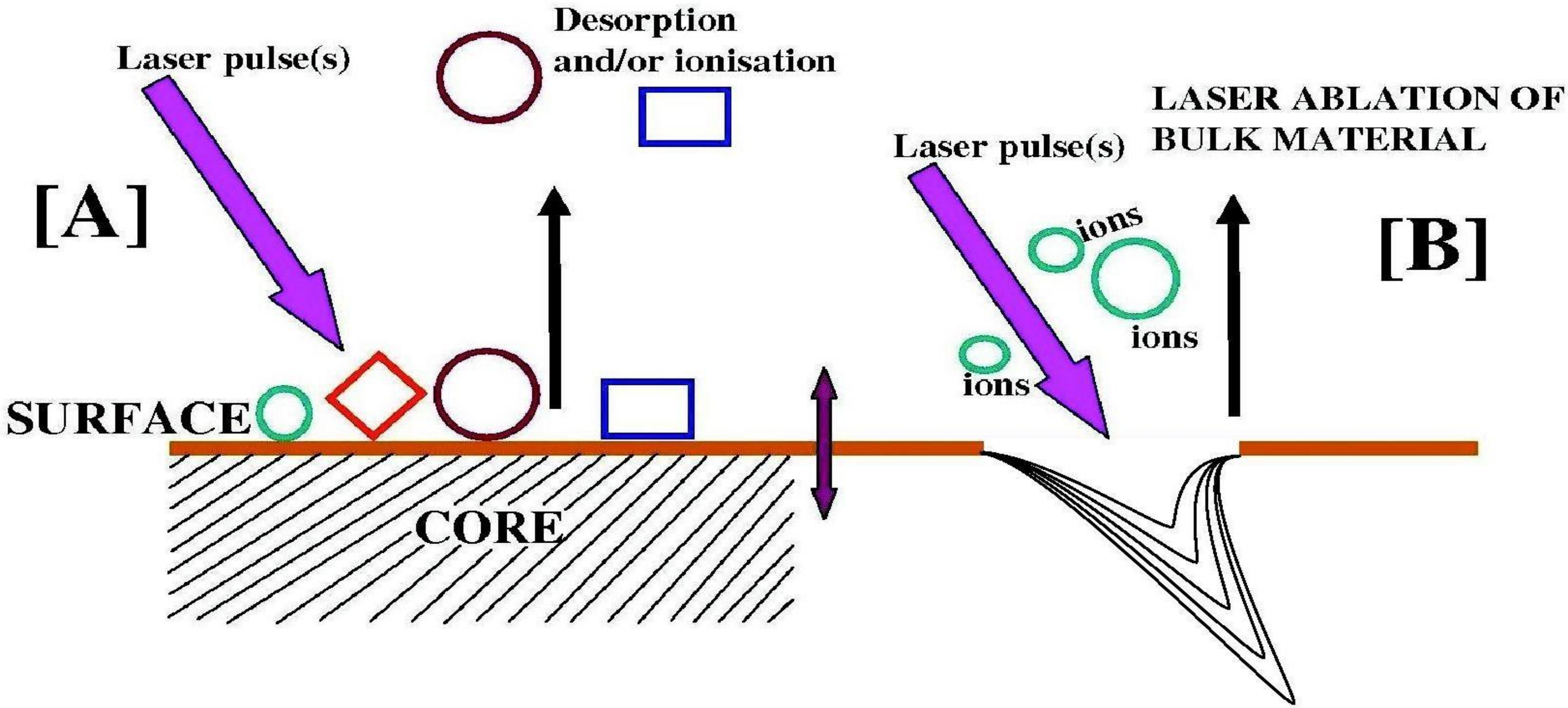

A. Pamreddy, D. Skácelová, M. Haničinec, P. Sťahel, M. Stupavská, M. Černák a J. Havel. Plasma cleaning and activation of silicon surface in Dielectric Coplanar Surface Barrier Discharge. *Surf. Coat. Technol.*, 2013, 236, 326-331.

LASER ABLATION synthesis

GOLD ARSENIDES

there are just a few known

Au + As → ?

GOLD ARSENIDES

there are just a few known

Au + As → ?

L. Prokeš, E. M. Peña-Méndez, J. E. Conde, N. R. Panyala, M. Alberti and J. Havel, Laser ablation synthesis of new gold arsenides using nano-gold and arsenic as precursors. LDI-TOF mass spectrometry and spectrophotom., **Rapid Commun. Mass Spectrom**. 2014 Mar 30;28(6):577-86 .

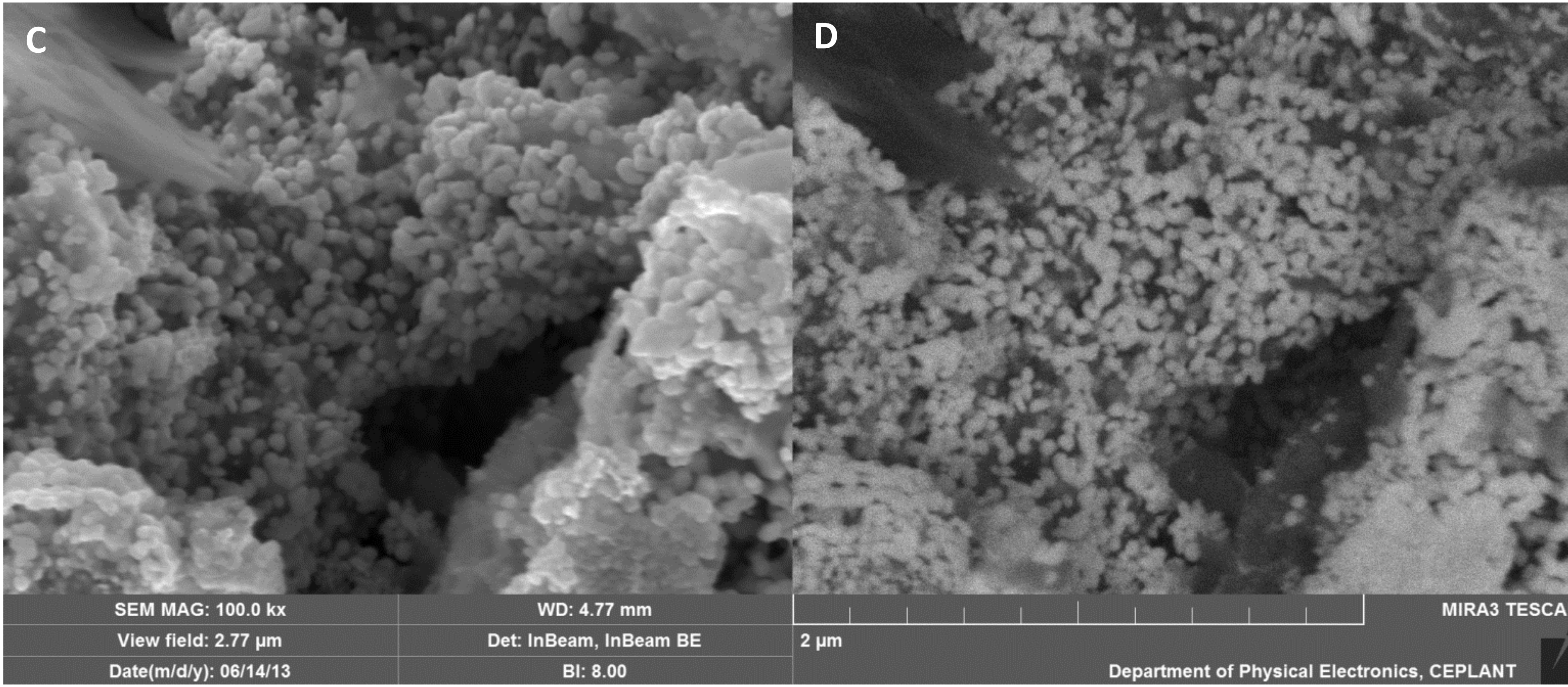
C
D
SEM MAG: 100.0 kx
WD: 4.77 mm
MIRA3 TESCAN
View field: 2.77 μm
Det: InBeam, InBeam BE
2 μm
Date(m/d/y): 06/14/13
BI: 8.00
Department of Physical Electronics, CEPLANT

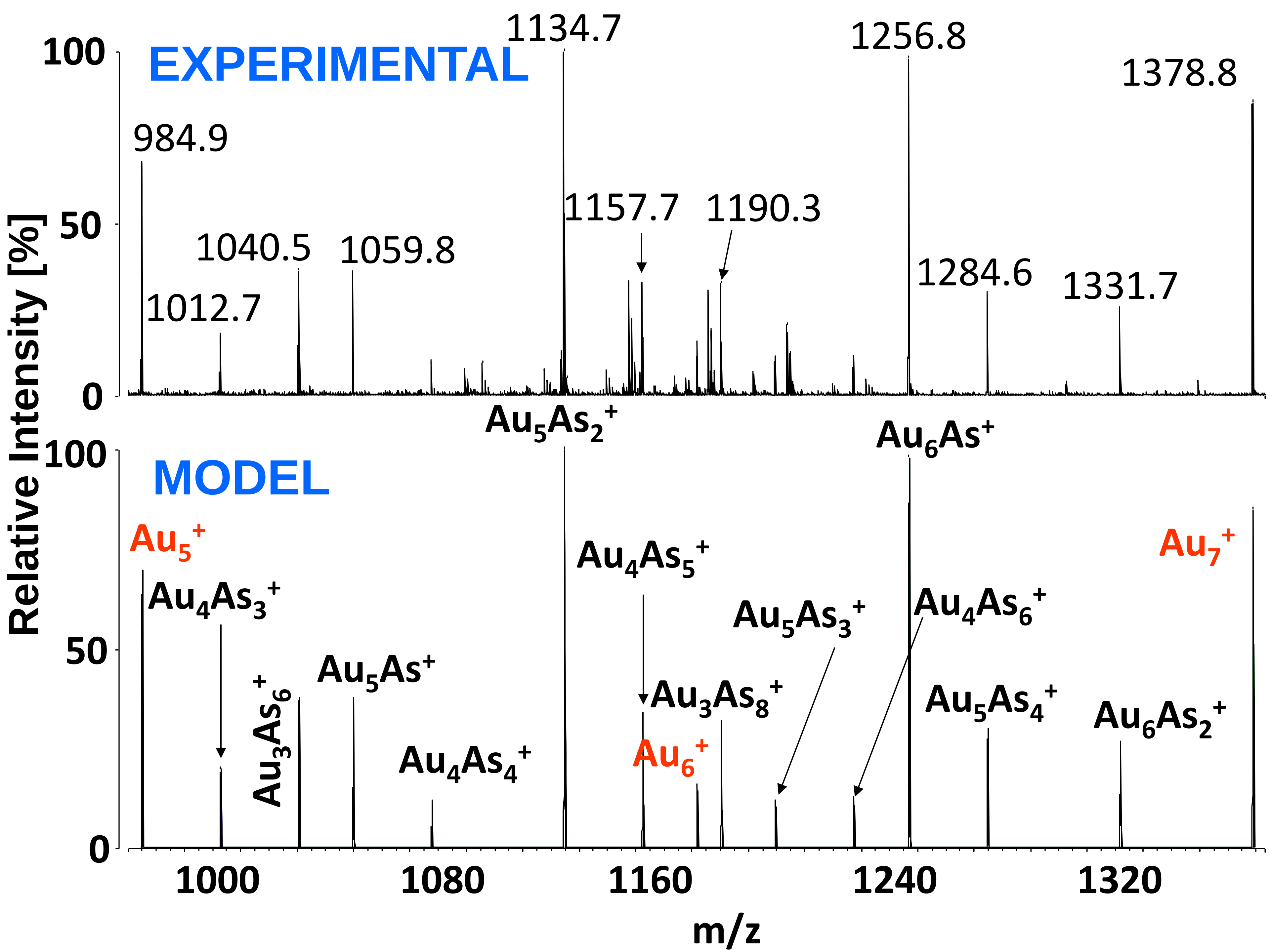

EXPERIMENTAL
MODEL
Relative Intensity [%]
m/z
100
50
0
1000
1080
1160
1240
1320
984.9
1012.7
1040.5
1059.8
1134.7
1157.7
1190.3
1256.8
1284.6
1331.7
1378.8
$Au_5As_2^+$
Au_6As^+
Au_5^+
$Au_4As_3^+$
$Au_3As_6^+$
Au_5As^+
$Au_4As_4^+$
$Au_4As_5^+$
$Au_3As_8^+$
Au_6^+
$Au_5As_3^+$
$Au_4As_6^+$
$Au_5As_4^+$
$Au_6As_2^+$
Au_7^+

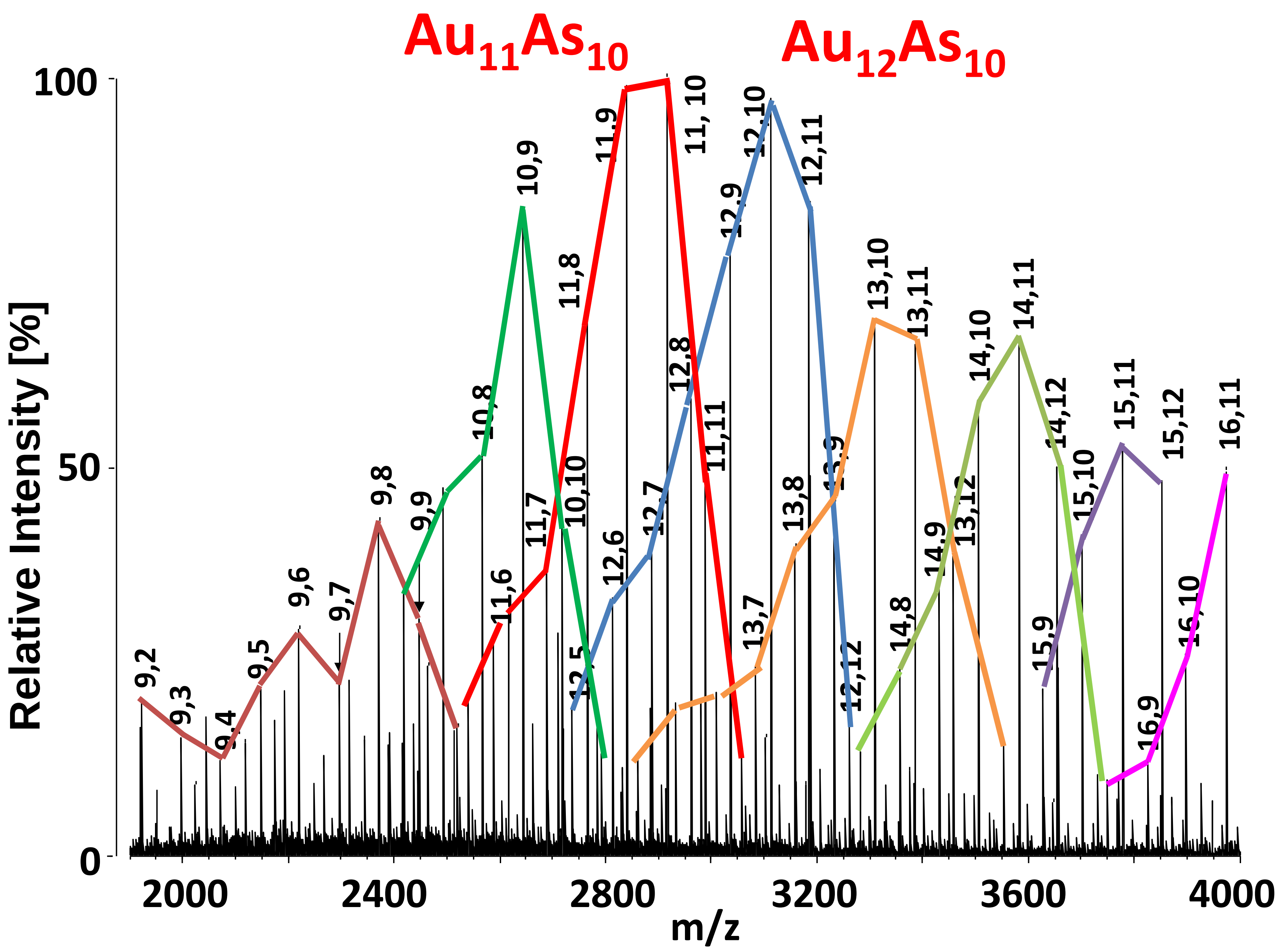

Au11As10
Au12As10
100
50
0
Relative Intensity [%]
2000
2400
2800
3200
3600
4000
m/z
9,2
9,3
9,4
9,5
9,6
9,7
9,8
9,9
10,8
10,9
10,10
11,6
11,7
11,8
11,9
11, 10
11,11
12,5
12,6
12,7
12,8
12,9
12,10
12,11
12,12
13,7
13,8
13,9
13,10
13,11
13,12
14,8
14,9
14,10
14,11
14,12
15,9
15,10
15,11
15,12
16,9
16,10
16,11

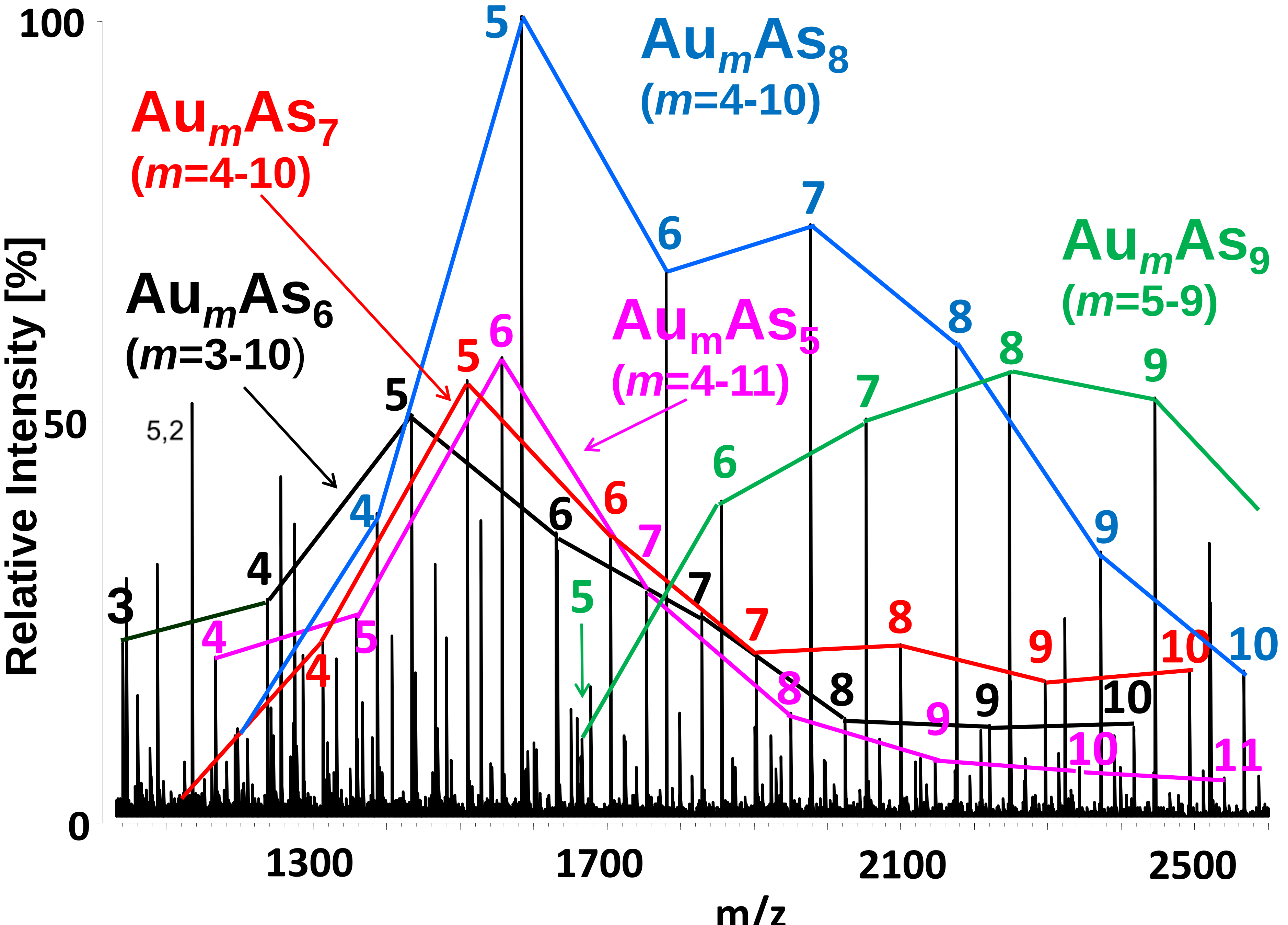

Au_mAs_8 (m=4-10)
Au_mAs_7 (m=4-10)
Au_mAs_6 (m=3-10)
Au_mAs_5 (m=4-11)
Au_mAs_9 (m=5-9)
5,2
Relative Intensity [%]
100
50
0
1300
1700
2100
2500
m/z

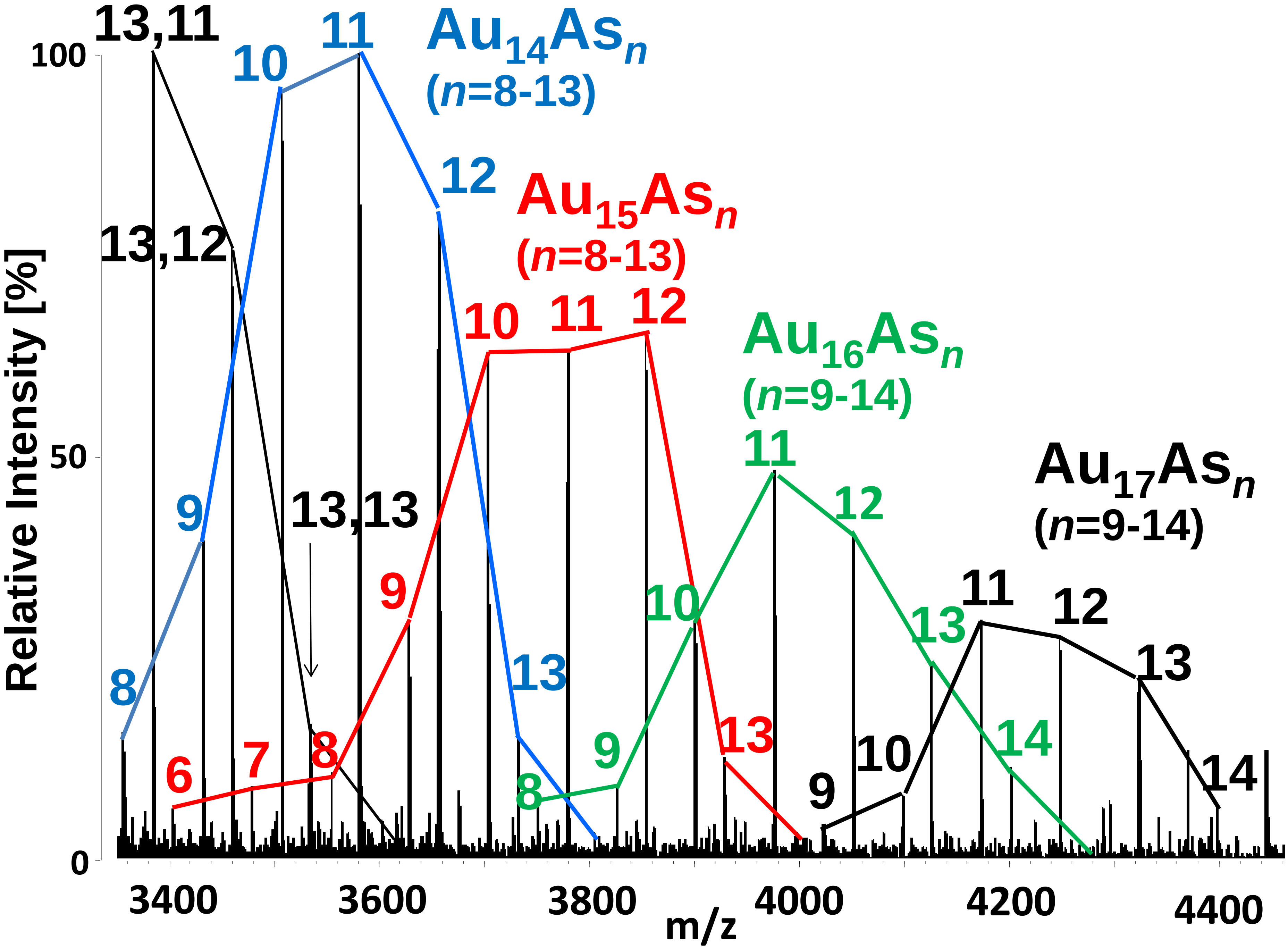

Au$_{14}$As$_n$ (n=8-13)
Au$_{15}$As$_n$ (n=8-13)
Au$_{16}$As$_n$ (n=9-14)
Au$_{17}$As$_n$ (n=9-14)
13,11
13,12
13,13
Relative Intensity [%]
m/z
100
50
0
3400
3600
3800
4000
4200
4400

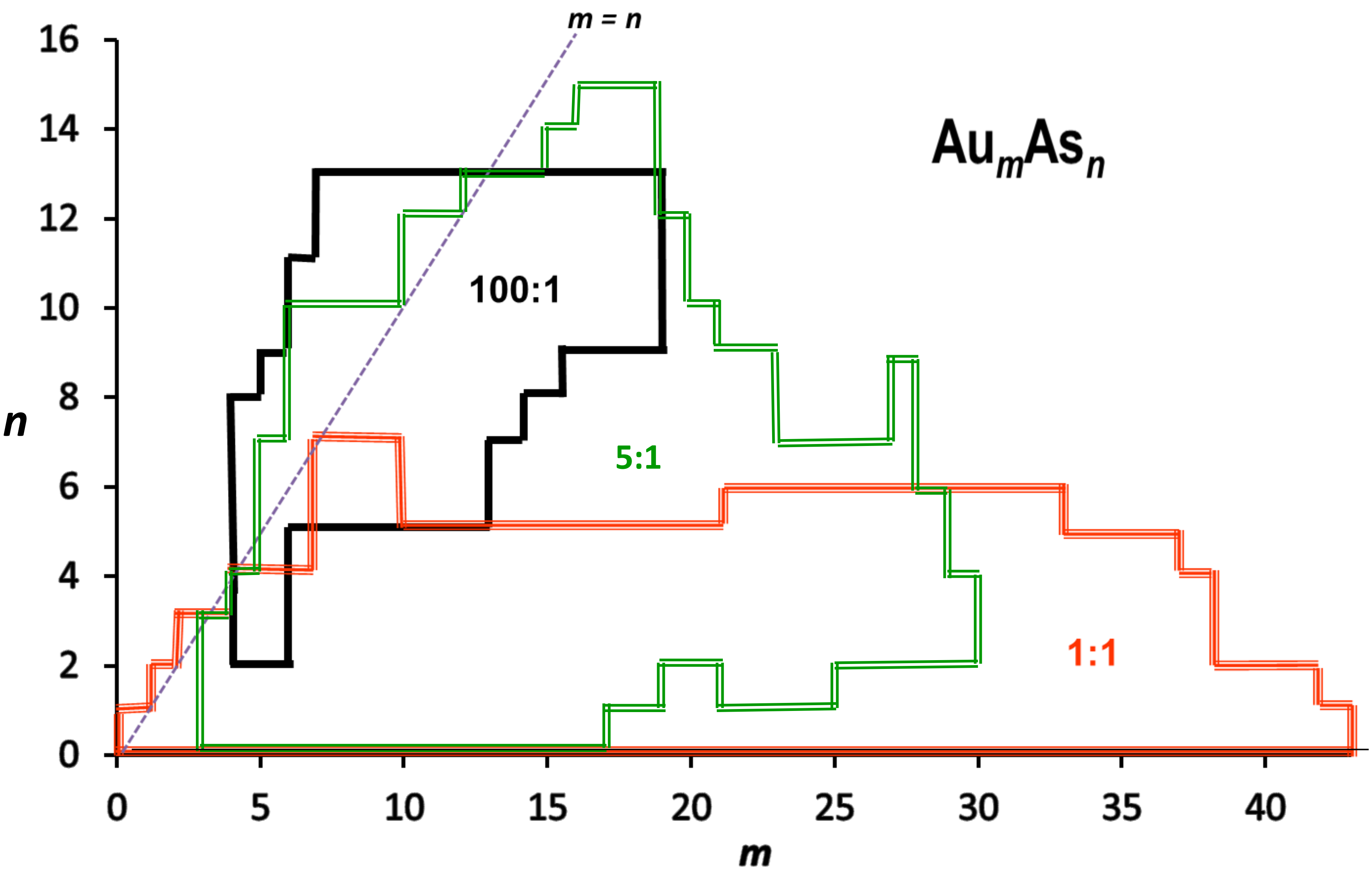

m = n
Au$_m$As$_n$
100:1
5:1
1:1
n
m
16
14
12
10
8
6
4
2
0
0
5
10
15
20
25
30
35
40

GOLD ARSENIDES

... more than

450

new gold arsenides were identified ...

L. Prokeš, E. M. Peña-Méndez, J. E. Conde, N. R. Panyala, M. Alberti and J. Havel,
Laser ablation synthesis of new gold arsenides using nano-gold and arsenic as precursors. LDI-TOF mass spectrometry and spectrophotometry, **Rapid Commun. Mass Spectrom**. 2014 Mar 30;28(6):577-86 .

MALDI TOF MS

Is first of all used for analysis peptides-proteins

In Proteomics

PROTEOMICS

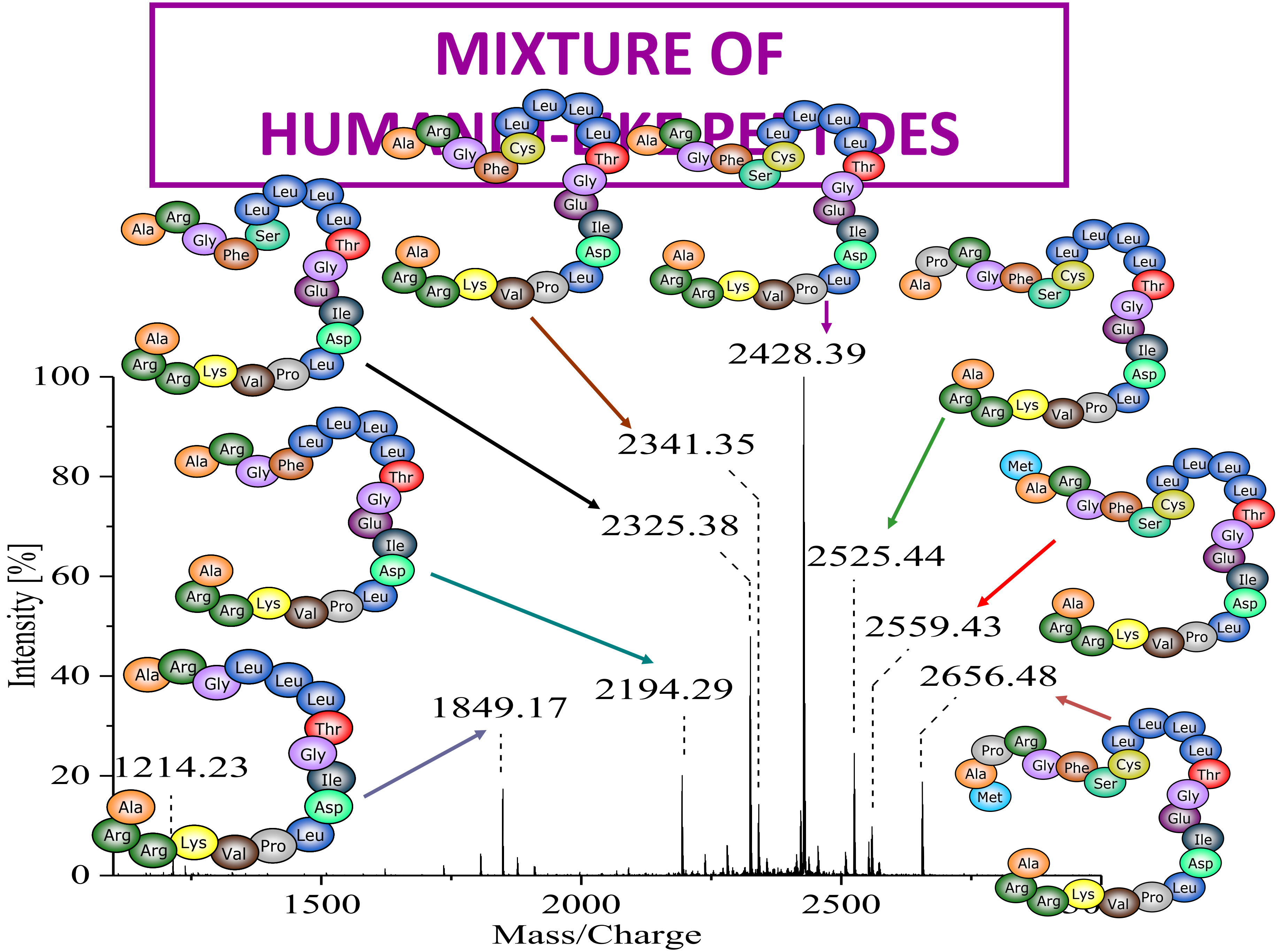
MIXTURE OF
2428.39
2341.35
2325.38
2525.44
2559.43
2656.48
2194.29
1849.17
1214.23
Intensity [%]
100
80
60
40
20
0
1500
2000
2500
Mass/Charge

use of MALDI TOF MS

peptides-proteins in Proteomics

But also

i) inorganic compounds and nano-materials

(ii) adsorbed organic and/or inorganic compounds on various surfaces

(iii) Elucidate chemical structure of coordination polymers MOF´s

(iv) Laser Ablation Synthesis

~~MALDI~~ -> SALDI -> SELDI -> NALDI

Surface Assisted LDI

Surface Enhanced LDI

NAno Particles LDI

Acknowledements

Lenka Kolářová
Katarína ŠÚTOROVÁ
Krístína HAJTMANOVÁ
Luboš PROKEŠ

José Elias CONDE-GONZÁLEZ
Eladia María PEŇA-MÉNDEZ
Catalina RUIZ-PÉREZ

MAT2014-57465-R
EU ERASMUS ULL-MU

ULL, La Laguna, Seminary of GRANT MAT2014-57465-R, Ministry of Economy and Competiveness, Spain, 13th October 2015

Gold nanoparticles (GNPs) used as a drug carriers

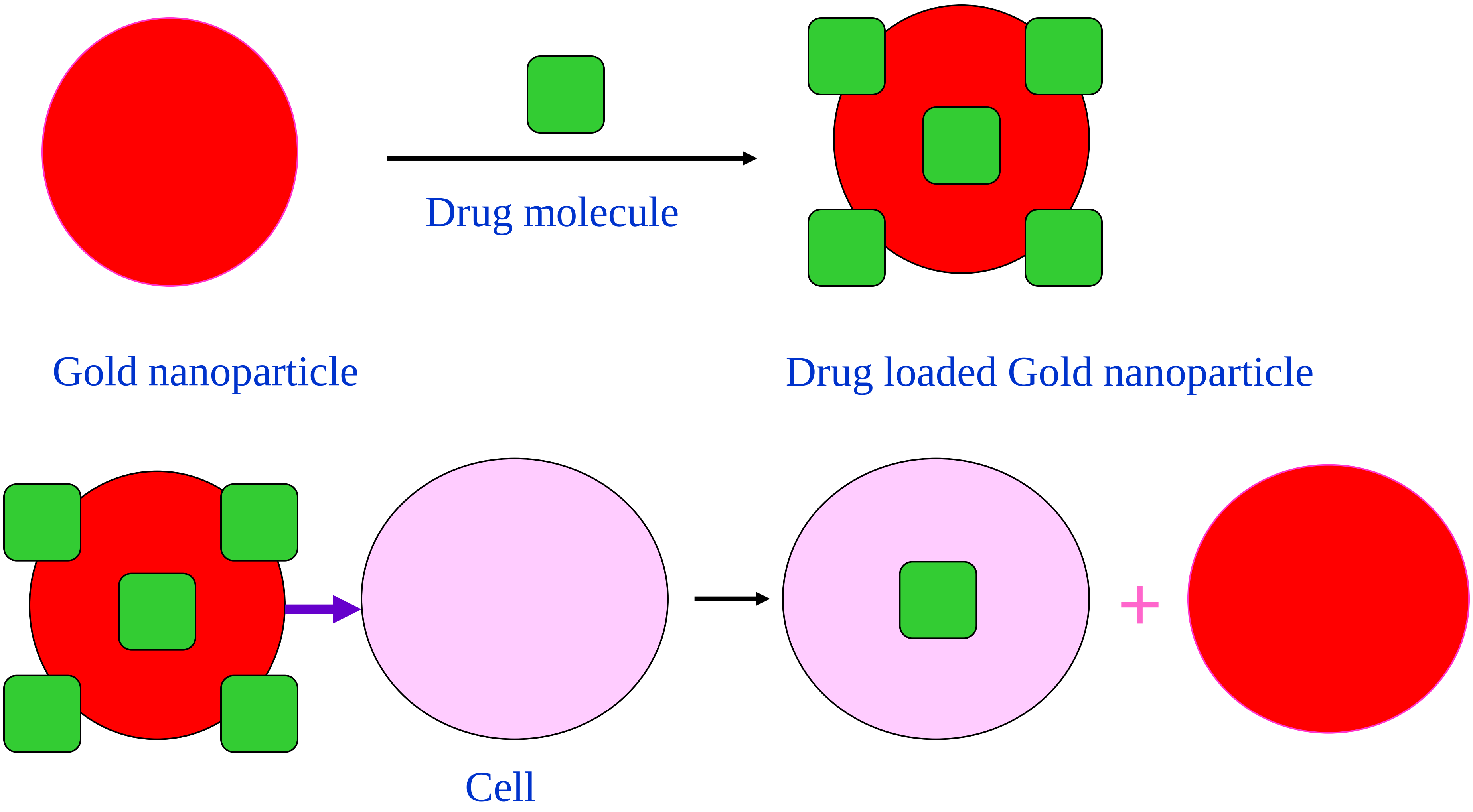

EXPLOADING Gold nanoparticles

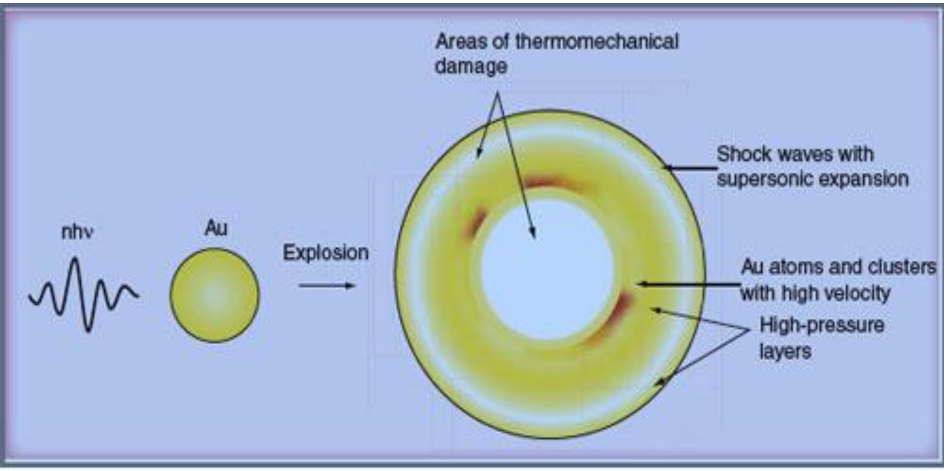

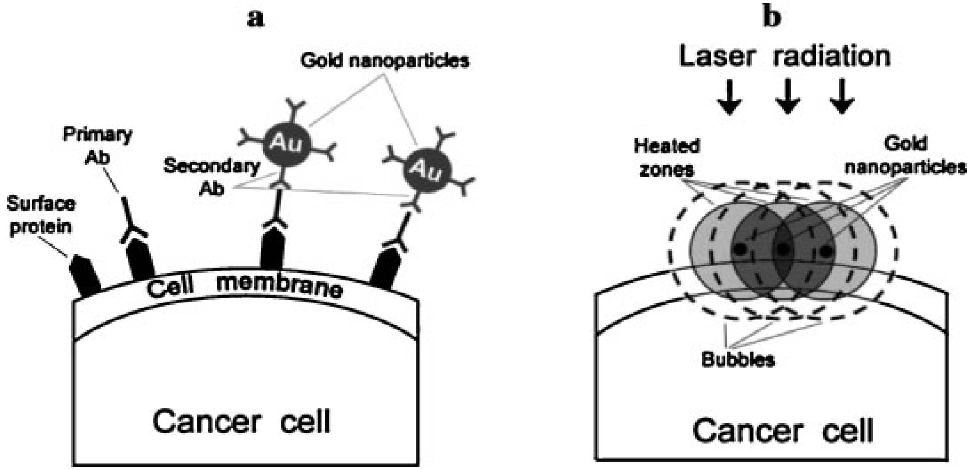

Nano photothermolysis of cancer cells

R. R. Letfullin, et al. Laser induced explosion of gold nanoparticles: potential role for nanophotothermolysis of cancer. *Nanomedicine* **2006**, 1, 473.

76

Titanium carbide, TiC

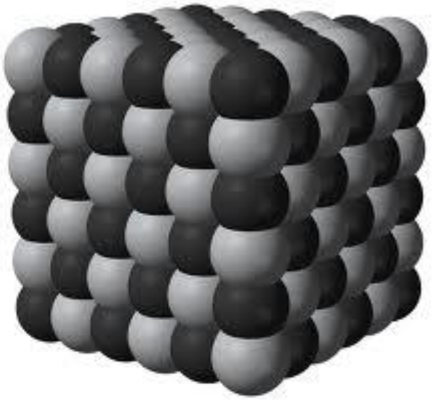

F. Amato, N. R. Panyala, P. Vašina, P. Souček, J. Havel. Laser desorption ionisation quadrupole ion trap time-of-flight mass spectrometry of titanium-carbon thin films. Rapid Commun. Mass Spectrom, 2013, 27, 1-7.

Titanium carbide, TiC

RESULTS:

Ti-C films were found to be composites of

(i) pure and hydrogenated TiC

(ii) **titanium oxycarbides,** and [$Ti_{8(9)}C_nO_p$:H].

(iii) titanium oxides of various degrees of hydrogenation (all embedded in an amorphous and/or diamond-like carbon matrix).

(iv) Hydrogenated titanium oxycarbide is was the main component of the surface layer, whereas while deeper layers are were composed mostly primarily of TiC and titanium oxides (also embedded in the carbon matrix).

[Ti8C25O10H8], [Ti8C25O10H9] , and [Ti8C25O10H10]

F. Amato, N. R. Panyala, P. Vašina, P. Souček, J. Havel. Laser desorption ionisation quadrupole ion trap time-of-flight mass spectrometry of titanium-carbon thin films. Rapid Commun. Mass Spectrom, 2013, 27, 1-7.

SURFACE ANALYSIS

and

CLEANING via PLASMA TREATMENT

A. Pamreddy, D. Skácelová, M. Haničinec, P. Sťahel, M. Stupavská, M. Černák a J. Havel. Plasma cleaning and activation of silicon surface in Dielectric Coplanar Surface Barrier Discharge. *Surf. Coat. Technol.*, 2013, 236, 326-331.

FIGURE X

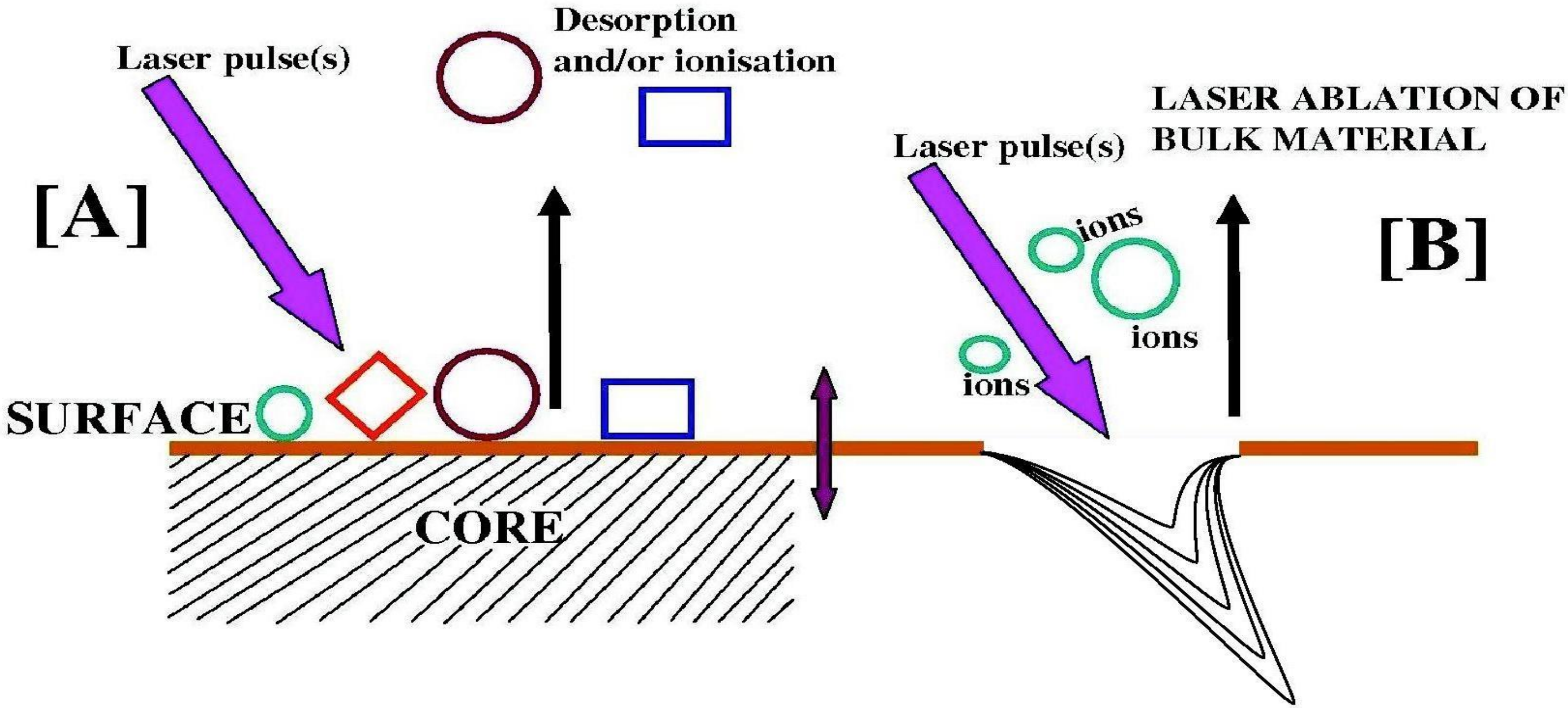

A. Pamreddy, D. Skácelová, M. Haničinec, P. Sťahel, M. Stupavská, M. Černák a J. Havel. Plasma cleaning and activation of silicon surface in Dielectric Coplanar Surface Barrier Discharge. *Surf. Coat. Technol.*, 2013, 236, 326-331.

CARBIDES, NITRIDES, ….

Boron nitrides

P_3N_5

CARBIDES, NITRIDES, ...

Boron nitrides

P_3N_5

Applications

Ceramic applications

-sintering additives

-pigments

-ionic conductors

-microporous materials

-for the doping of semiconductors

Aims

-to study laser ablation ionization of solid P_3N_5 and analyse $P_mN_n^{+/-}$ clusters formed in order to understand the formation of phosphorus-nitrogen clusters

-and/or also to check the possibility of **generating nitrogen rich compounds**

As POSSIBLE HIGH ENERGY CONTENT MATERIALs

LDI TOF MS

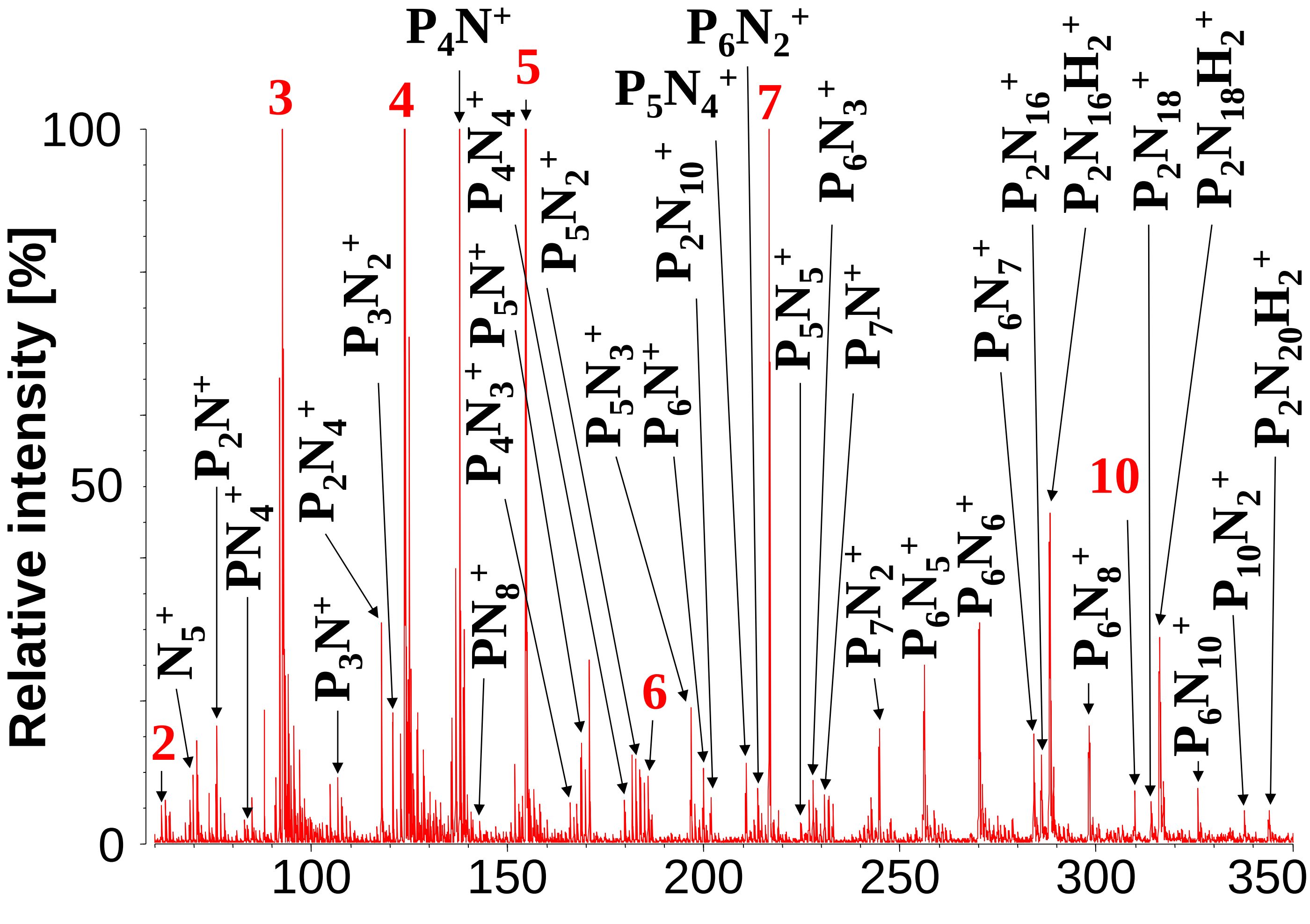

Relative intensity [%]
m/z
100
50
0
100
150
200
250
300
350
2
3
4
5
6
7
10
N_5^+
P_2N^+
PN_4^+
$P_2N_4^+$
P_3N^+
$P_3N_2^+$
P_4N^+
PN_8^+
$P_4N_3^+$
P_5N^+
$P_4N_4^+$
$P_5N_2^+$
$P_5N_3^+$
P_6N^+
$P_2N_{10}^+$
$P_5N_4^+$
$P_6N_2^+$
$P_5N_5^+$
$P_6N_3^+$
P_7N^+
$P_7N_2^+$
$P_6N_5^+$
$P_6N_6^+$
$P_6N_7^+$
$P_2N_{16}^+$
$P_2N_{16}H_2^+$
$P_6N_8^+$
$P_2N_{18}^+$
$P_2N_{18}H_2^+$
$P_6N_{10}^+$
$P_{10}N_2^+$
$P_2N_{20}H_2^+$

Matrices

- 2,5-dihydroxybenzoic acid (DHB)
- fullerene (C_{60})
- a-cyano-4-hydroxycinnamic acid (CHC)
- 1,8-dihydroxy-9[10H]-anthracenone (DIT)
- 3-hydroxypicolinic acid (HPA)
- trans-2-[3-(4-terc-butylphenyl)-2-methyl-2-propenylidene]-malononitrile (TMN)
- 2-amino-5-nitropyridine (ANP)
- Sulfur
- Selenium

HPA

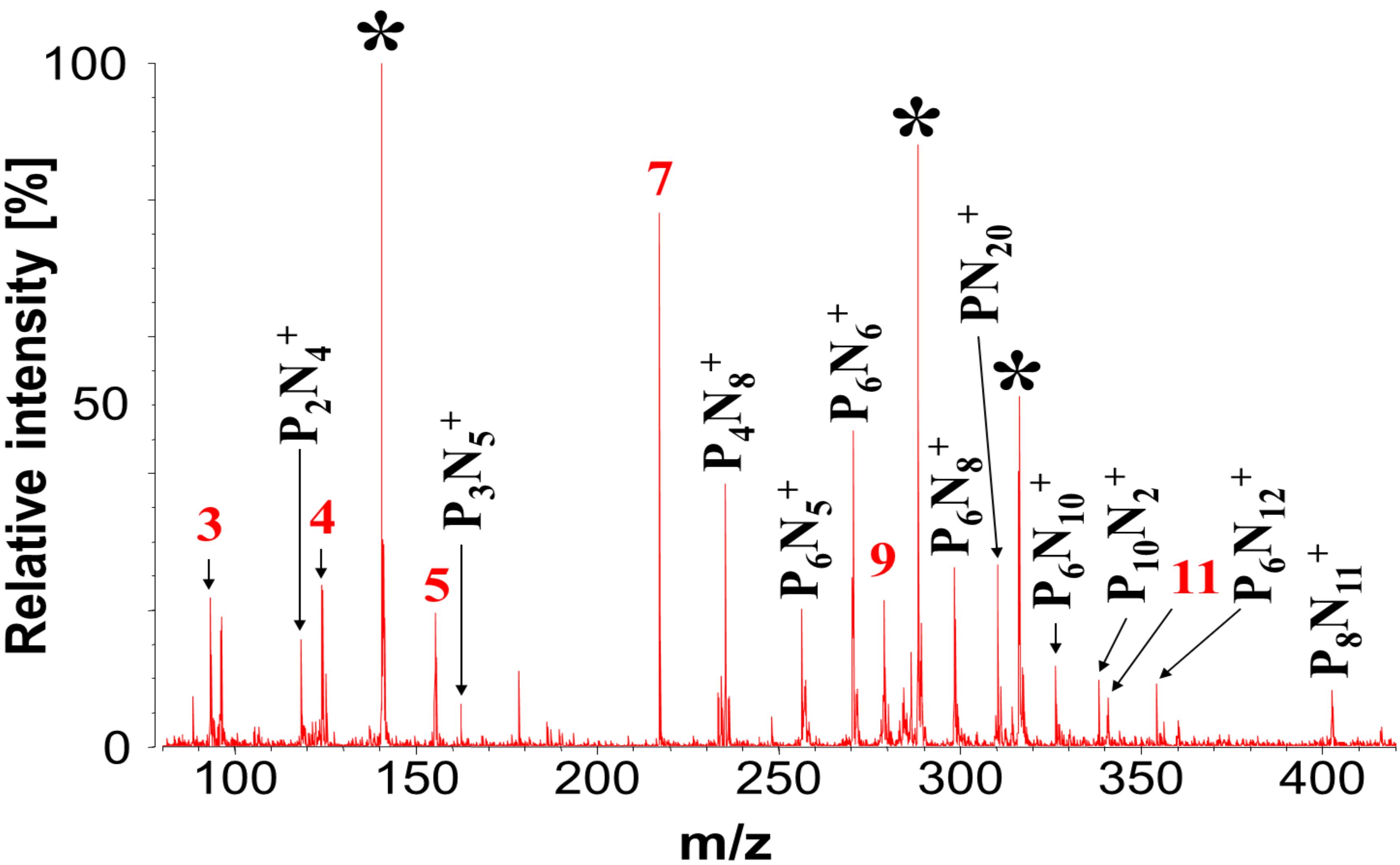

Relative intensity [%]
100
50
0
m/z
100
150
200
250
300
350
400
*
3
4
5
7
9
11
$P_2N_4^+$
$P_3N_5^+$
$P_4N_8^+$
$P_6N_5^+$
$P_6N_6^+$
$P_6N_8^+$
PN_{20}^+
$P_6N_{10}^+$
$P_{10}N_2^+$
$P_6N_{12}^+$
$P_8N_{11}^+$

TMN

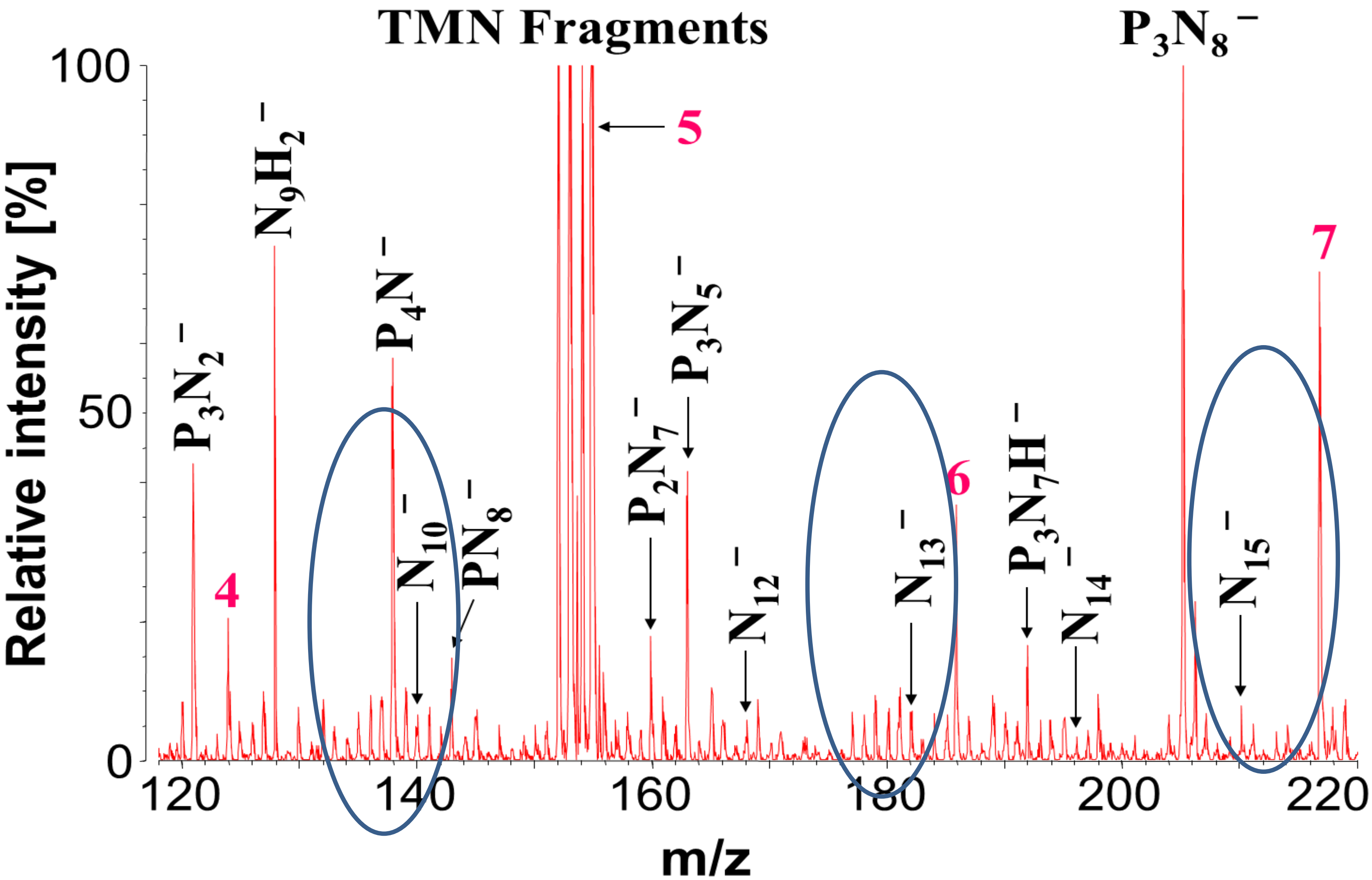

TMN Fragments
$P_3N_8^-$
Relative intensity [%]
100
50
0
120
140
160
180
200
220
m/z
$P_3N_2^-$
4
$N_9H_2^-$
P_4N^-
N_{10}^-
PN_8^-
5
$P_2N_7^-$
$P_3N_5^-$
N_{12}^-
N_{13}^-
6
$P_3N_7H^-$
N_{14}^-
N_{15}^-
7

P_3N_5

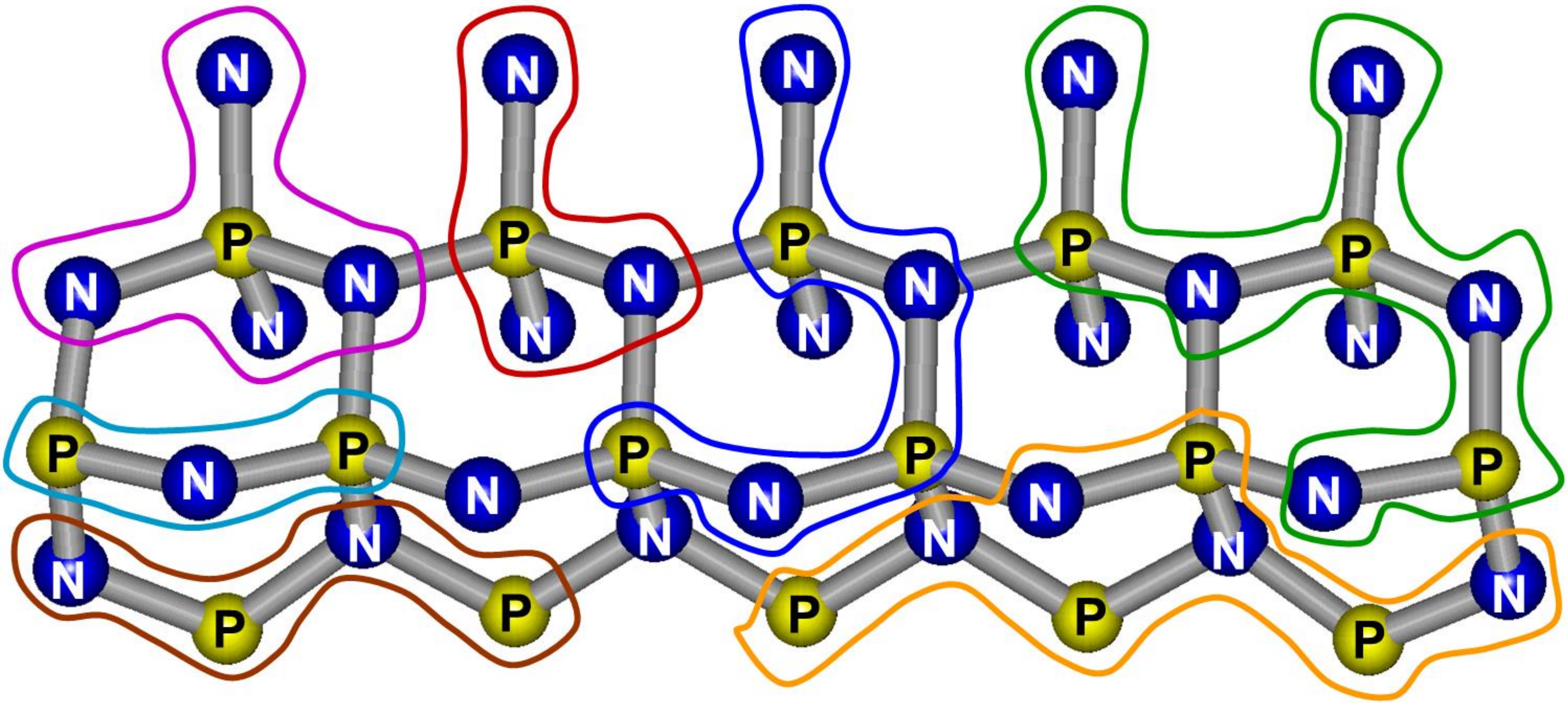

S. D. Pangavhane, L. Hebedová, M. Alberti and J. Havel, Laser ablation synthesis of new phosphorus nitride clusters from α-P3N5. Laser desorption ionization and MALDI time of flight mass spectrometry, Rapid Commun. Mass Spectrom., Rapid Commun. Mass Spectrom. 2011, 25, 1(wileyonlinelibrary.com) DOI: 10.1002/rcm.4937.

Summary

Phosphorus nitride

- Many new N_n and binary P_mN_n cluster ions were identified in positive and negative ion modes
- It was found that HPA is the most suitable matrix to generate nitrogen rich P_mN_n clusters in positive ion mode
- high nitrogen clusters (up to N_{15}^{-}) generated by laser from a solid material are described for the first time

FIGURE 1

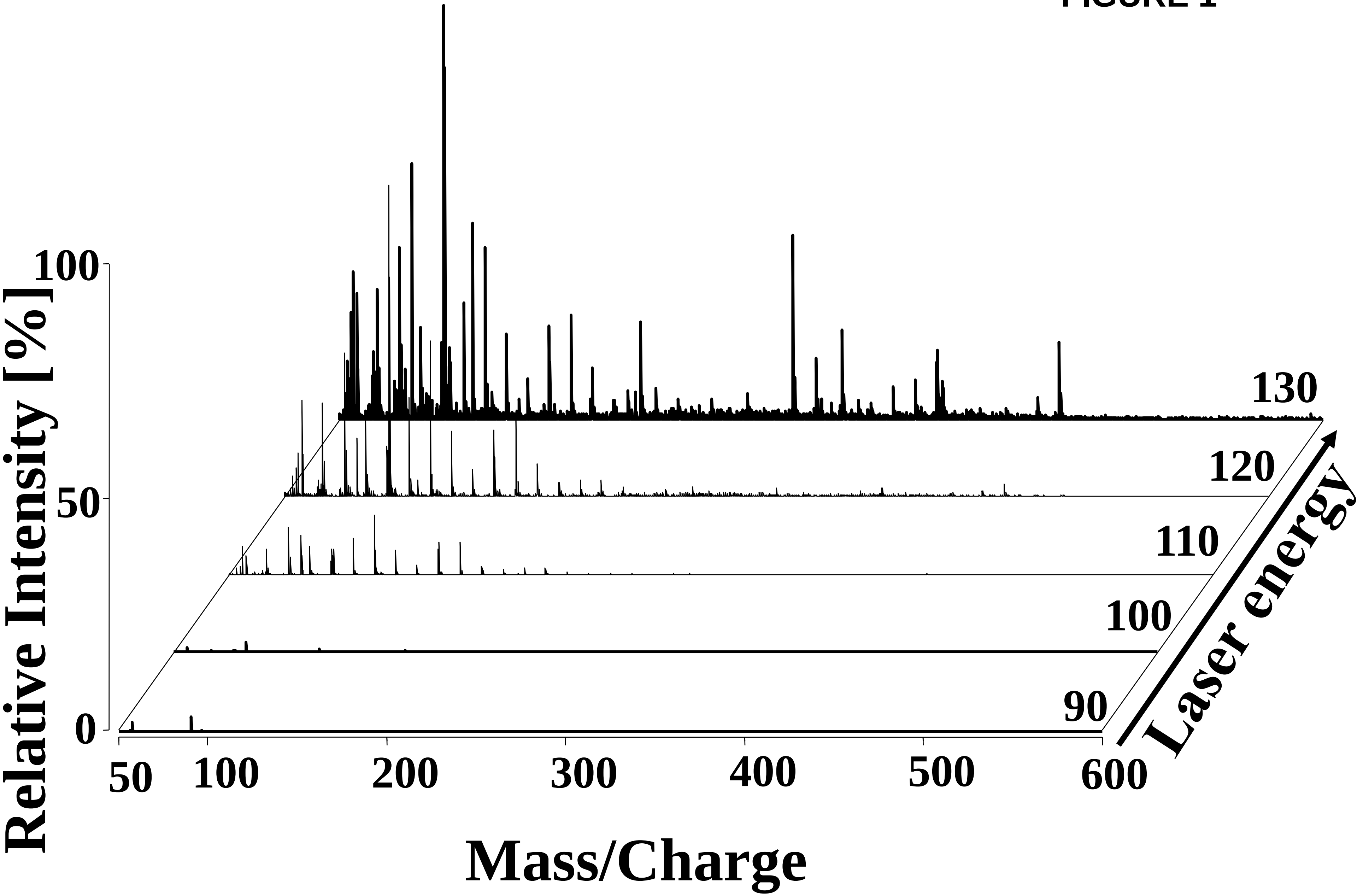

Relative Intensity [%]
100
50
0
130
120
110
100
90
Laser energy
50
100
200
300
400
500
600
Mass/Charge

SILICON WAFERS

FIGURE 2A

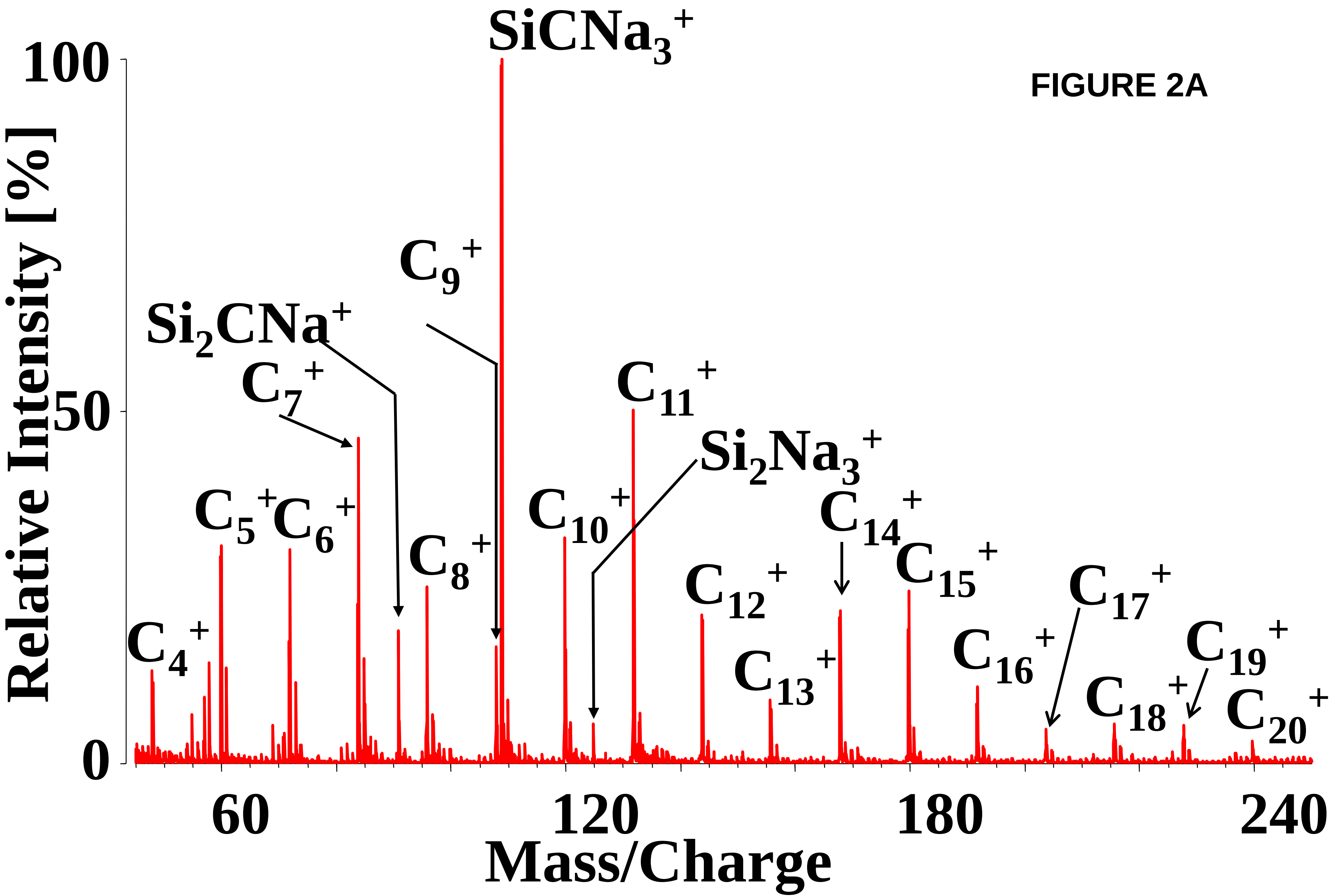

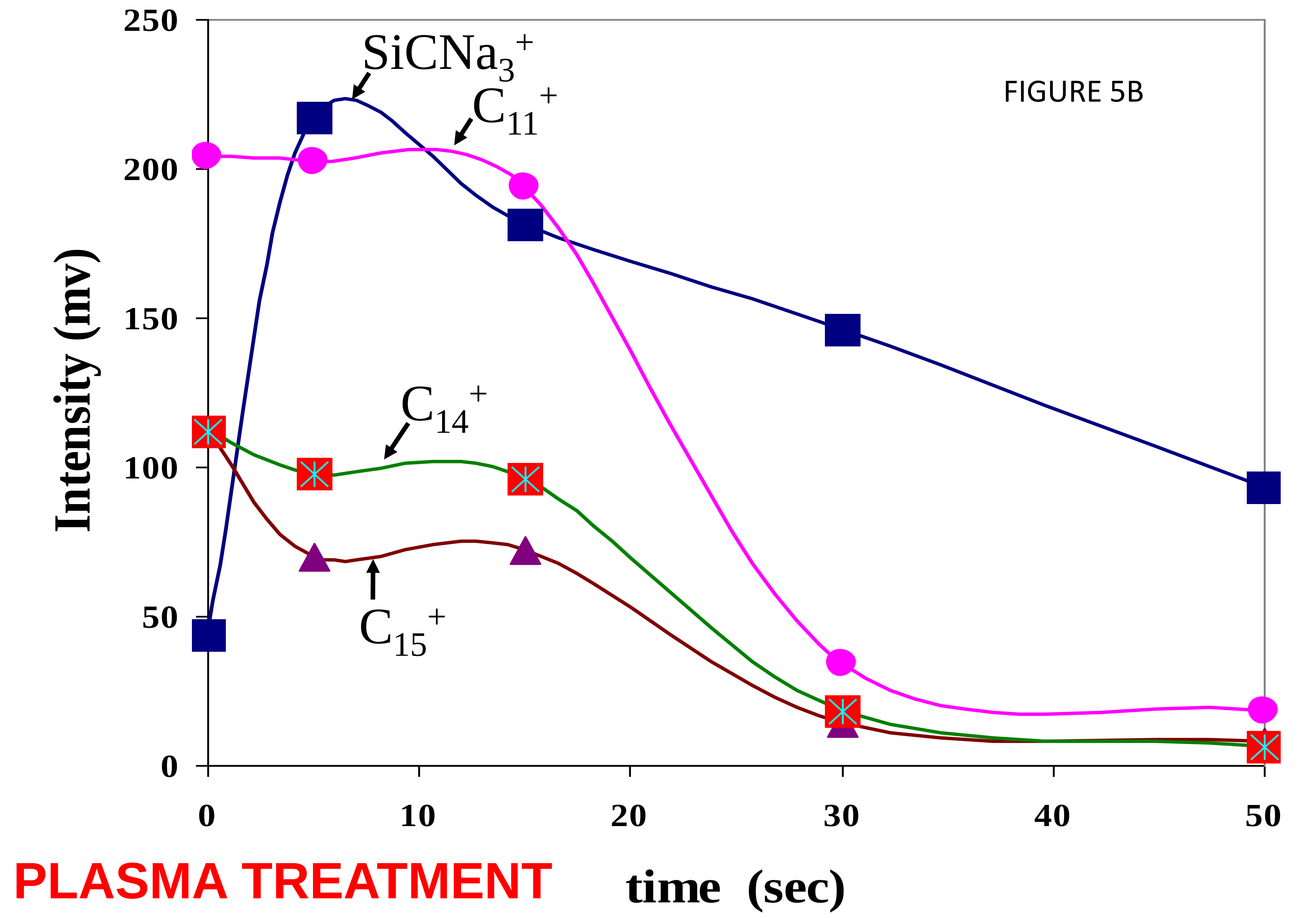

FIGURE 5B
Intensity (mv)
250
200
150
100
50
0
SiCNa$_3^+$
C_{11}^+
C_{14}^+
C_{15}^+
0
10
20
30
40
50
PLASMA TREATMENT
time (sec)

CHALCOGENIDE GLASSES

Chalcogenide elements in Mendeleev Table

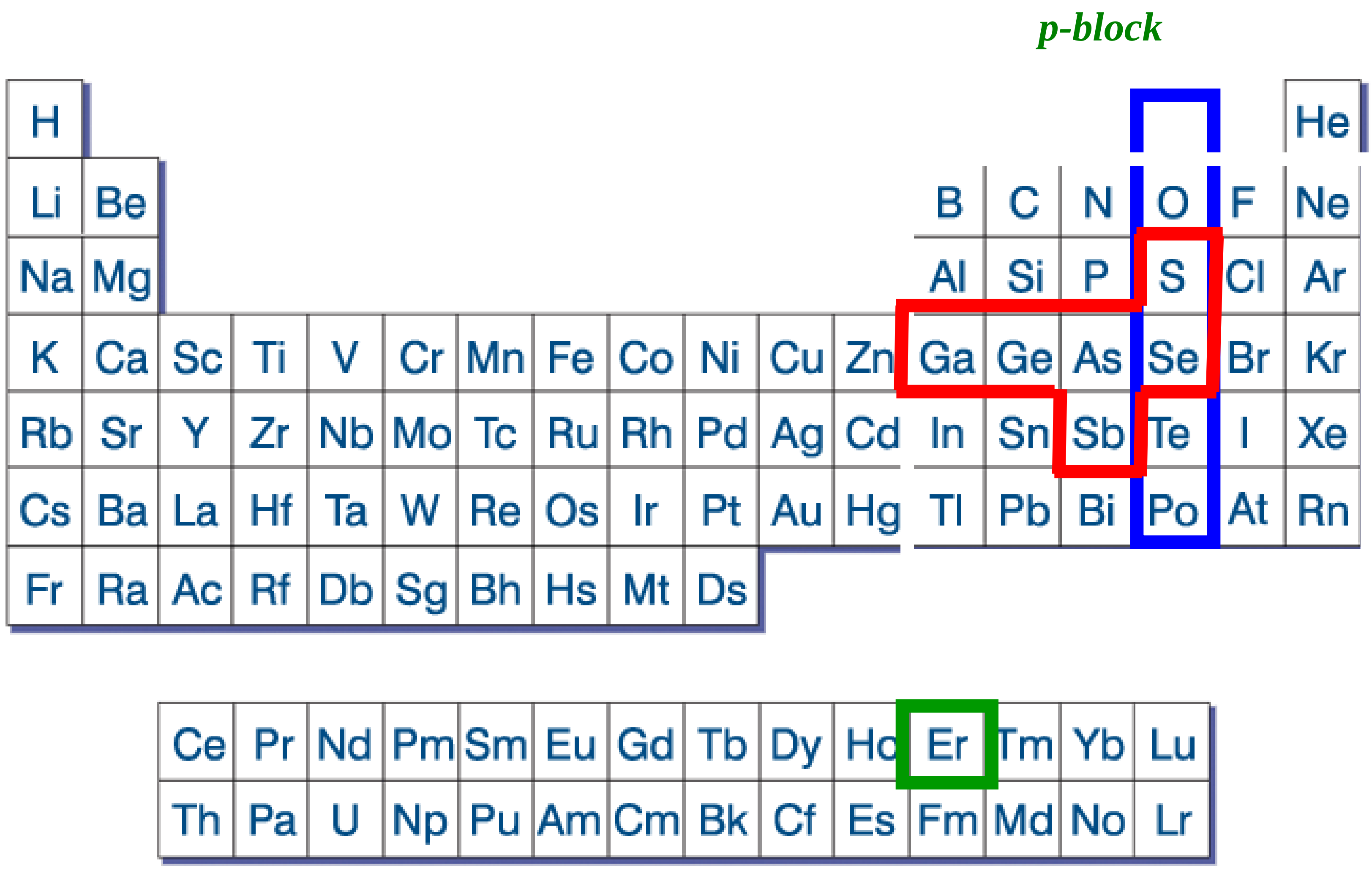

Chalcogenide glasses

$Ga_5Ge_{20}Sb_{10}S_{65}$

S

Te

Se

transmit focus light

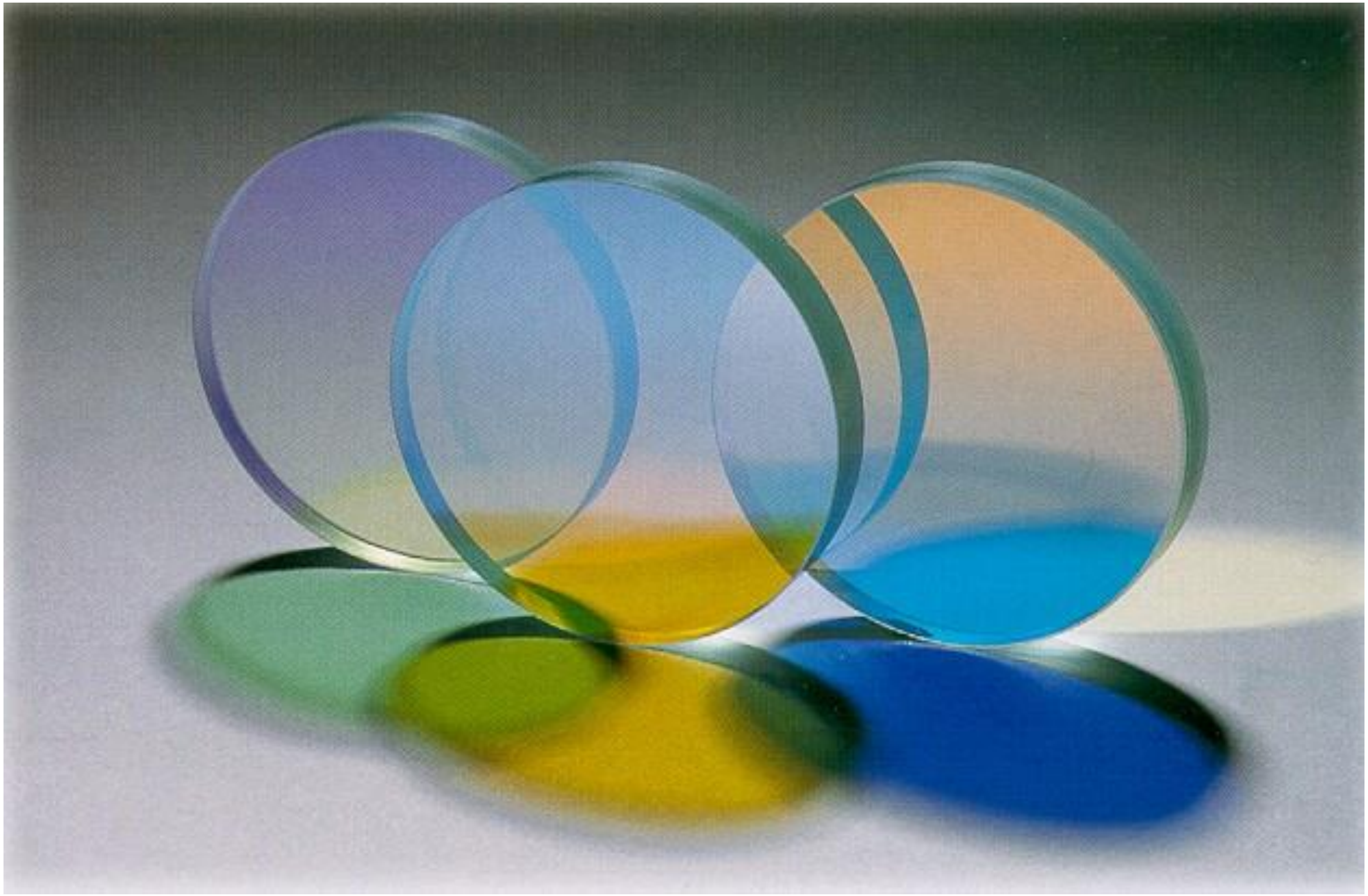



OLYMPUS

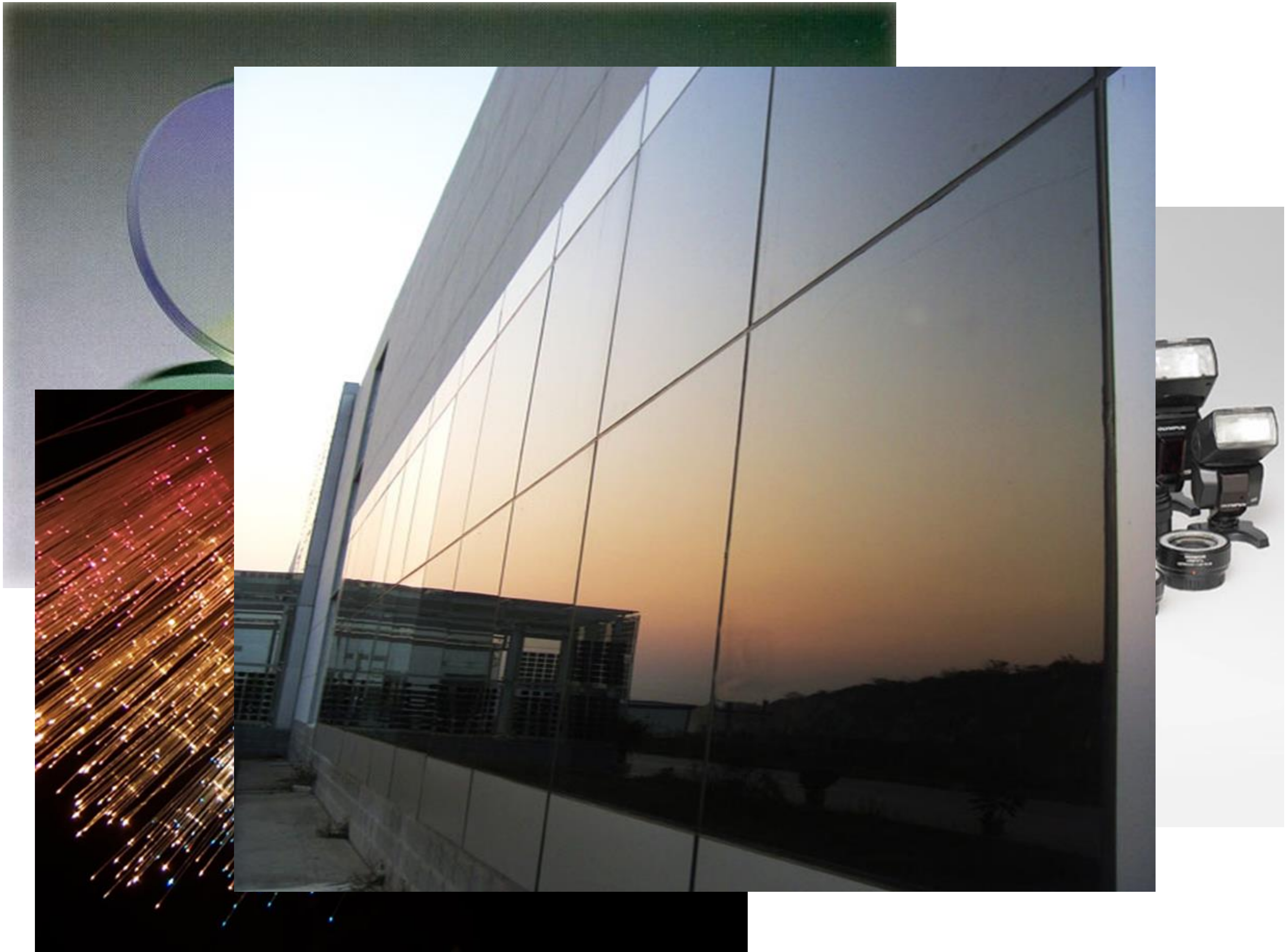

Pulsed laser deposition

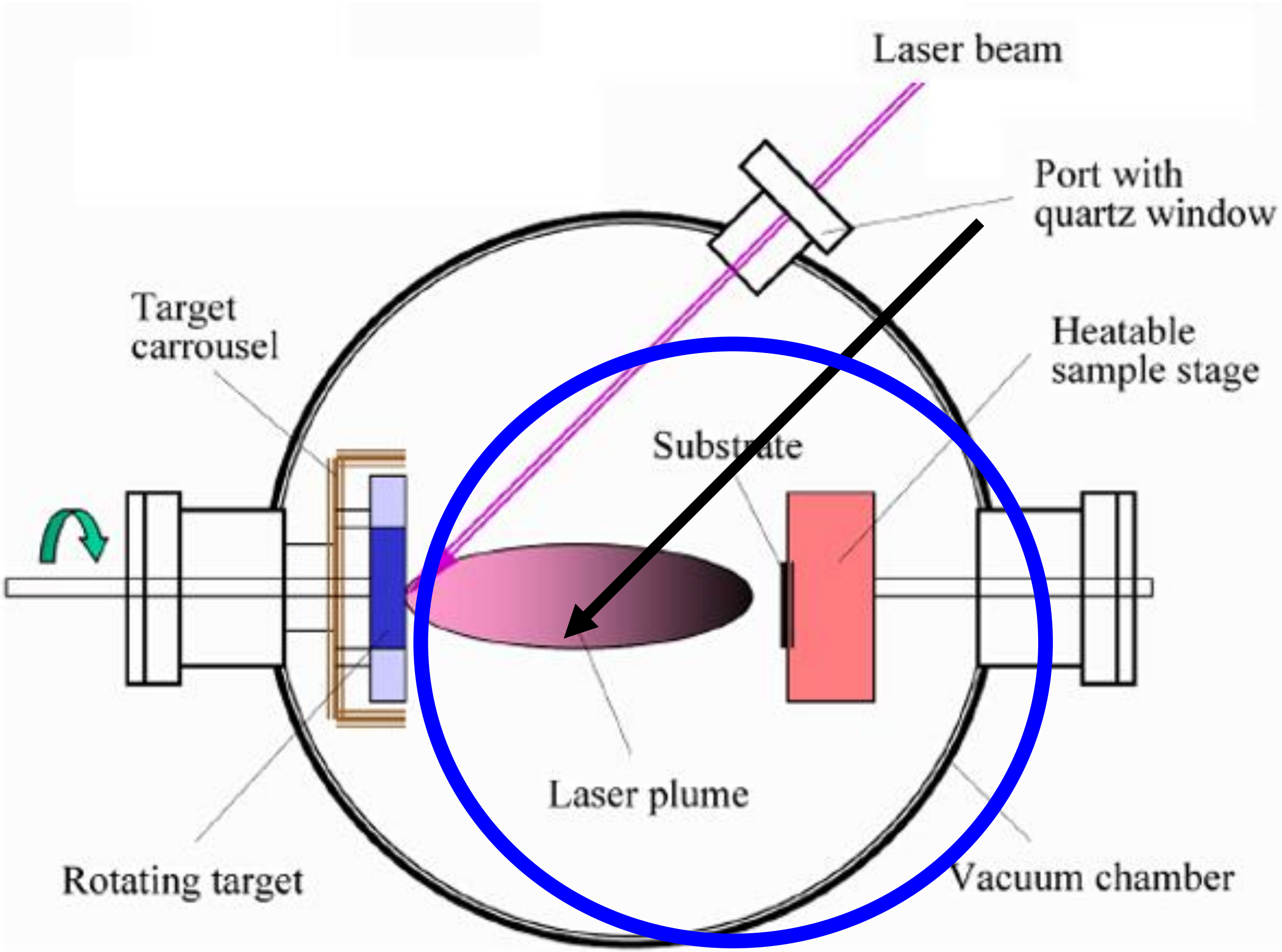

Phase change random access memory chip

Scientific instruments

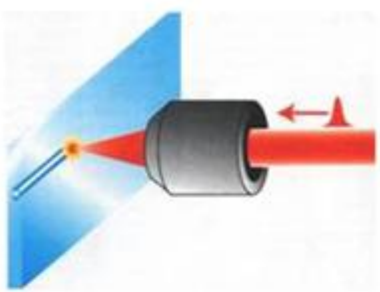

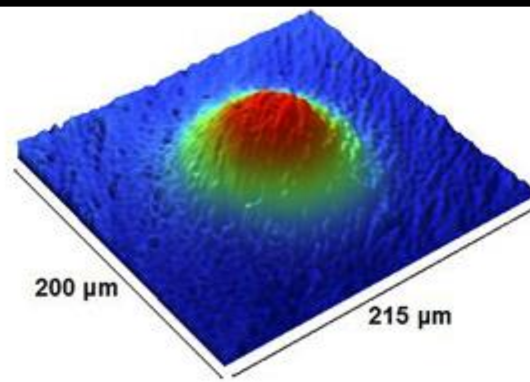

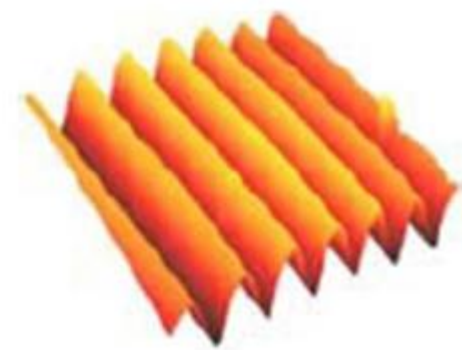

Waveguides Micro-lenses Relief Gratings

Chalcogenide glass photonic chip

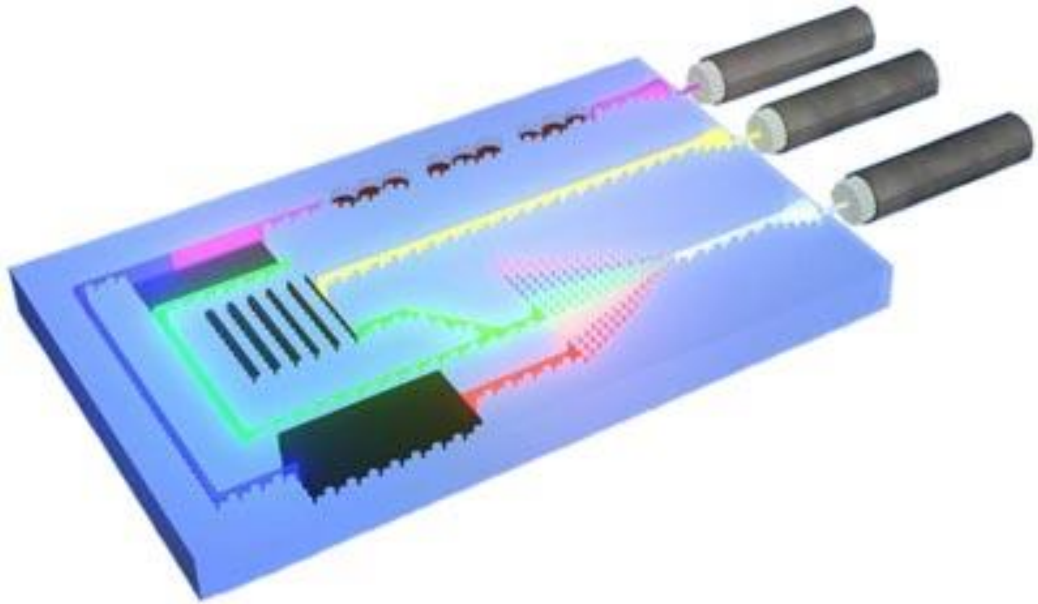

Push internet speeds


Infrared Wireless
Communication

Infrared technology in communication

Main advantages for this technology are:

-stable and scalable communication method.
-high-speed communication with low cost.
-does not interfere nor is it disturbed by other radiofrequency devices.
-Information is secured
-license free and can be used worldwide.

Live-Cell based bio-optic sensors

-**Live human lung cells** are coated onto an IR transparent chalcogenide **glasses fibres**

-**Biochemical change** in the living cells

-Detection minute quantities of **bio-hazardous and toxic molecules**

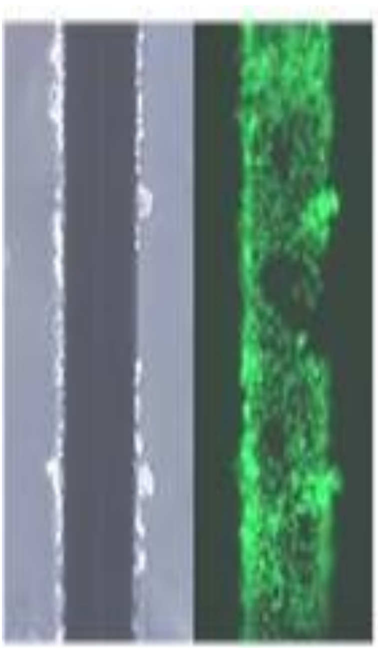

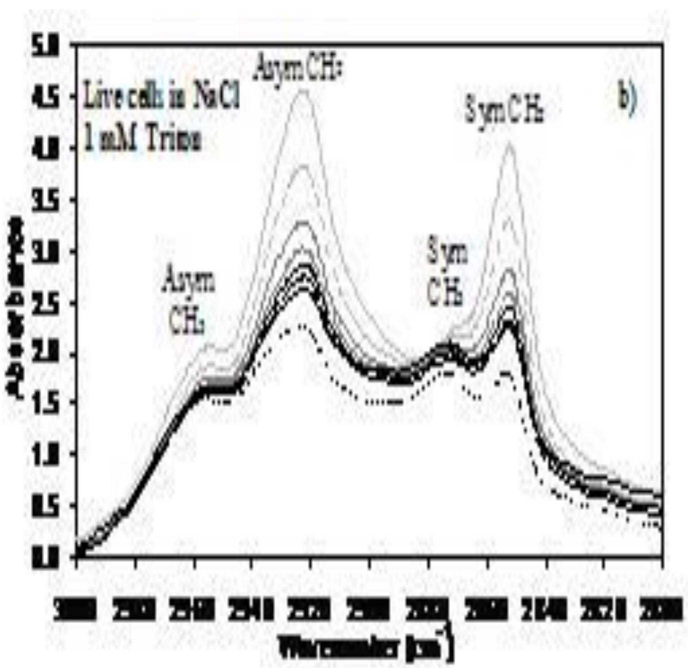

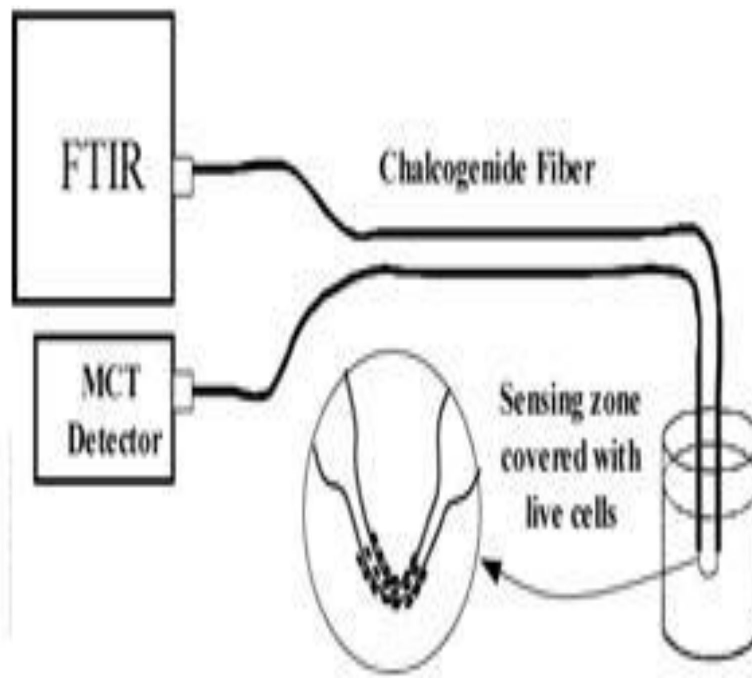

Minimally invasive surgery

Fibre optic camera for endoscopy

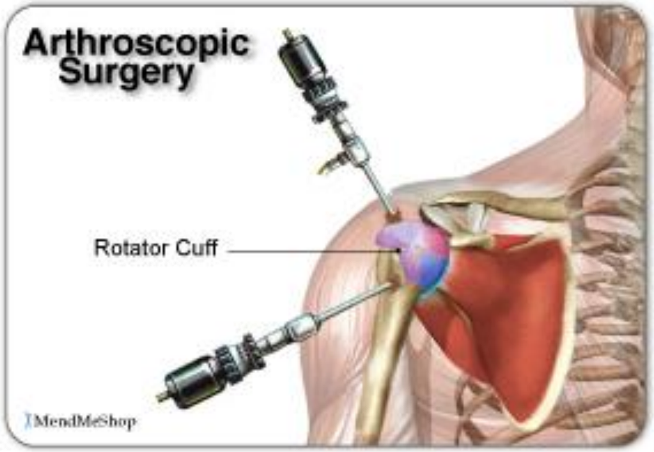

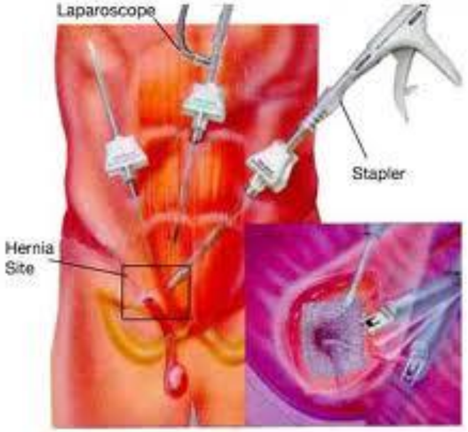

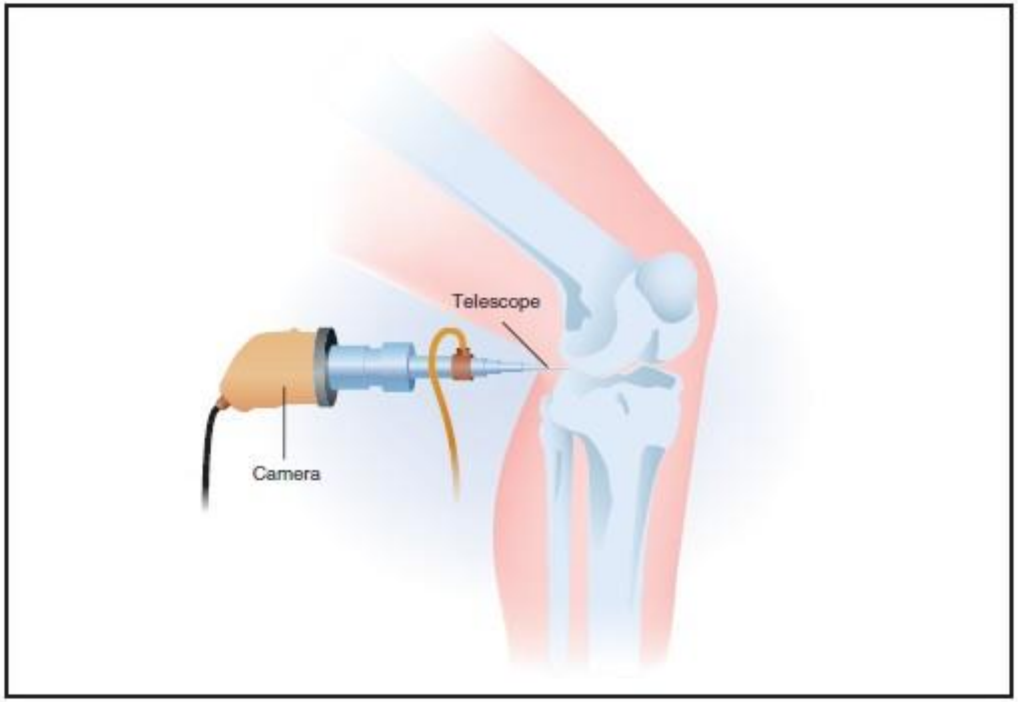

An arthroscope uses optical fibers to form an image of the damged cartilage, which it sends to a television monitor that helps the surgeon perform surgery. *(Illustration by Argosy Inc.)*

Gastroscopy

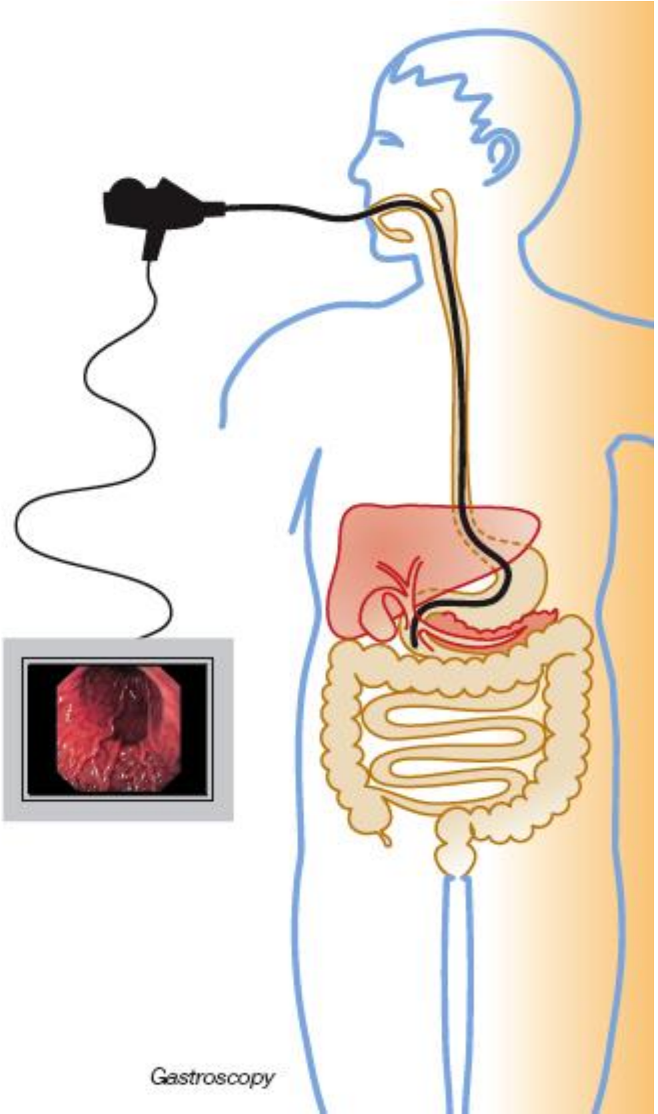

Colonoscopy

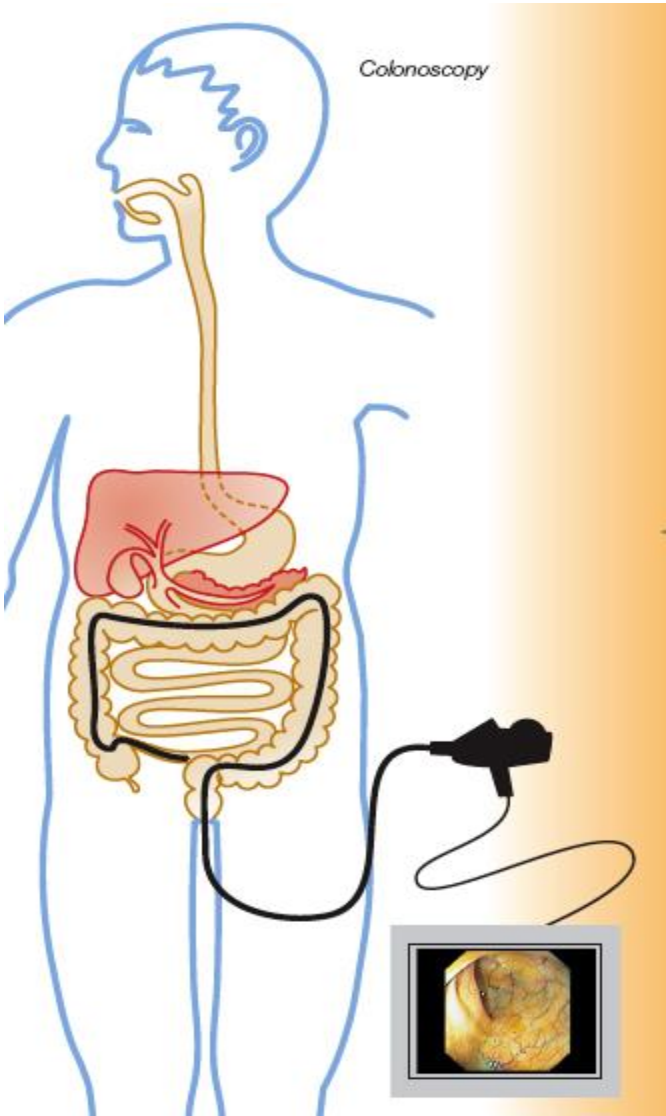

Growth of Brain tumour

3D image of brain helps to understand growth of tumour

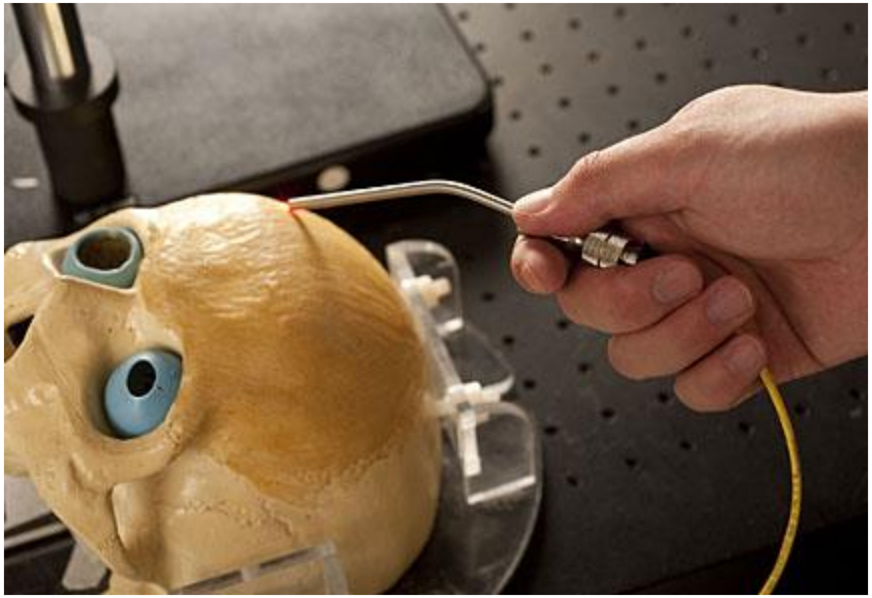

What is the structure for?

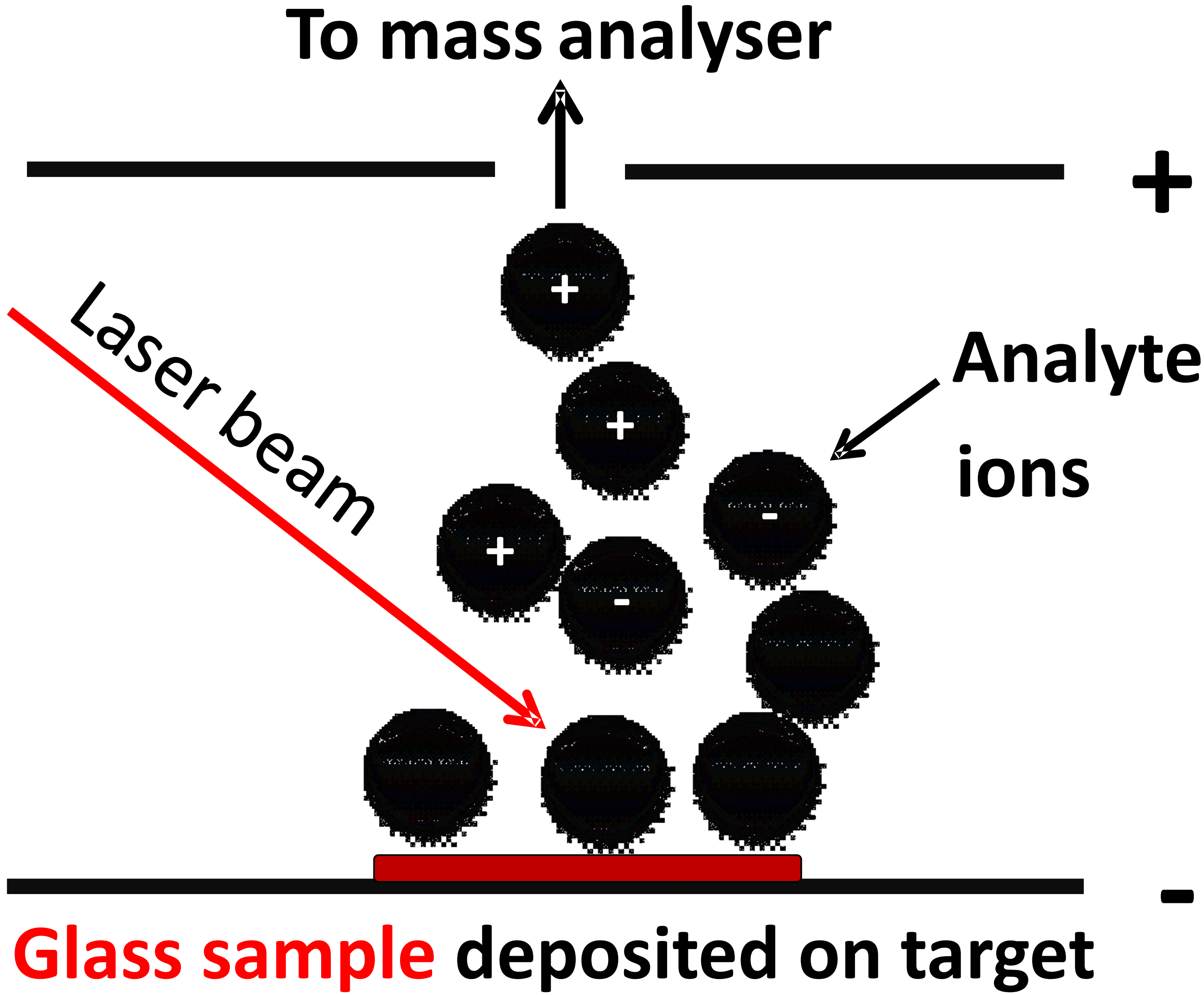
To mass analyser
+
Laser beam
Analyte
ions
+
+
+
-
-
-
Glass sample deposited on target

Isotopic envelope

Theoretical model

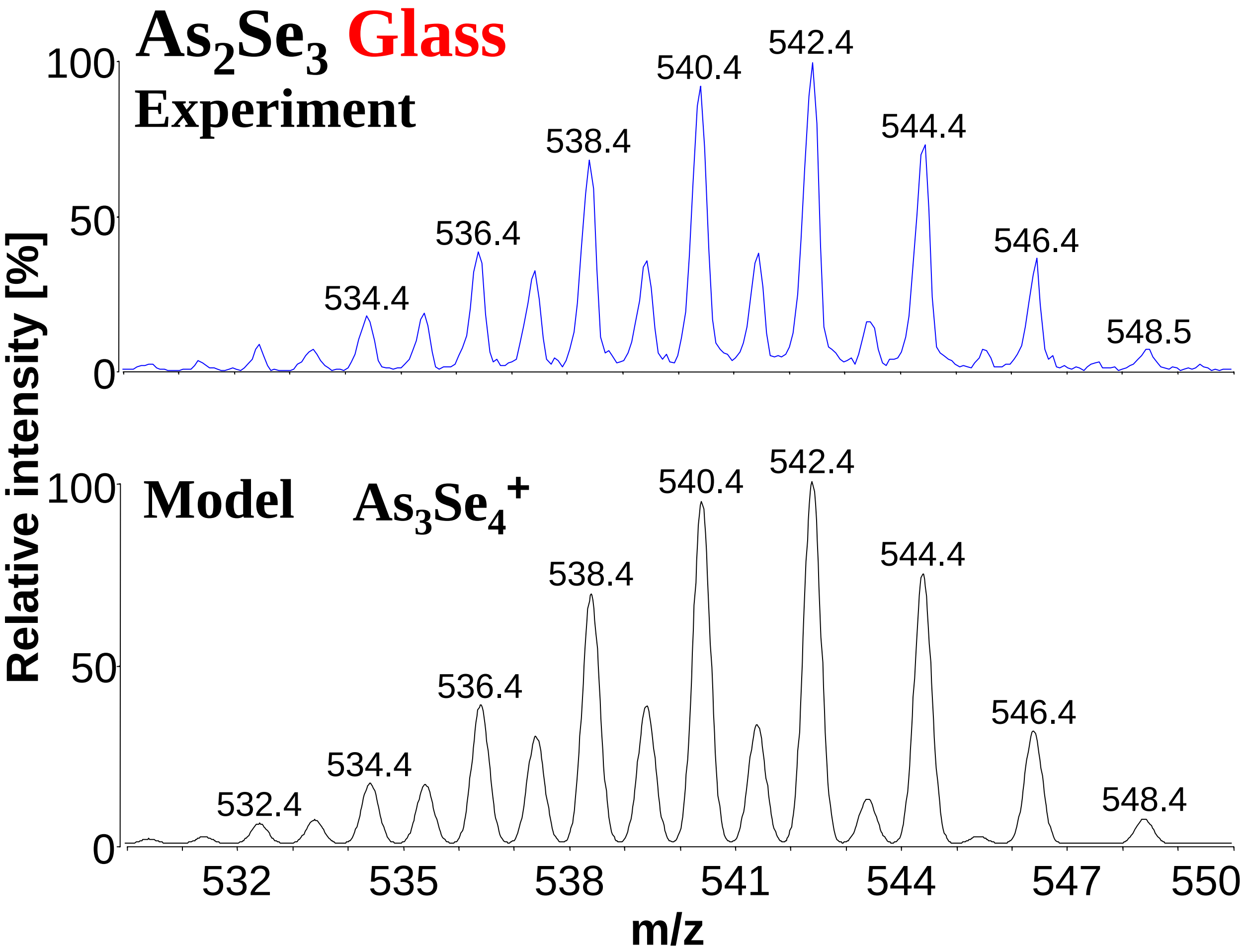

Composition of the glasses studied

As-Se

$AsSe_2$, As_2Se_3, As_4Se_4, As_4Se_3, and As_7Se_3

As-S-Se

$As_{33}S_{33.5}Se_{33.5}$, $As_{33}S_{50}Se_{17}$, and $As_{33}S_{17}Se_{50}$

$Ga_5Ge_{20}Sb_{10}S_{65}$

Er doping: 0.05, 0.1, 0.5 w.%

As_pSe_r: Glasses of the composition studied

- $AsSe_2$
- As_2Se_3

Selenium rich

- As_4Se_4 → 1:1

- As_4Se_3
- As_7Se_3

Arsenic rich

Effect of laser energy: As_7Se_3 Glass

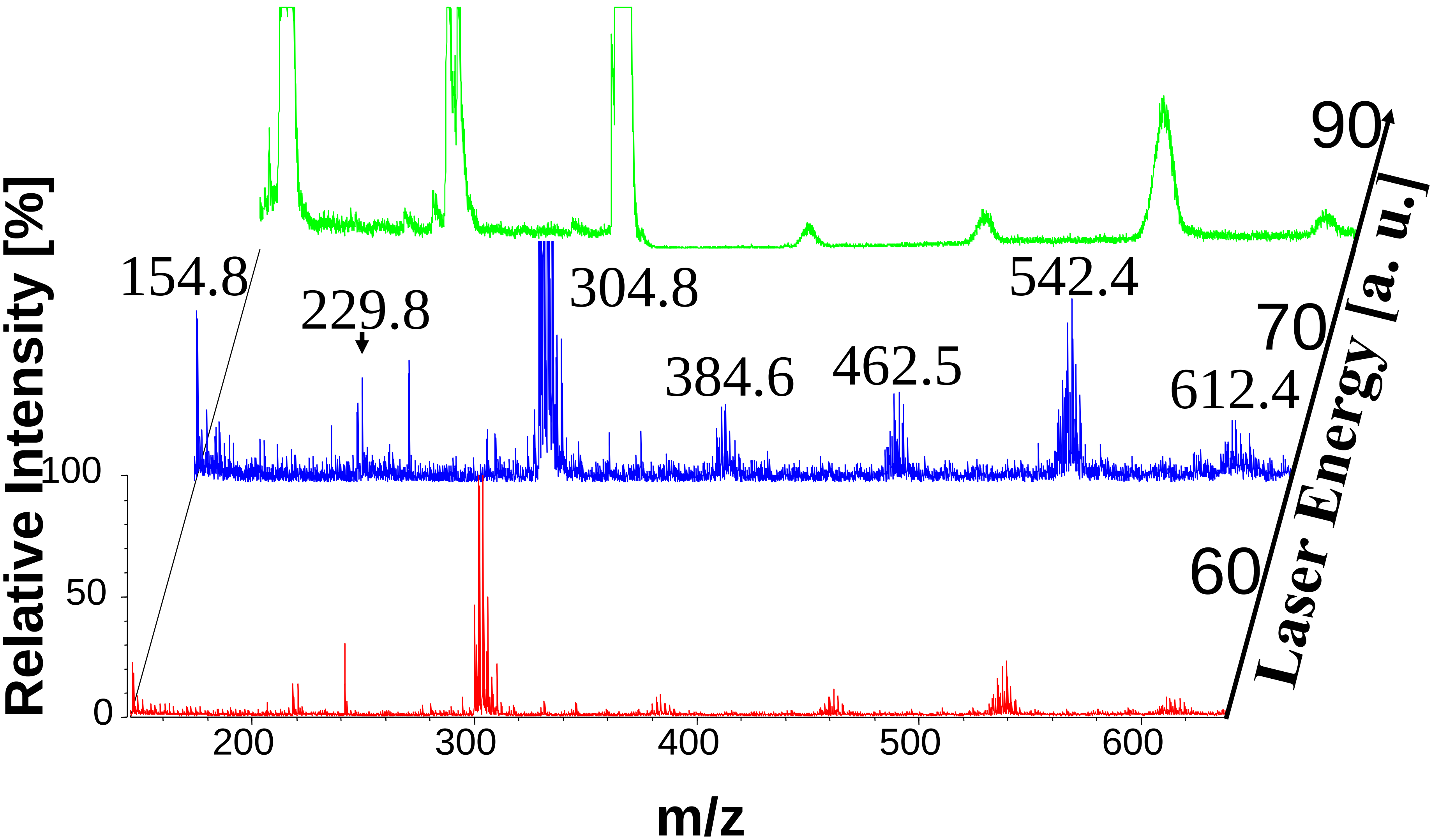

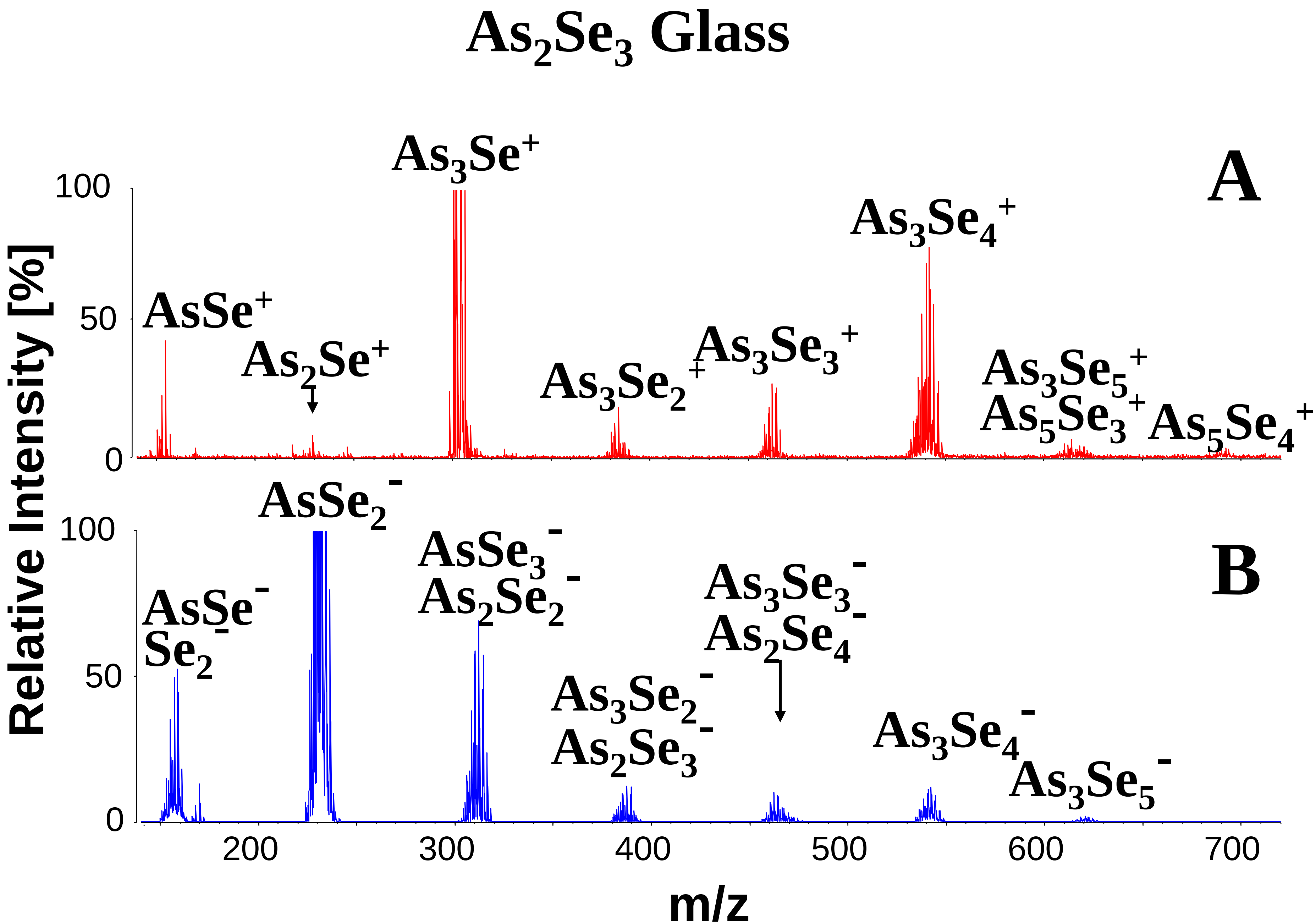

As2Se3 Glass
A
B
Relative Intensity [%]
m/z
100
50
0
AsSe+
As2Se+
As3Se+
As3Se2+
As3Se3+
As3Se4+
As3Se5+
As5Se3+
As5Se4+
AsSe-
Se2-
AsSe2-
AsSe3-
As2Se2-
As3Se2-
As2Se3-
As3Se3-
As2Se4-
As3Se4-
As3Se5-
200
300
400
500
600
700

Raman spectra for As-Se glasses

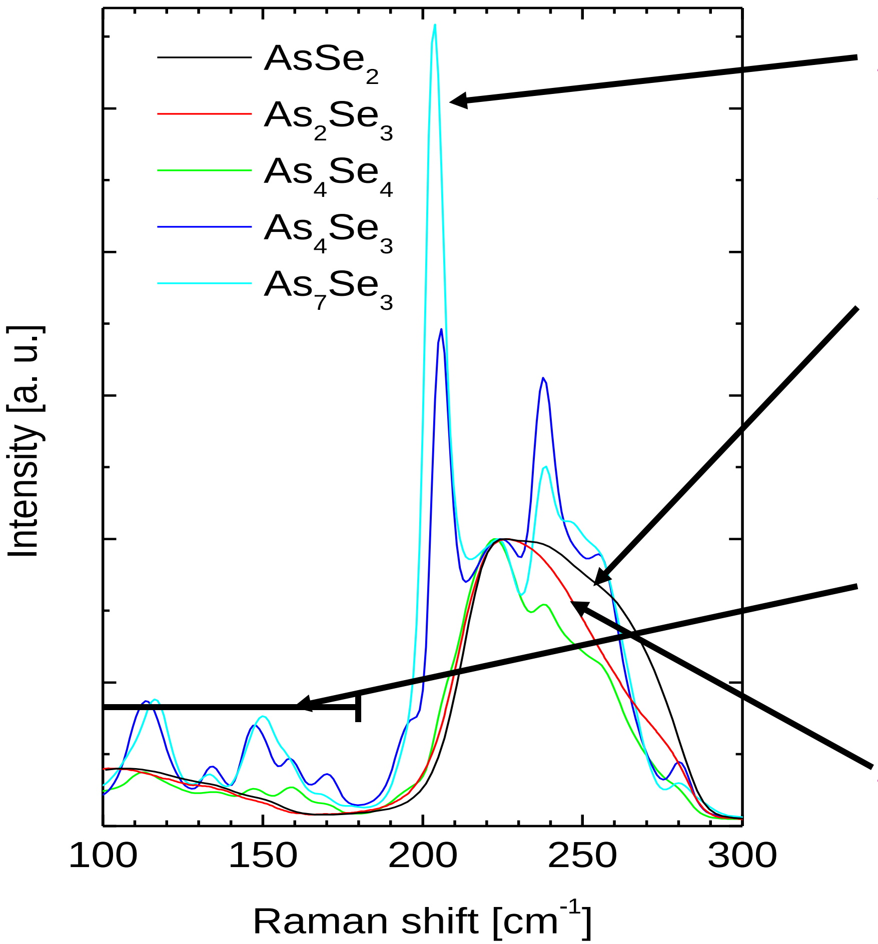

As rich glass (As_7Se_3): As_4 Raman band at 206 cm^{-1}
As_3Se, As_2Se_2

Se rich glass ($AsSe_2$): -Se-Se-Se- chains or $AsSe_3$ units, band at 238 cm^{-1}

As rich cage like structures As_4Se_4 and As_4Se_3

$AsSe_3$ pyramidal units (broad band at 220-230 cm^{-1})

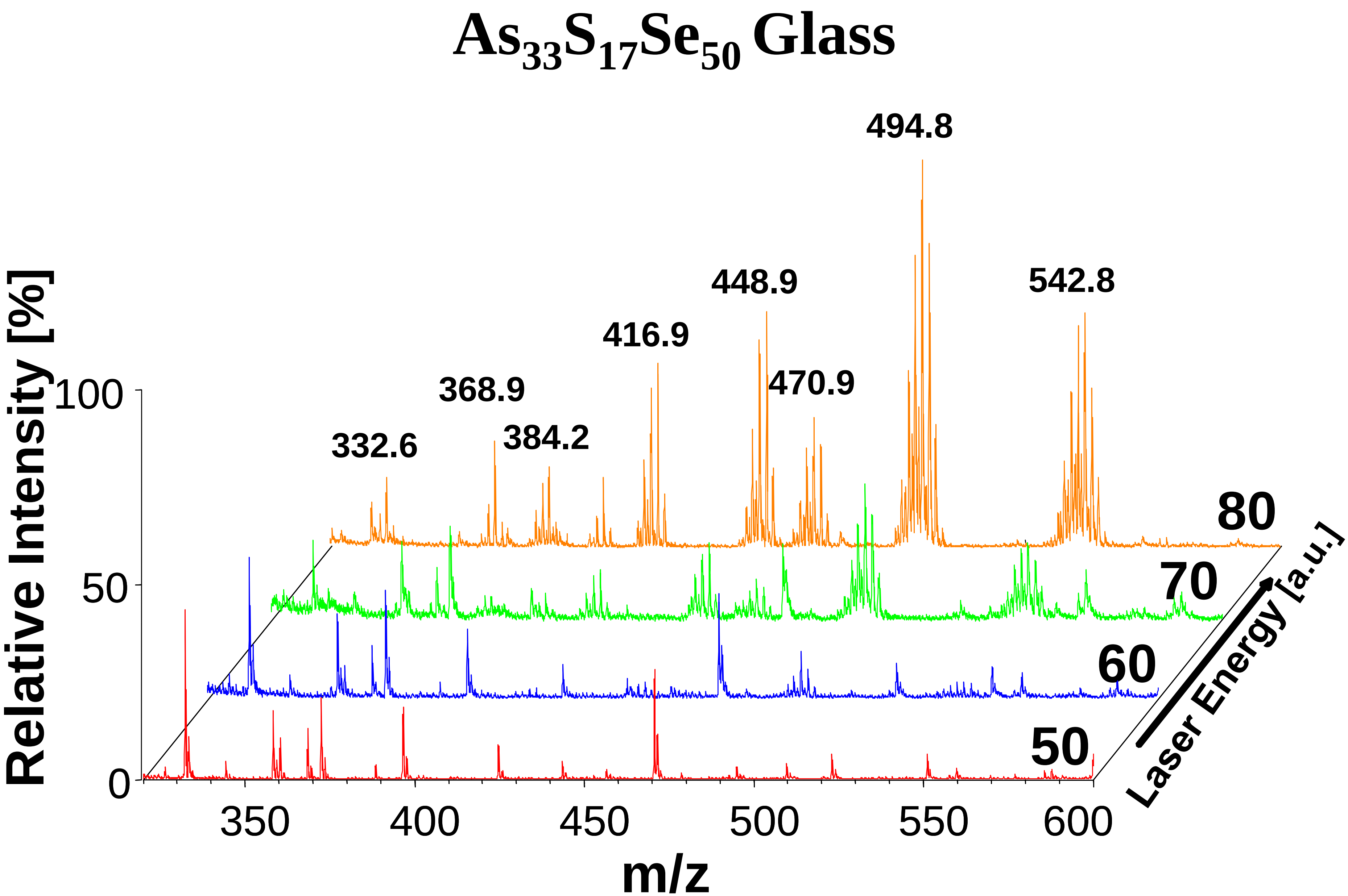

As$_{33}$S$_{17}$Se$_{50}$ Glass
494.8
448.9
542.8
416.9
470.9
368.9
332.6
384.2
100
50
0
Relative Intensity [%]
80
70
60
50
Laser Energy [a.u.]
350
400
450
500
550
600
m/z

$As_{33}S_{17}Se_{50}$ Glass

(A)

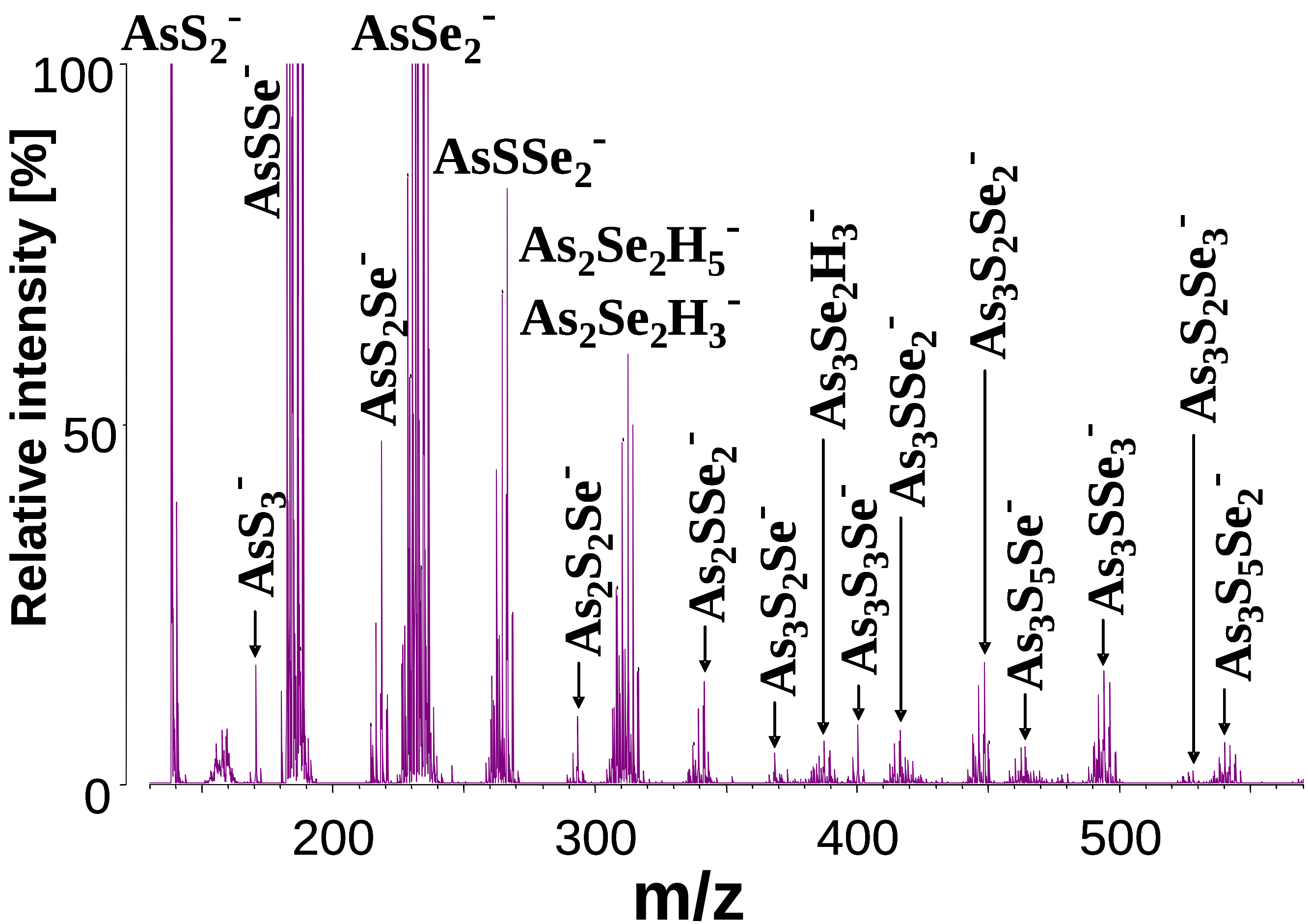

$As_{33}S_{33.5}Se_{33.5}$ glass

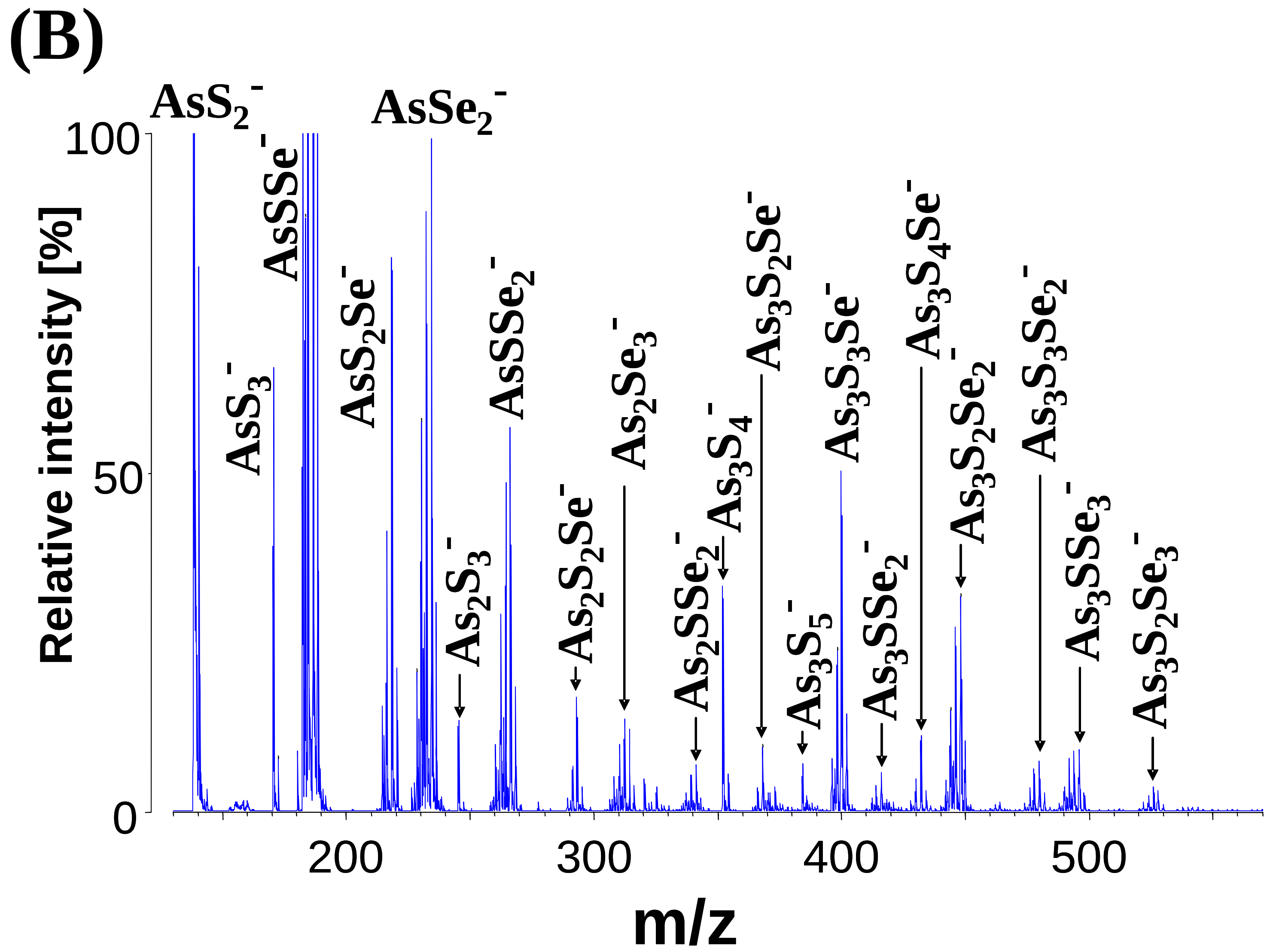

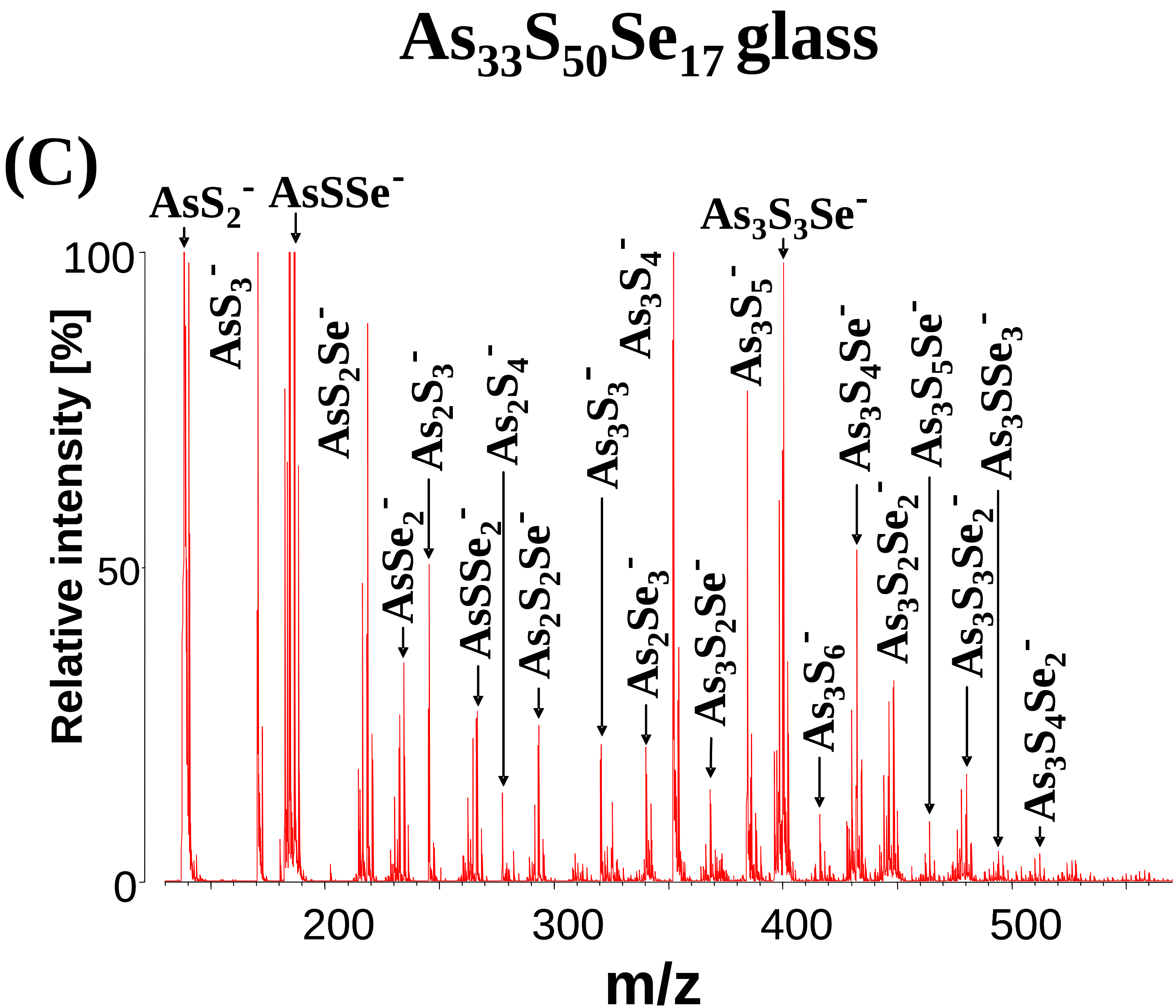

As33S50Se17 glass
(C)
AsS2-
AsSSe-
As3S3Se-
AsS3-
AsS2Se-
AsSe2-
As2S3-
AsSSe2-
As2S4-
As2S2Se-
As3S3-
As2Se3-
As3S4-
As3S2Se-
As3S5-
As3S6-
As3S4Se-
As3S2Se2-
As3S5Se-
As3S3Se2-
As3SSe3-
As3S4Se2-
Relative intensity [%]
100
50
0
200
300
400
500
m/z

$As_{33}S_{17}Se_{50}$ Glass

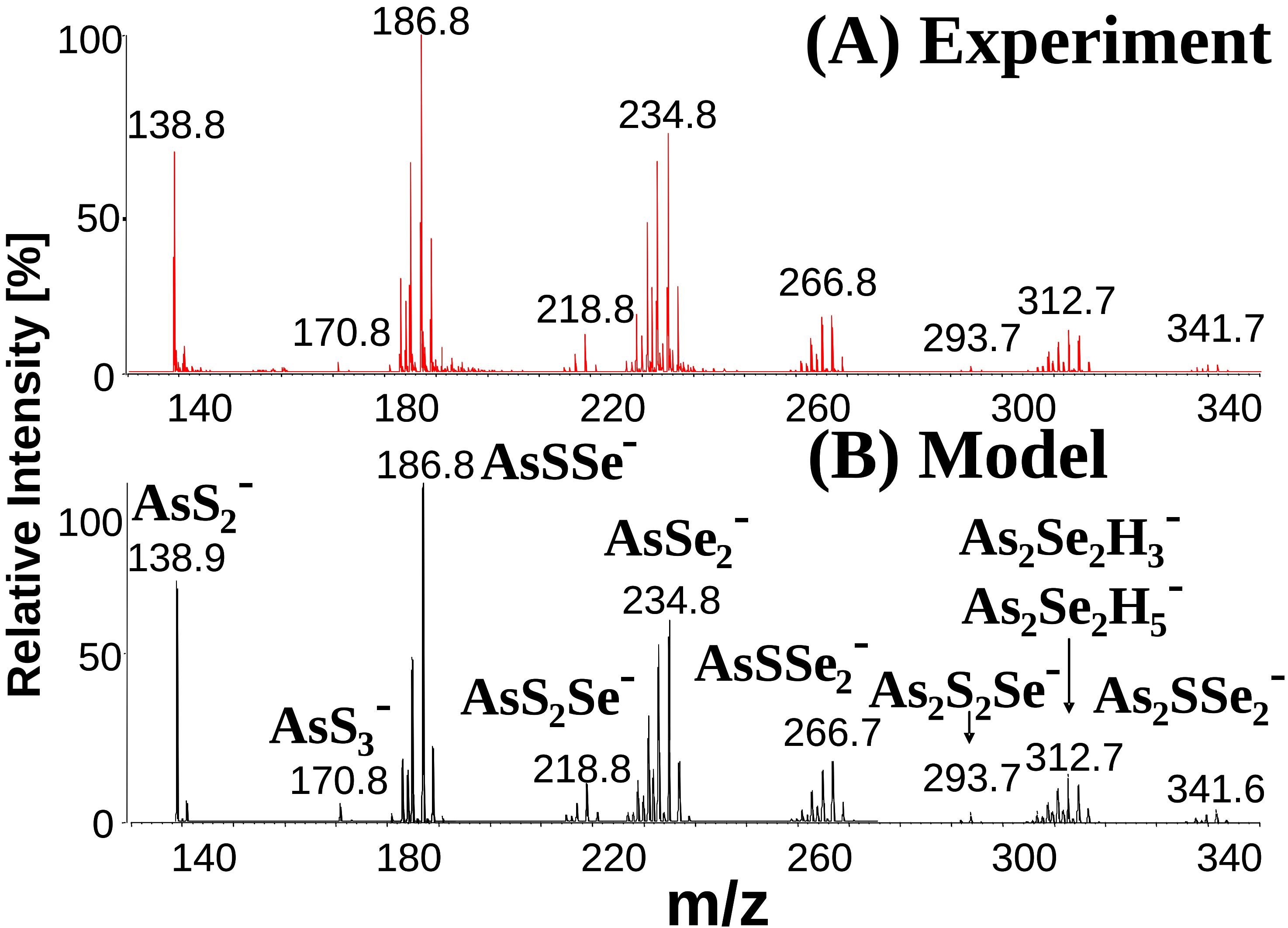

Clusters common to all samples

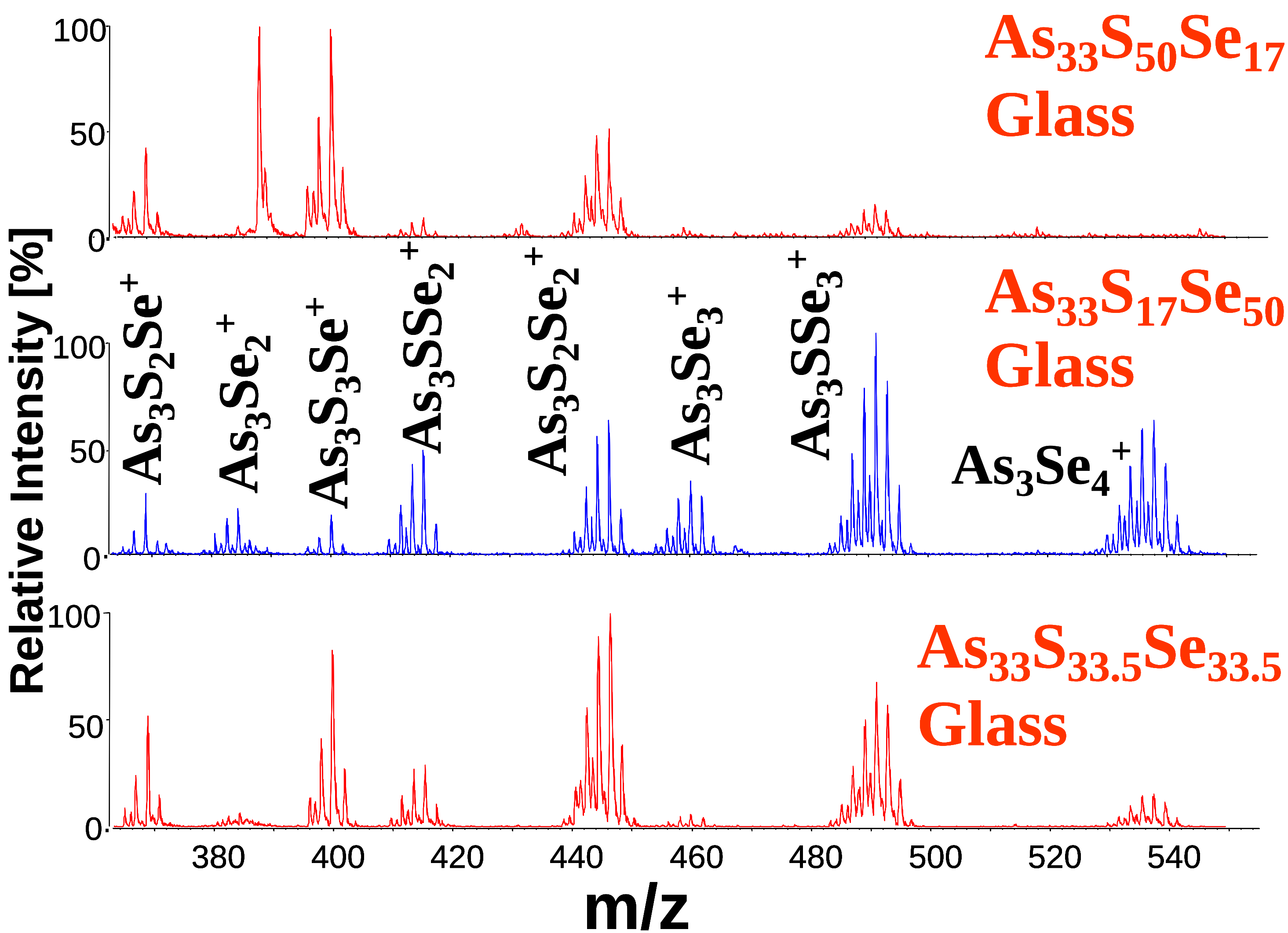

Spectra of bulk and nano layer of glasses

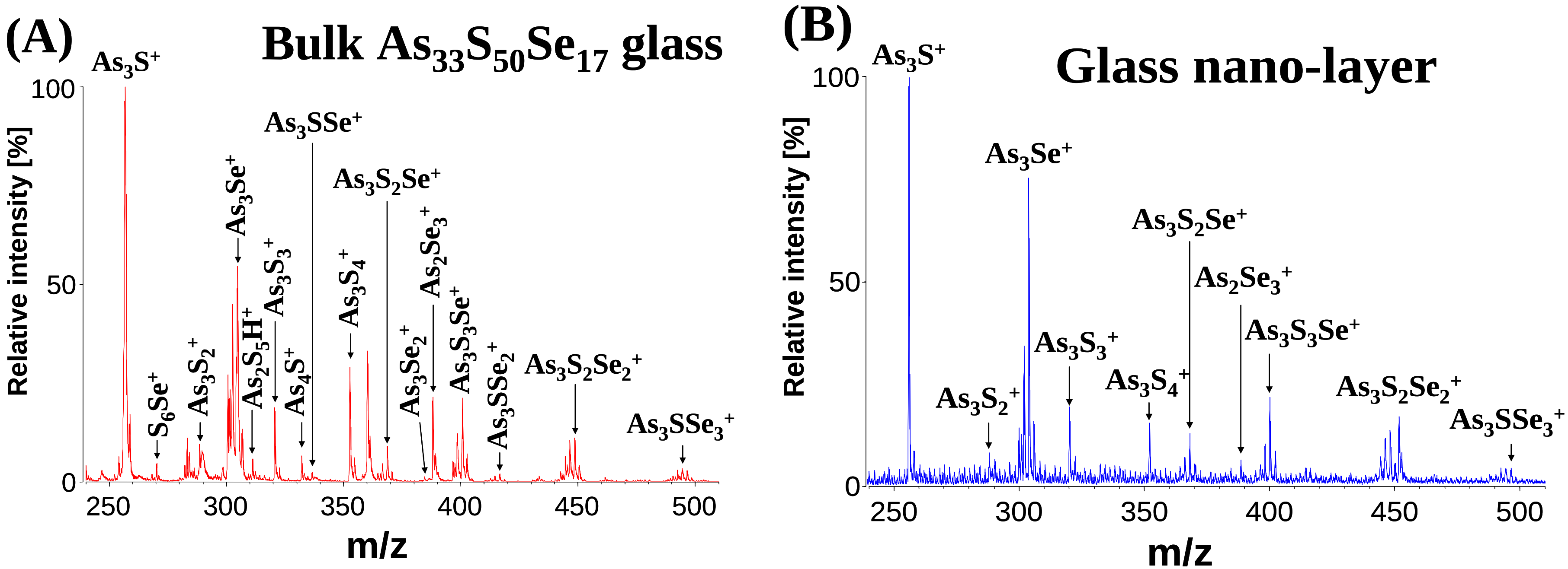

Er Doped glass: Ga-Ge-Sb-S

Erbium doped $Ga_5Ge_{25}Sb_{10}S_{60}$ glass

1. Suitable thermo-mechanical properties for optical fibre drawing

2. Gallium allows better solubilisation of erbium ions

3. Erbium posses mid-IR emission around 4.5 µm
   IR emissions beyond 3 µm are scarcely reported using other rare earth elements (Terbium, Dysprosium, Holmium, Thulium, etc).

$Ga_5Ge_{20}Sb_{10}S_{65}$ glass

Er doping: 0.05, 0.1, 0.5 w.%

- Strong luminescence
- Laser action

} Fiber amplifier and near/mid infrared laser devices

- IR emission at std telecommunication wavelength ~1540 nm

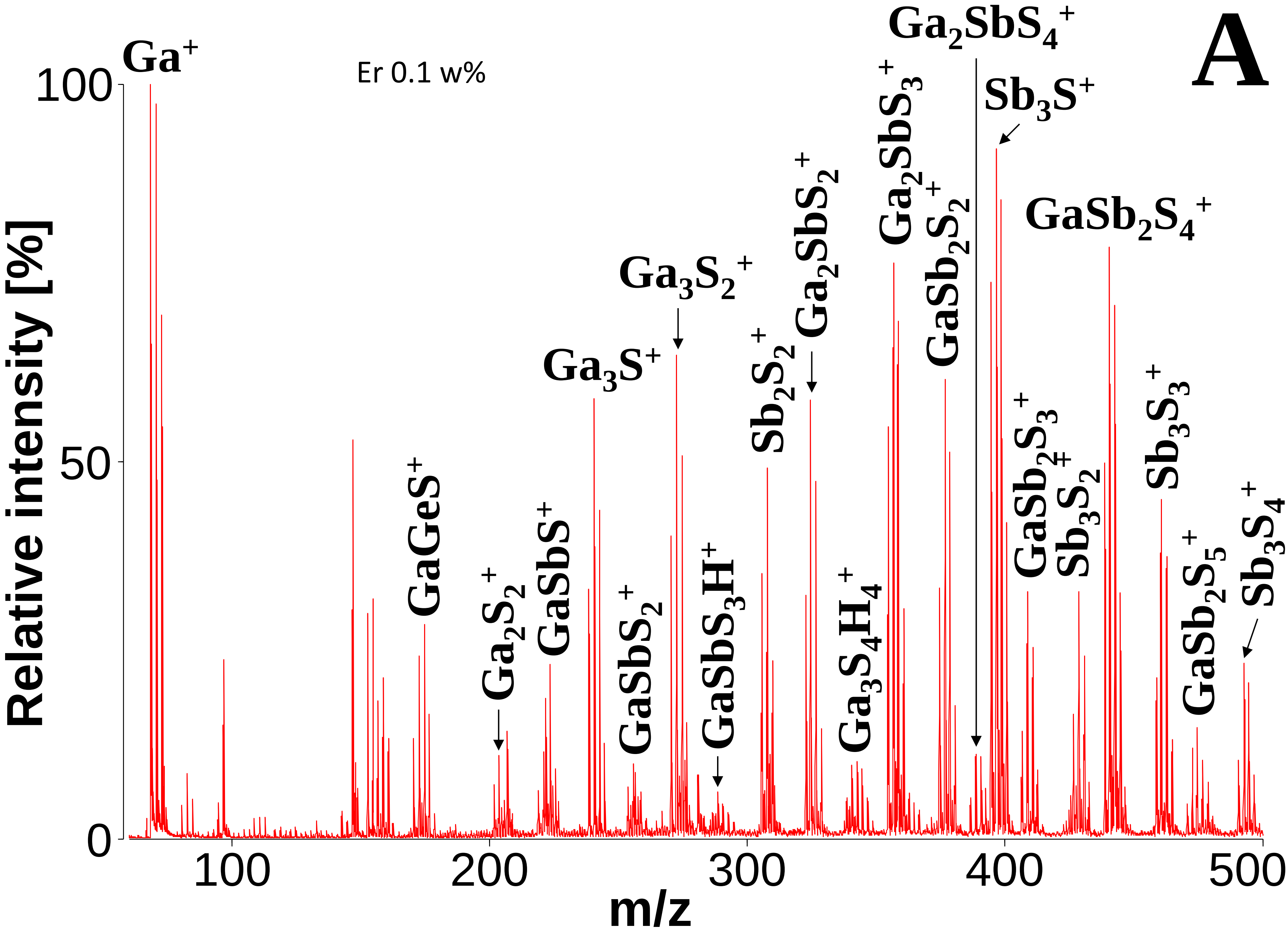
A
Er 0.1 w%
Relative intensity [%]
m/z
0
50
100
100
200
300
400
500
Ga+
GaGeS+
Ga2S2+
GaSbS+
Ga3S+
GaSbS2+
Ga3S2+
GaSbS3H+
Sb2S2+
Ga2SbS2+
Ga3S4H4+
Ga2SbS3+
GaSb2S2+
Ga2SbS4+
Sb3S+
GaSb2S3+
Sb3S2+
GaSb2S4+
Sb3S3+
GaSb2S5+
Sb3S4+

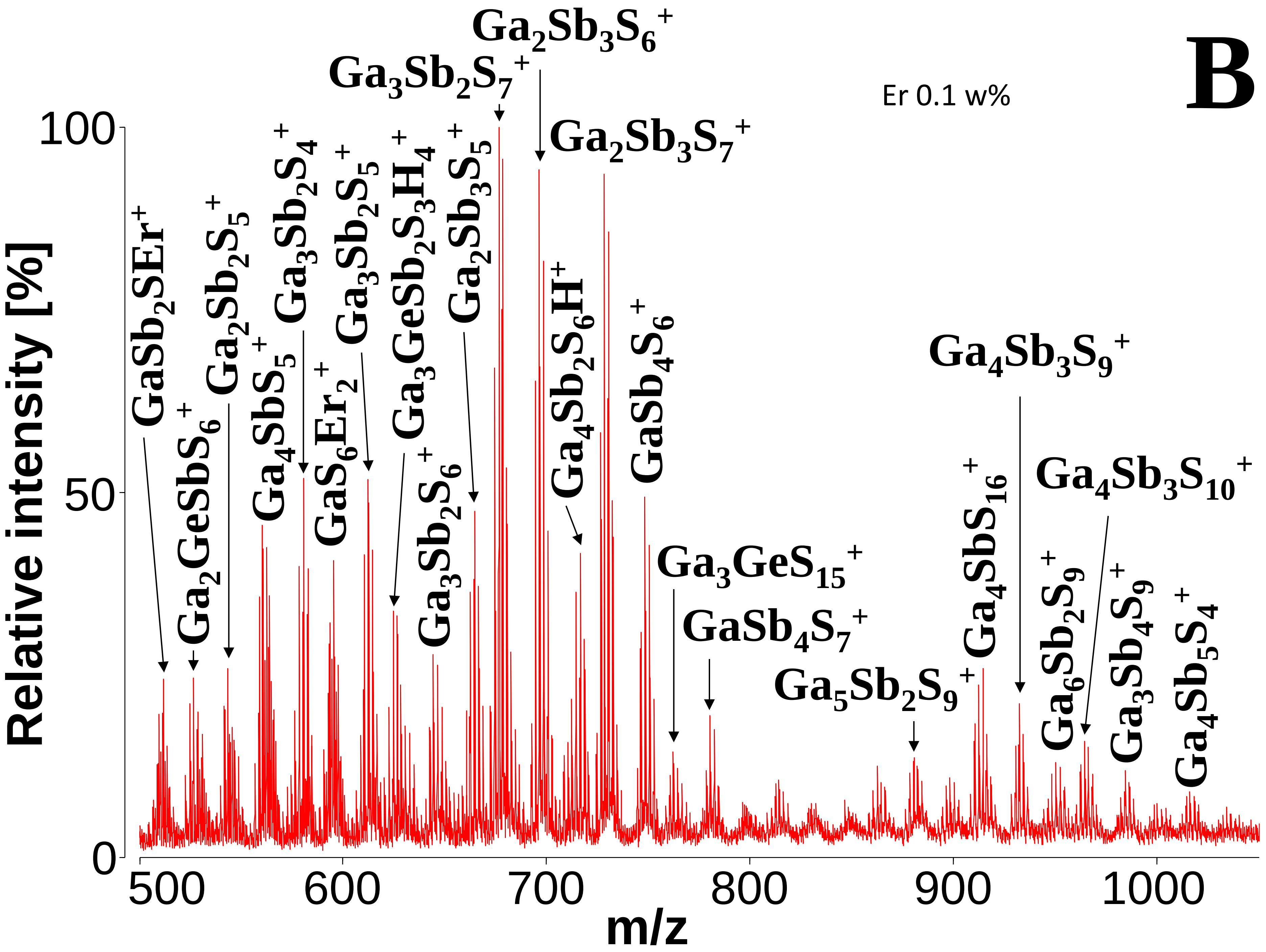

B
Er 0.1 w%
Relative intensity [%]
m/z
100
50
0
500
600
700
800
900
1000
$Ga_2Sb_3S_6^+$
$Ga_3Sb_2S_7^+$
$Ga_2Sb_3S_7^+$
$GaSb_2SEr^+$
$Ga_2GeSbS_6^+$
$Ga_2Sb_2S_5^+$
$Ga_4SbS_5^+$
$Ga_3Sb_2S_4^+$
$GaS_6Er_2^+$
$Ga_3Sb_2S_5^+$
$Ga_3GeSb_2S_3H_4^+$
$Ga_3Sb_2S_6^+$
$Ga_2Sb_3S_5^+$
$Ga_4Sb_2S_6H^+$
$GaSb_4S_6^+$
$Ga_3GeS_{15}^+$
$GaSb_4S_7^+$
$Ga_5Sb_2S_9^+$
$Ga_4SbS_{16}^+$
$Ga_4Sb_3S_9^+$
$Ga_4Sb_3S_{10}^+$
$Ga_6Sb_2S_9^+$
$Ga_3Sb_4S_9^+$
$Ga_4Sb_5S_4^+$

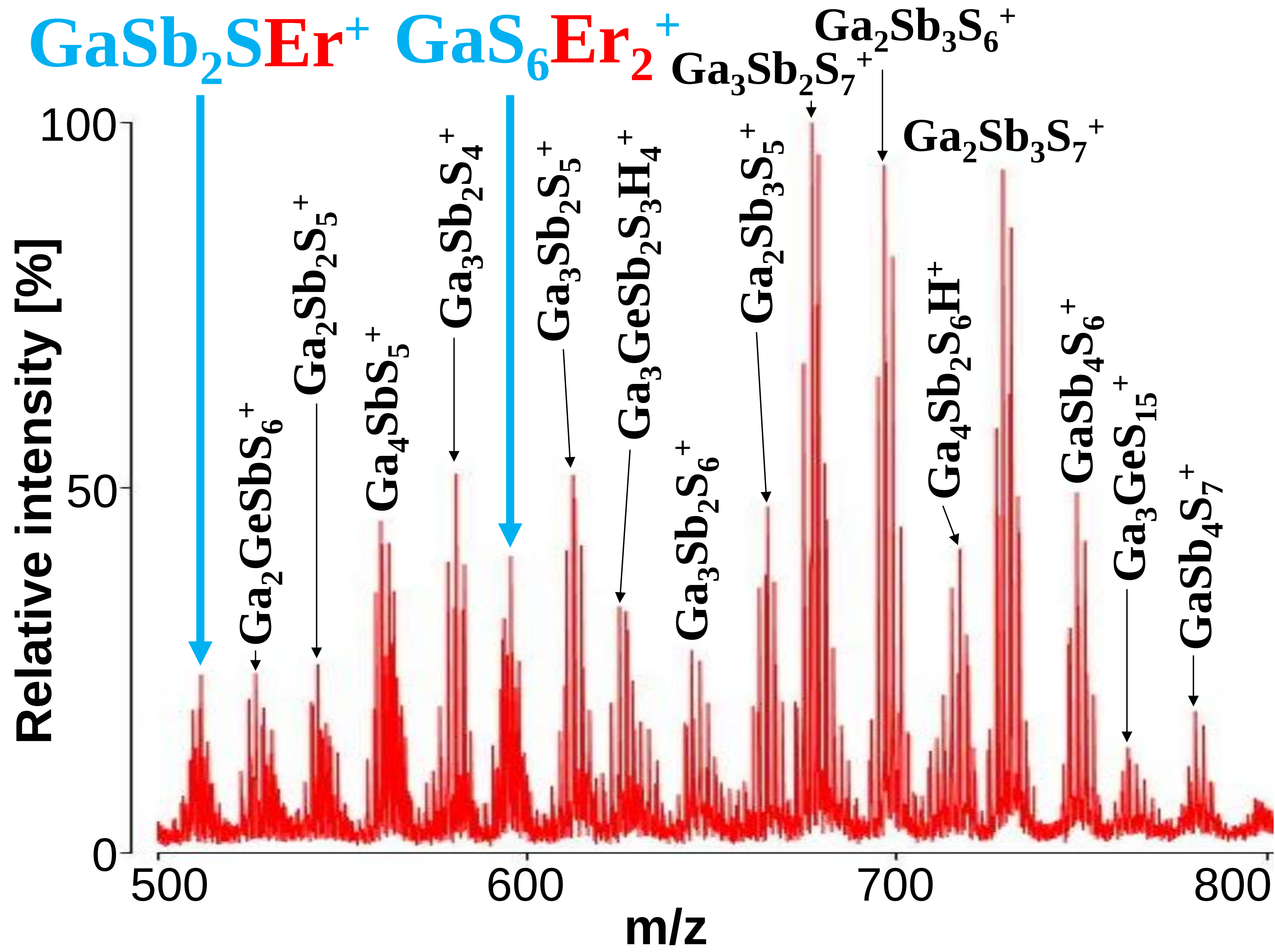

GaSb2SEr+
GaS6Er2+
Ga2Sb3S6+
Ga3Sb2S7+
Ga2Sb3S7+
Relative intensity [%]
100
50
0
Ga2GeSbS6+
Ga2Sb2S5+
Ga4SbS5+
Ga3Sb2S4+
Ga3Sb2S5+
Ga3GeSb2S3H4+
Ga3Sb2S6+
Ga2Sb3S5+
Ga4Sb2S6H+
GaSb4S6+
Ga3GeS15+
GaSb4S7+
500
600
700
800
m/z

$Ga_5Ge_{20}Sb_{10}S_{65}$ glass Er 0.1 w.%

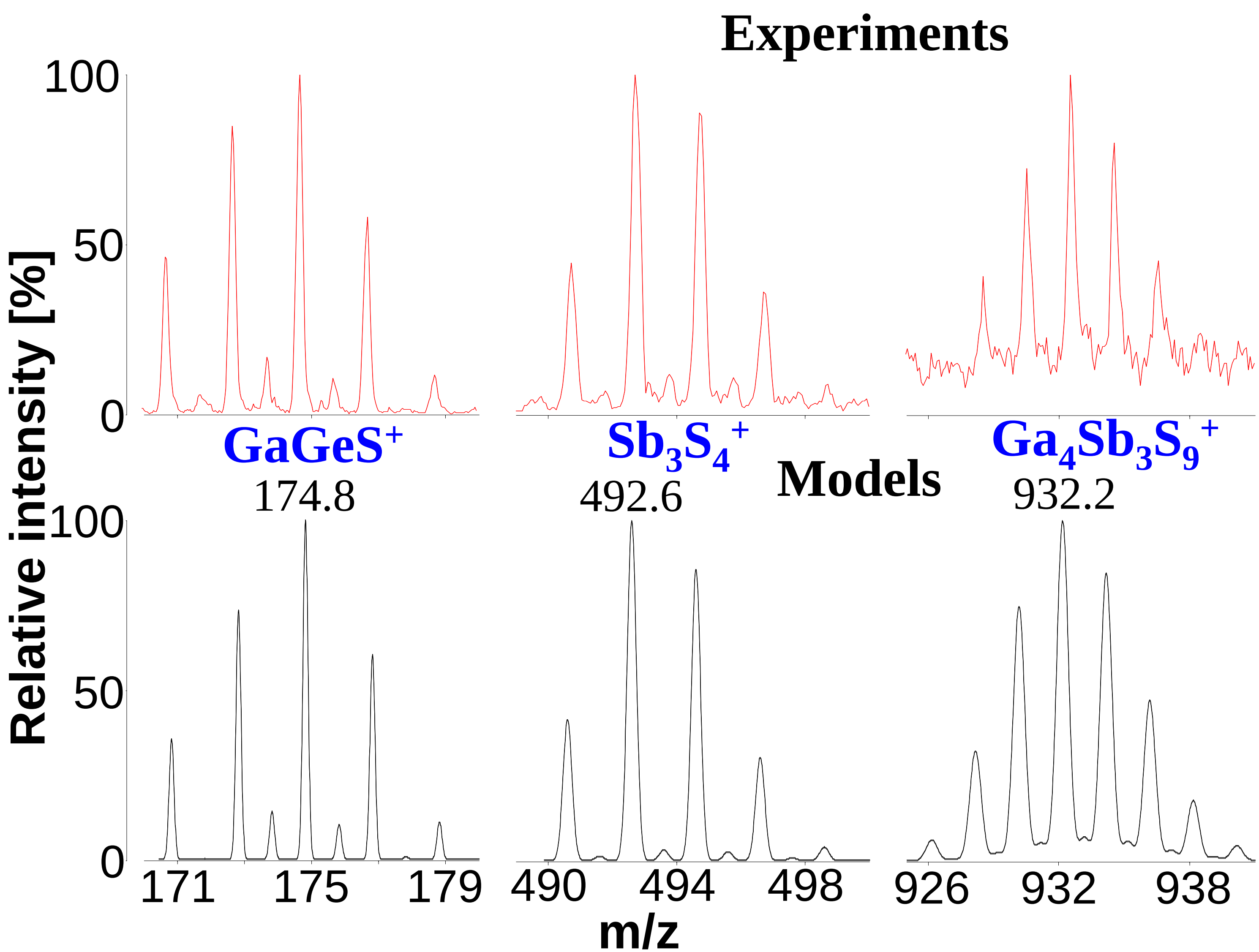

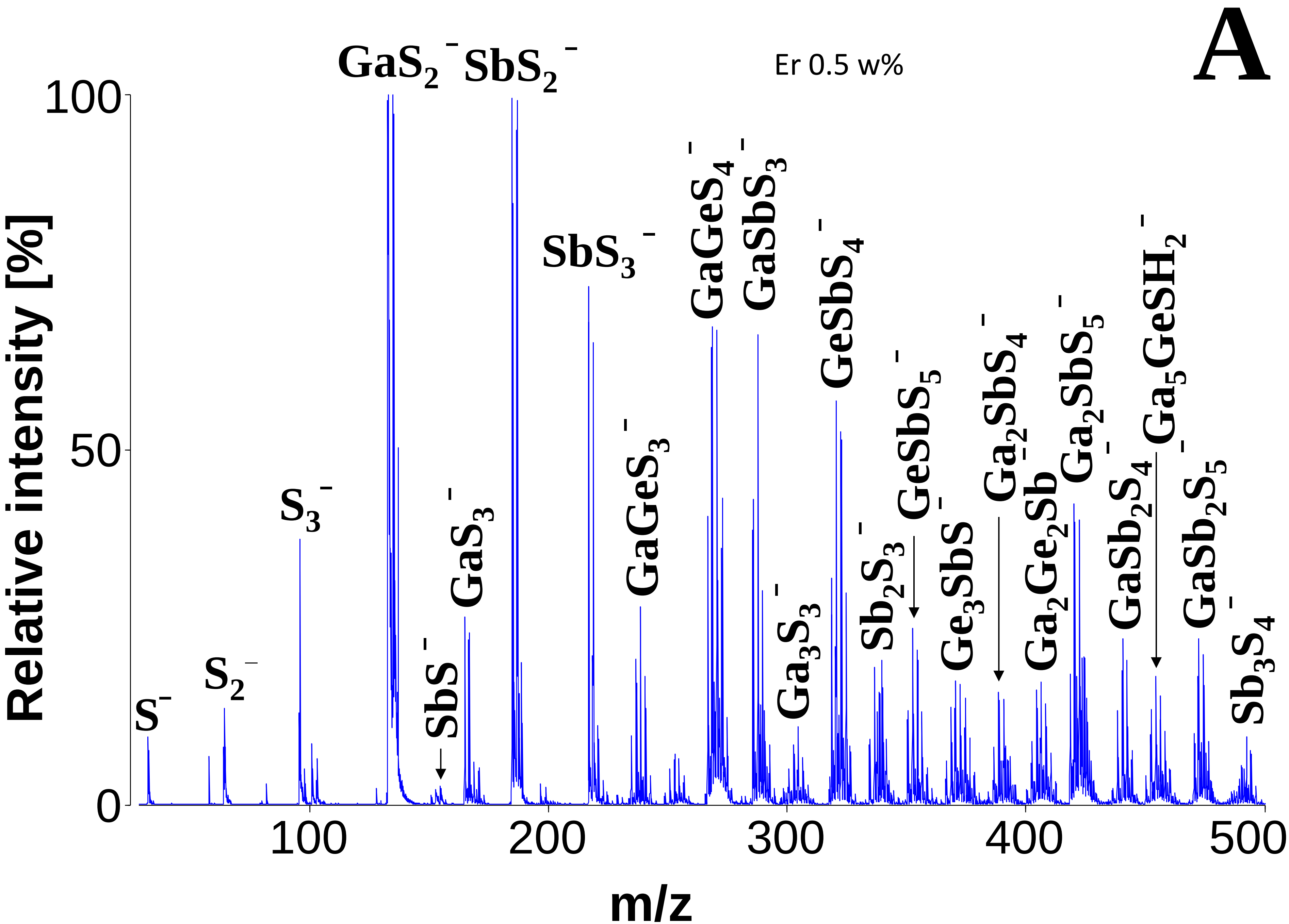

A
Er 0.5 w%
Relative intensity [%]
m/z
100
50
0
100
200
300
400
500
S⁻
S2⁻
S3⁻
GaS2⁻
SbS2⁻
SbS⁻
GaS3⁻
SbS3⁻
GaGeS3⁻
GaGeS4⁻
GaSbS3⁻
Ga3S3⁻
GeSbS4⁻
Sb2S3⁻
GeSbS5⁻
Ge3SbS⁻
Ga2SbS4⁻
Ga2Ge2Sb⁻
Ga2SbS5⁻
GaSb2S4⁻
Ga5GeSH2⁻
GaSb2S5⁻
Sb3S4⁻

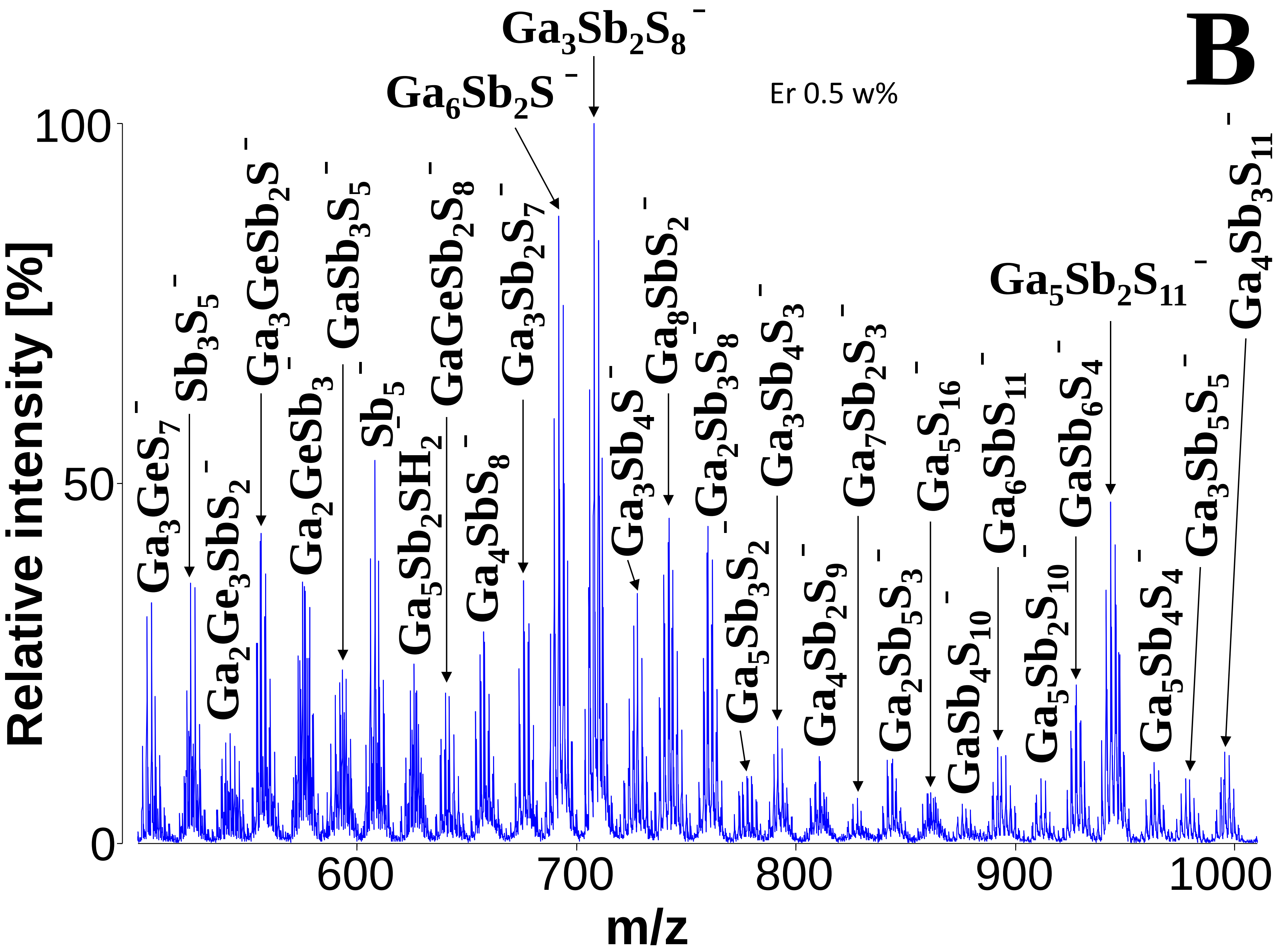
B
Er 0.5 w%
$Ga_3Sb_2S_8^-$
$Ga_6Sb_2S^-$
$Ga_3GeS_7^-$
$Sb_3S_5^-$
$Ga_2Ge_3SbS_2^-$
$Ga_3GeSb_2S^-$
$Ga_2GeSb_3^-$
$GaSb_3S_5^-$
Sb_5^-
$Ga_5Sb_2SH_2^-$
$GaGeSb_2S_8^-$
$Ga_4SbS_8^-$
$Ga_3Sb_2S_7^-$
$Ga_3Sb_4S^-$
$Ga_8SbS_2^-$
$Ga_2Sb_3S_8^-$
$Ga_5Sb_3S_2^-$
$Ga_3Sb_4S_3^-$
$Ga_4Sb_2S_9^-$
$Ga_7Sb_2S_3^-$
$Ga_2Sb_5S_3^-$
$Ga_5S_{16}^-$
$GaSb_4S_{10}^-$
$Ga_6SbS_{11}^-$
$Ga_5Sb_2S_{10}^-$
$GaSb_6S_4^-$
$Ga_5Sb_2S_{11}^-$
$Ga_3Sb_5S_5^-$
$Ga_5Sb_4S_4^-$
$Ga_4Sb_3S_{11}^-$
Relative intensity [%]
100
50
0
600
700
800
900
1000
m/z

$Ga_5Ge_{20}Sb_{10}S_{65}$ glass Er 0.5 w.%

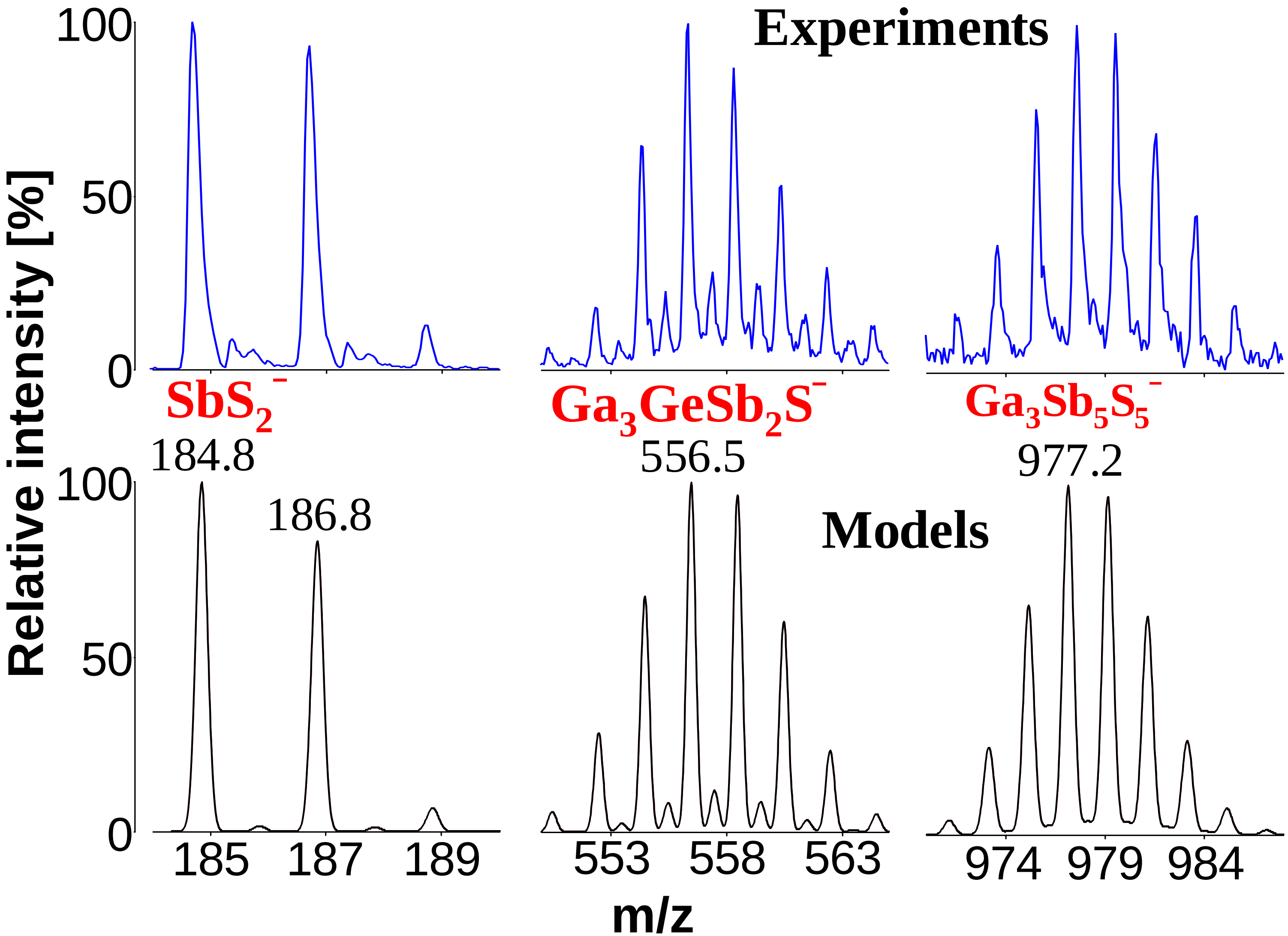

Raman Spectra

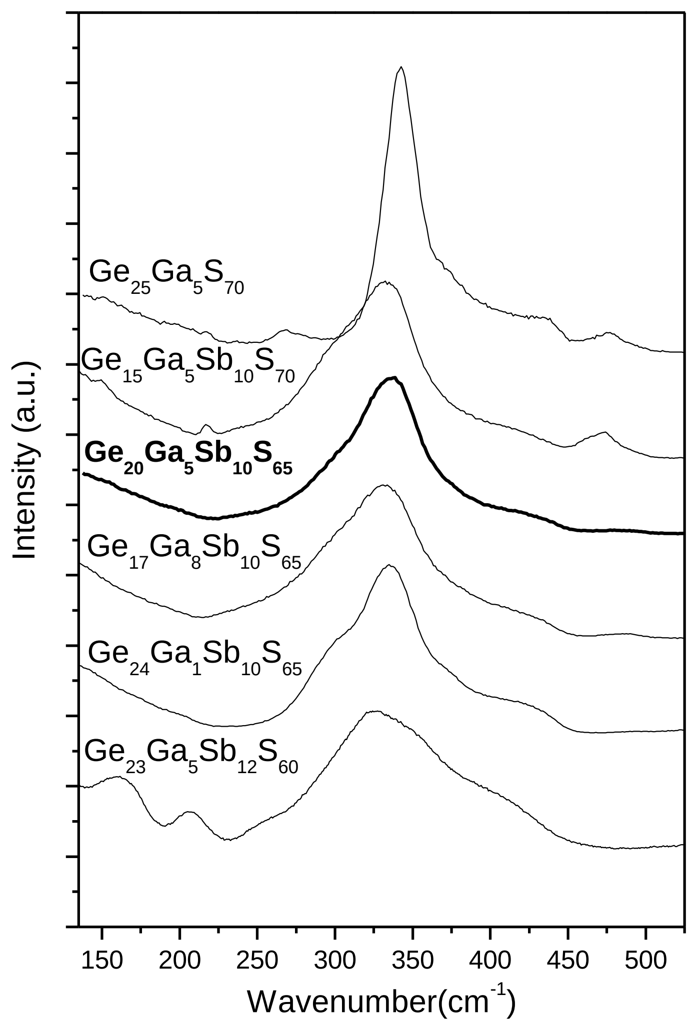

[$GeS_{4/2}$] tetrahedra

~330-340 cm^{-1}

[$GaS_{4/2}$] tetrahedra

~320 cm^{-1}

[$SbS_{3/2}$] pyramids

~290-300 cm^{-1}

STRUCTURE of CLUSTERS

Structures: series of clusters
Arsenic:chalcogen = 3:3 and 3:4

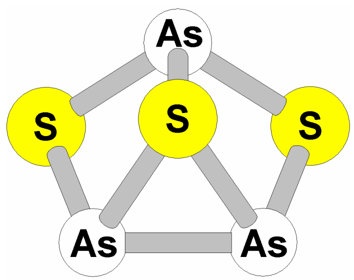

$As_3S_3^+$

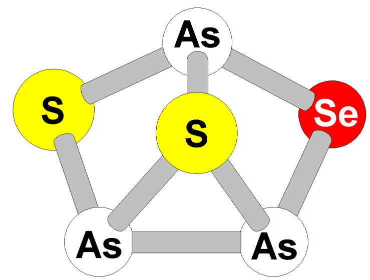

$As_3S_2Se^+$

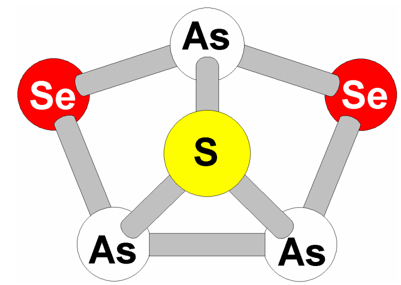

$As_3SSe_2^+$

Structures: series of clusters
Arsenic:chalcogen = 3:3 and 3:4

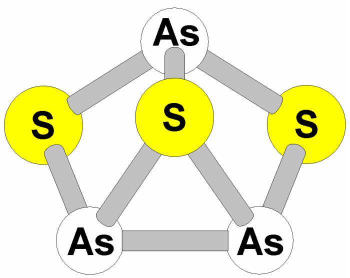

$As_3S_3^+$

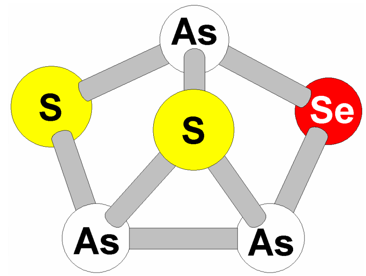

$As_3S_2Se^+$

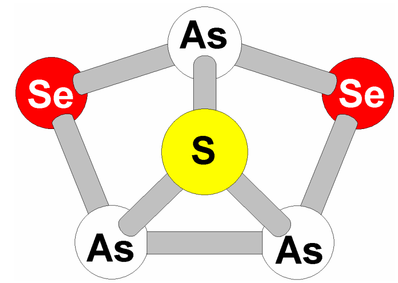

$As_3SSe_2^+$

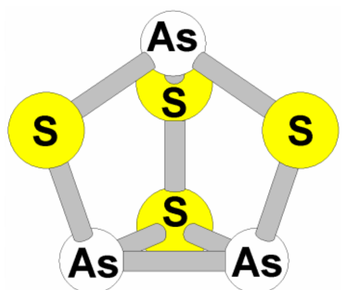

$As_3S_4^+$

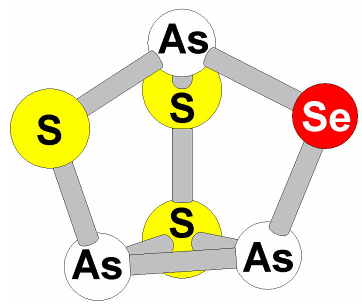

$As_3S_3Se^+$

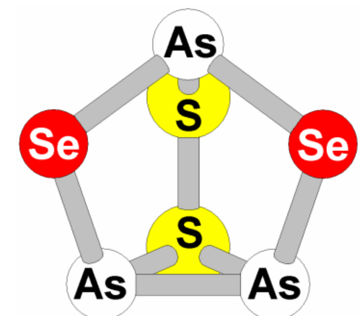

$As_3S_2Se_2^+$

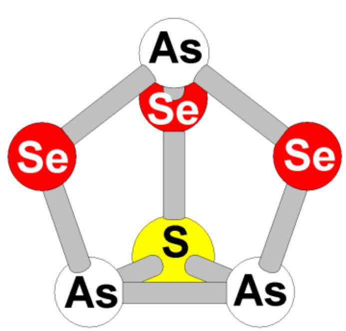

$As_3SSe_3^+$

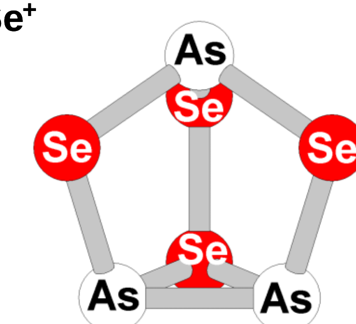

$As_3Se_4^+$

Mass spectra of a mixture (1:1) of As_2S_3 and S_8 as precursors

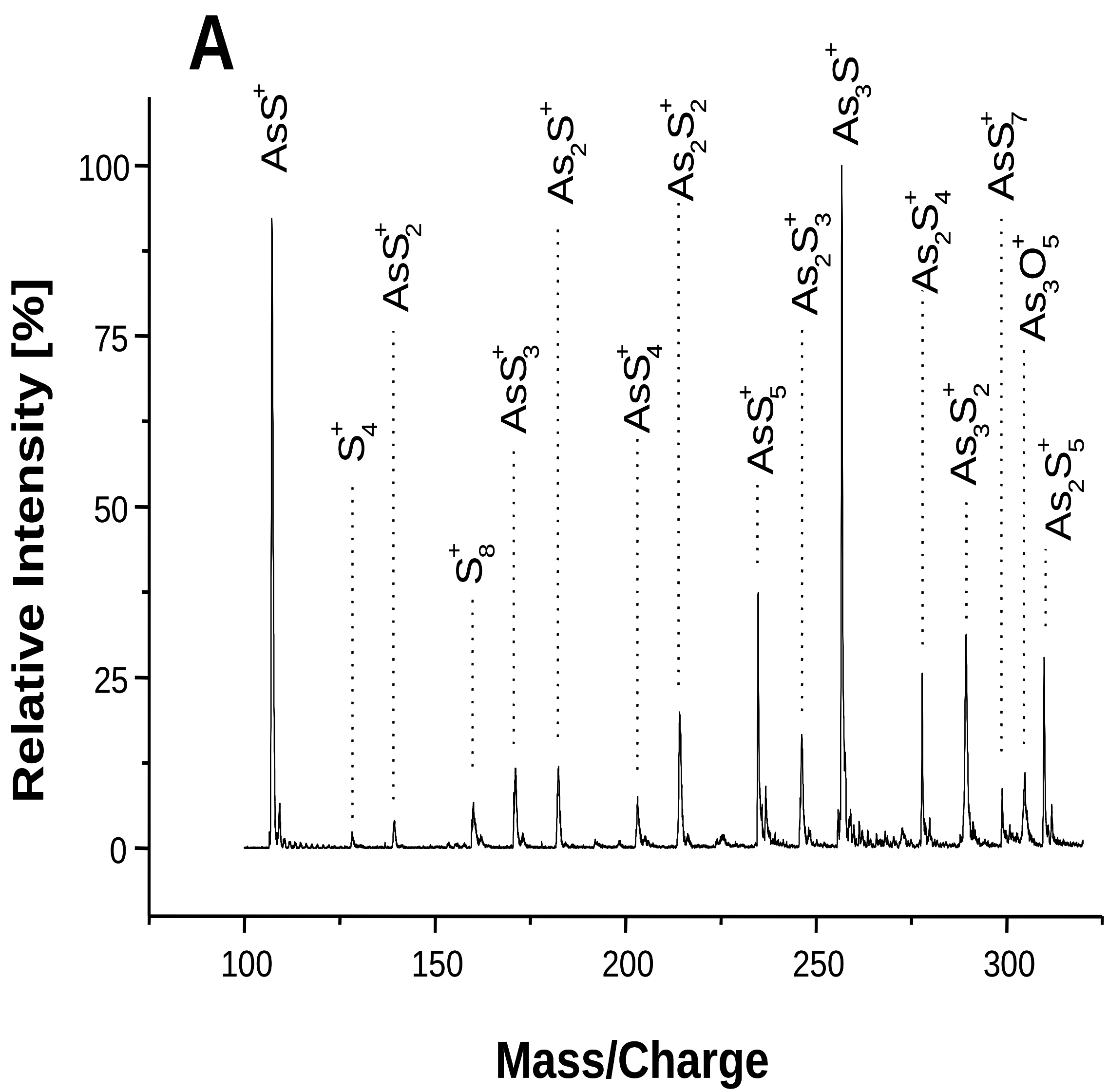

Mass spectra of a mixture (1:1) of As_2S_3 and S_8 as precursors

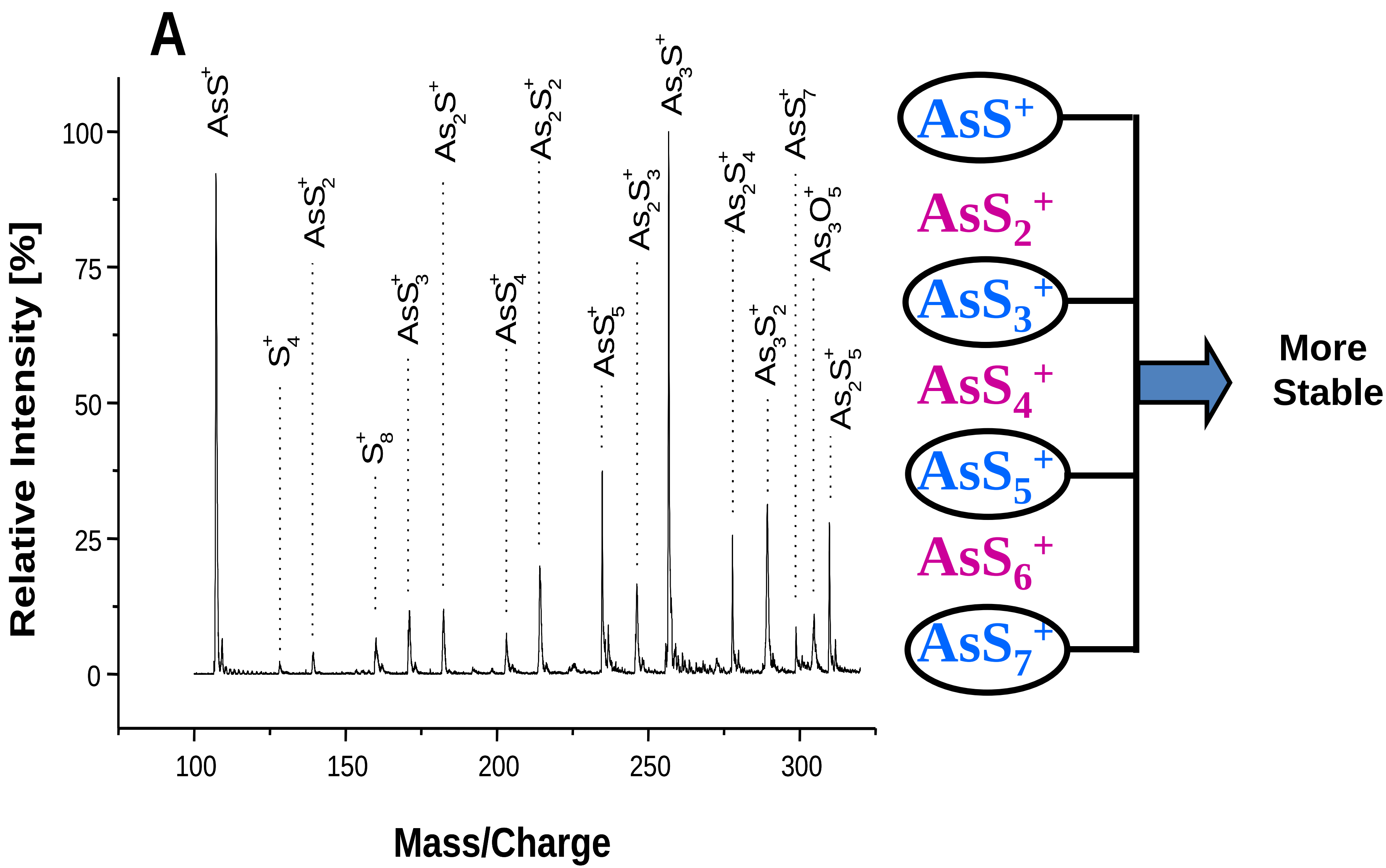

Comparison of theoretical and experimental mass spectra of AsS_7^+

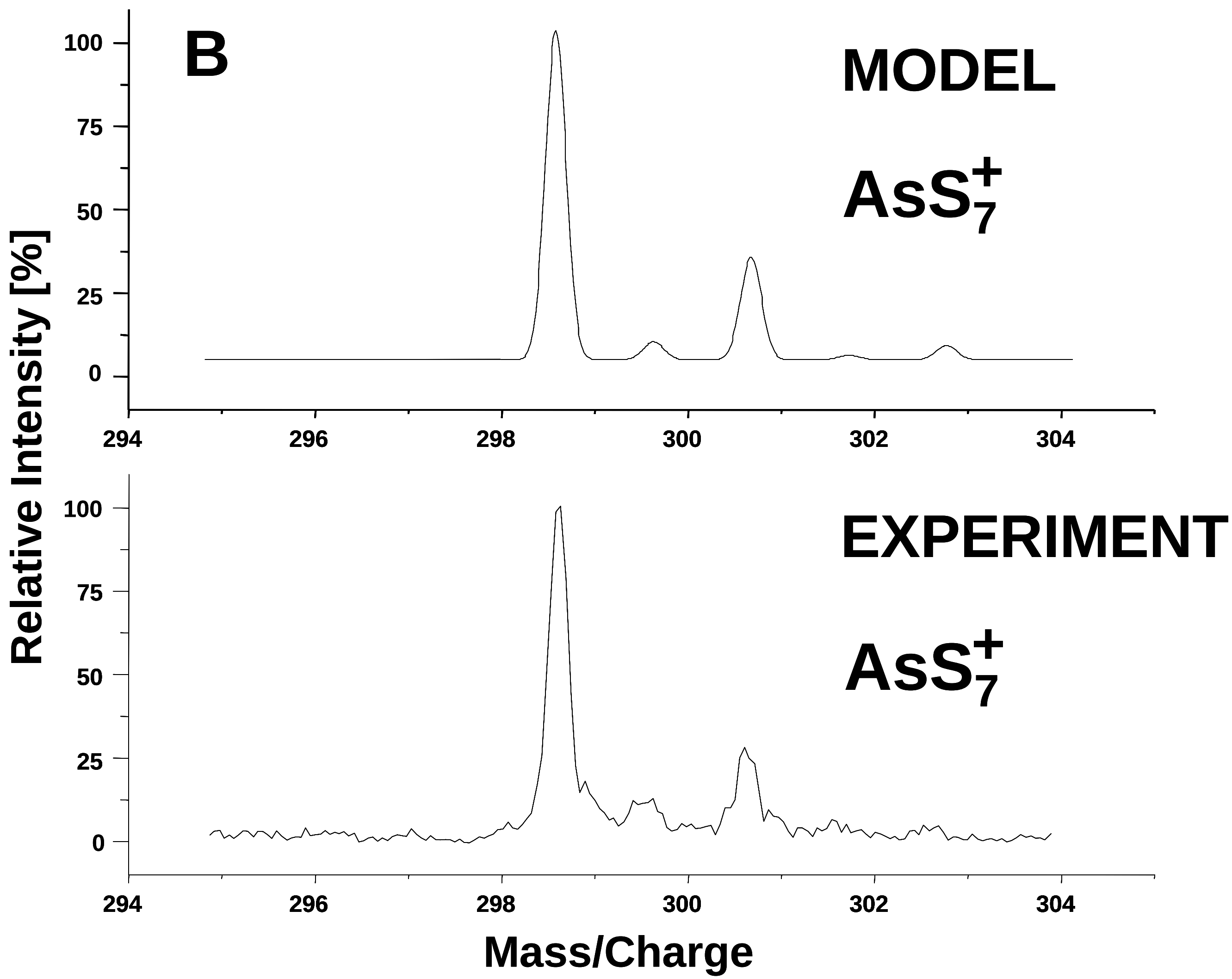

Some structures of AsS_n (n=1-7) clusters were demonstrated by QUANTUM CHEMISTRY MODELLING

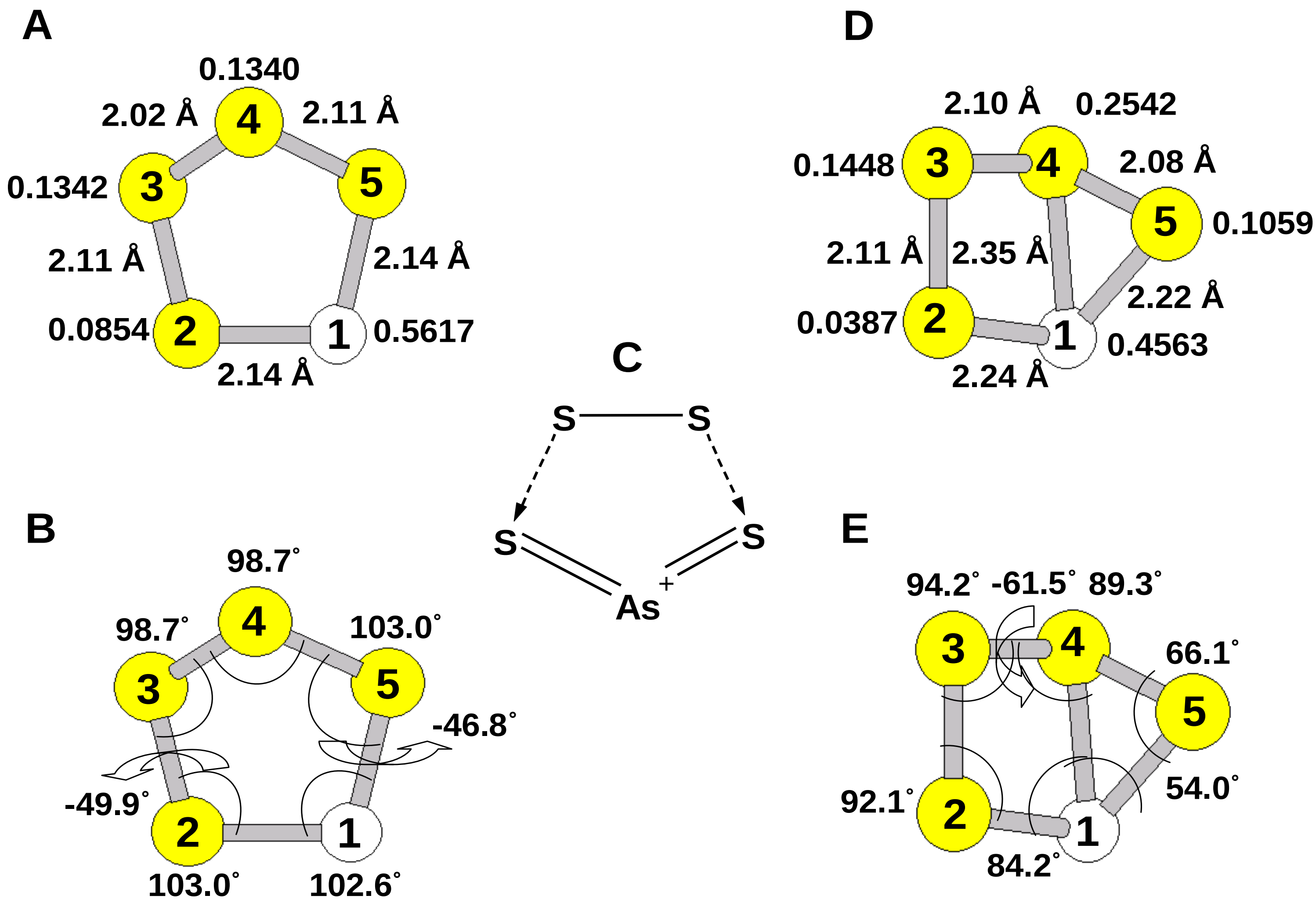

G. Ramirez-Galicia, E. M. Peña-Méndez, S. D. Pangavhane, M. Alberti, J. Havel, Mass spectrometry and ab initio calculation of AsS_n (n = 1–7) ion structures, Polyhedron 29 (2010) 1567–1574.

Do Mass Spectra Reflect Condensed-Phase Chemistry of Glasses?

YES,

Mass spectrometry is giving (some) information about the structure of the glasses

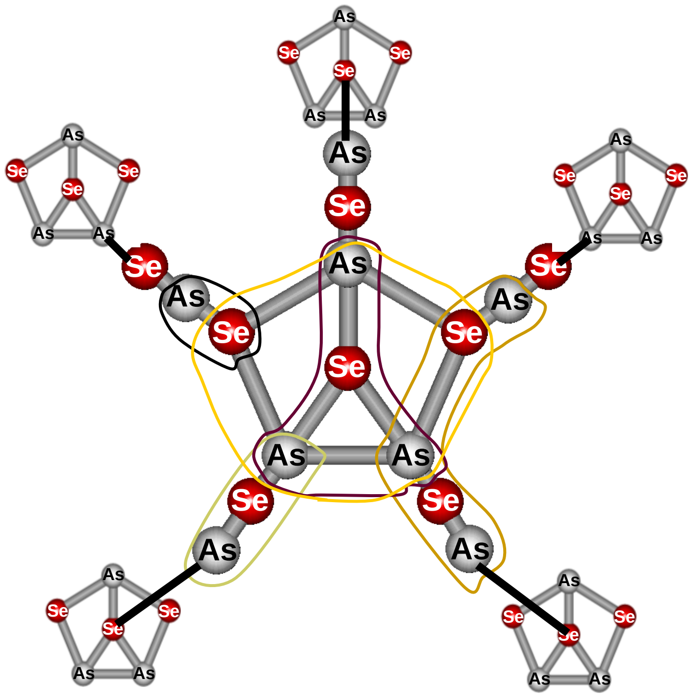

S. Dagurao Pangavhane, J. Houška, T. Wágner, M. Pavlišta and Josef Havel, Laser ablation of ternary As-S-Se glasses and clusters analysis by time of flight mass spectrometry, Rapid Commun. Mass Spectrom., 2010, 24: 95-102.

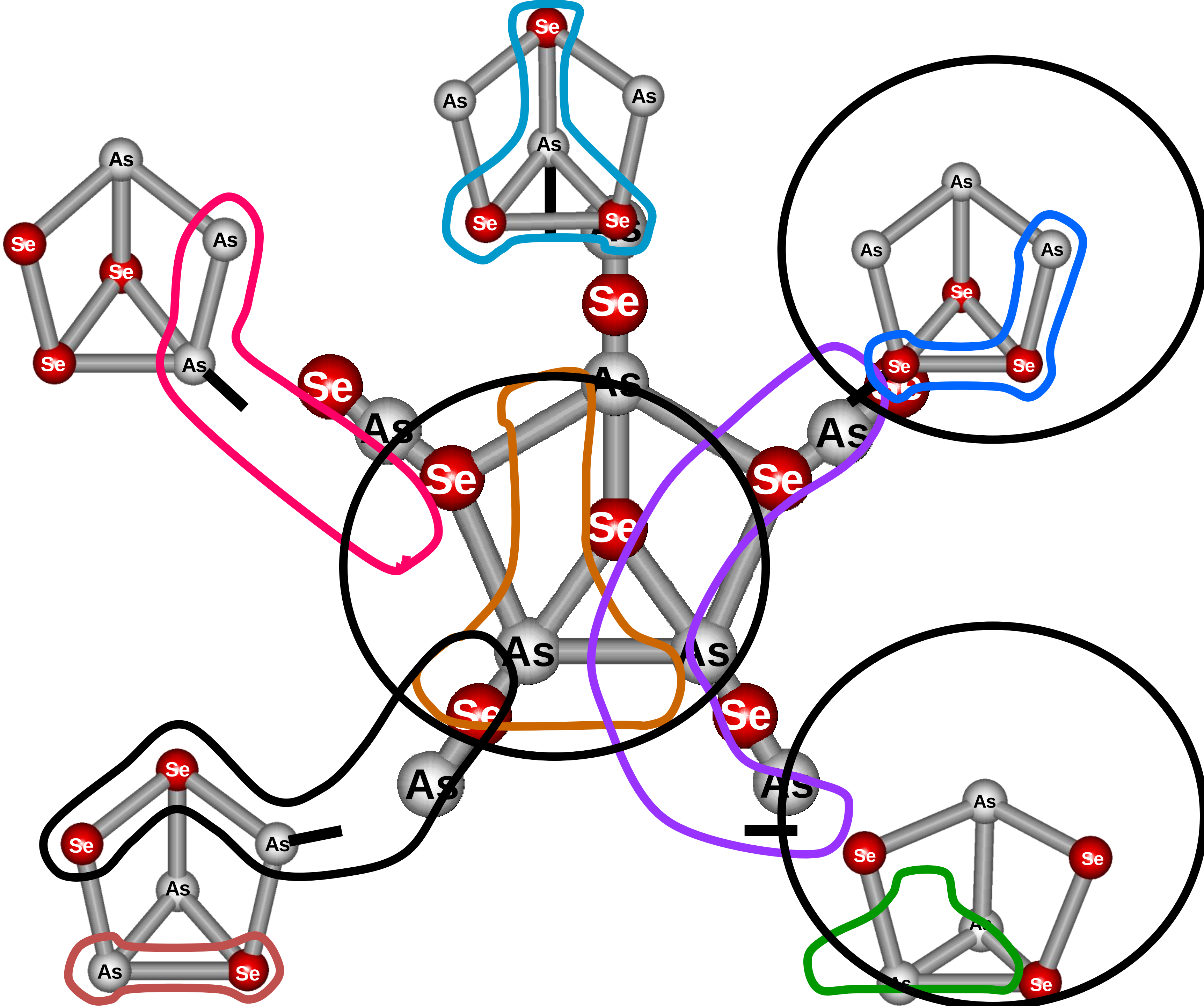
Se
As
As
As
Se
Se
As
Se
As
Se
As
Se
As
As
Se
Se
As
As
Se
As
As
Se
Se
Se
As
Se
As
As
Se
As
As
Se
As
Se
Se
As
As
Se
As
Se
As
Se
Se

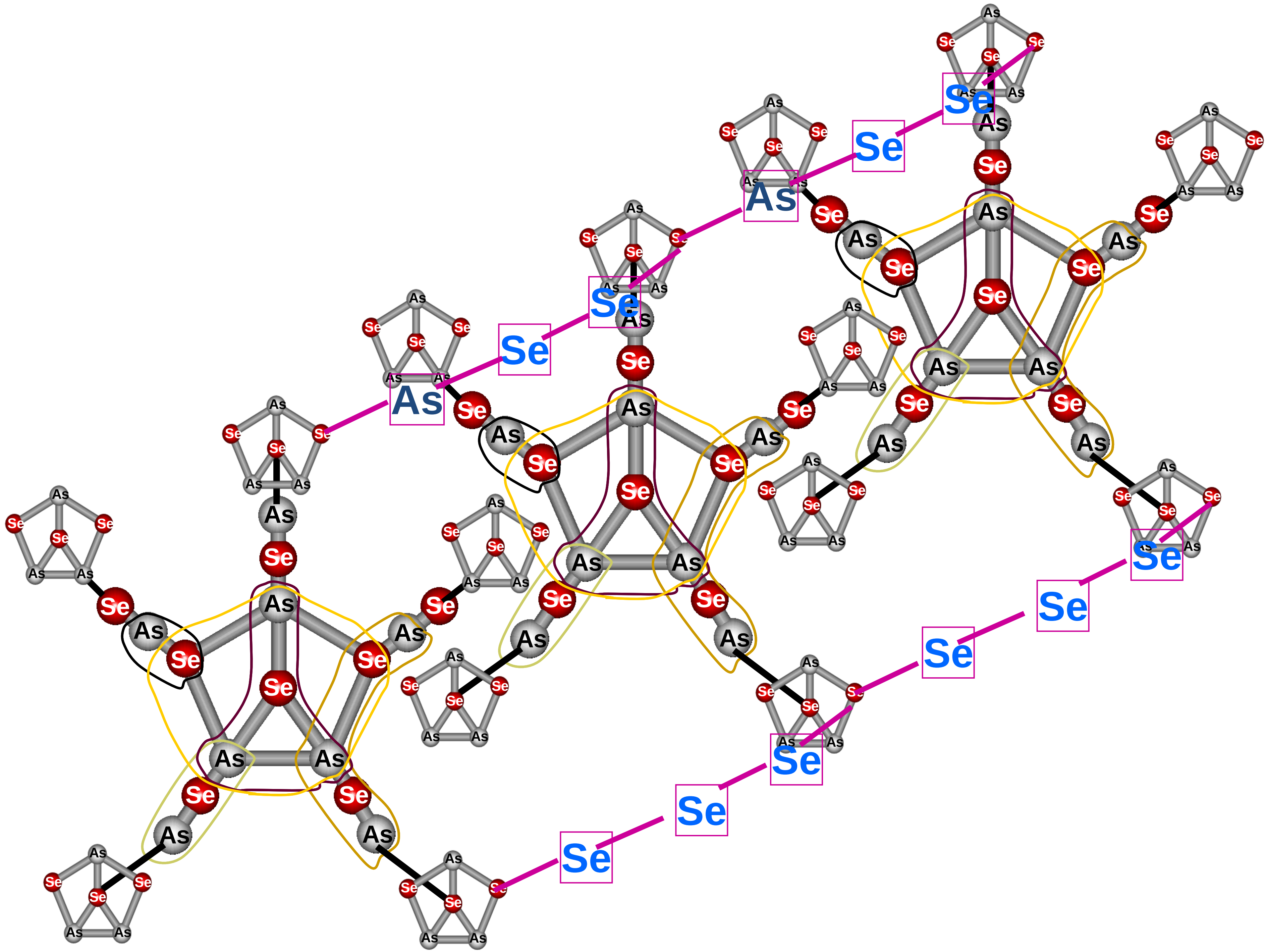
As
Se

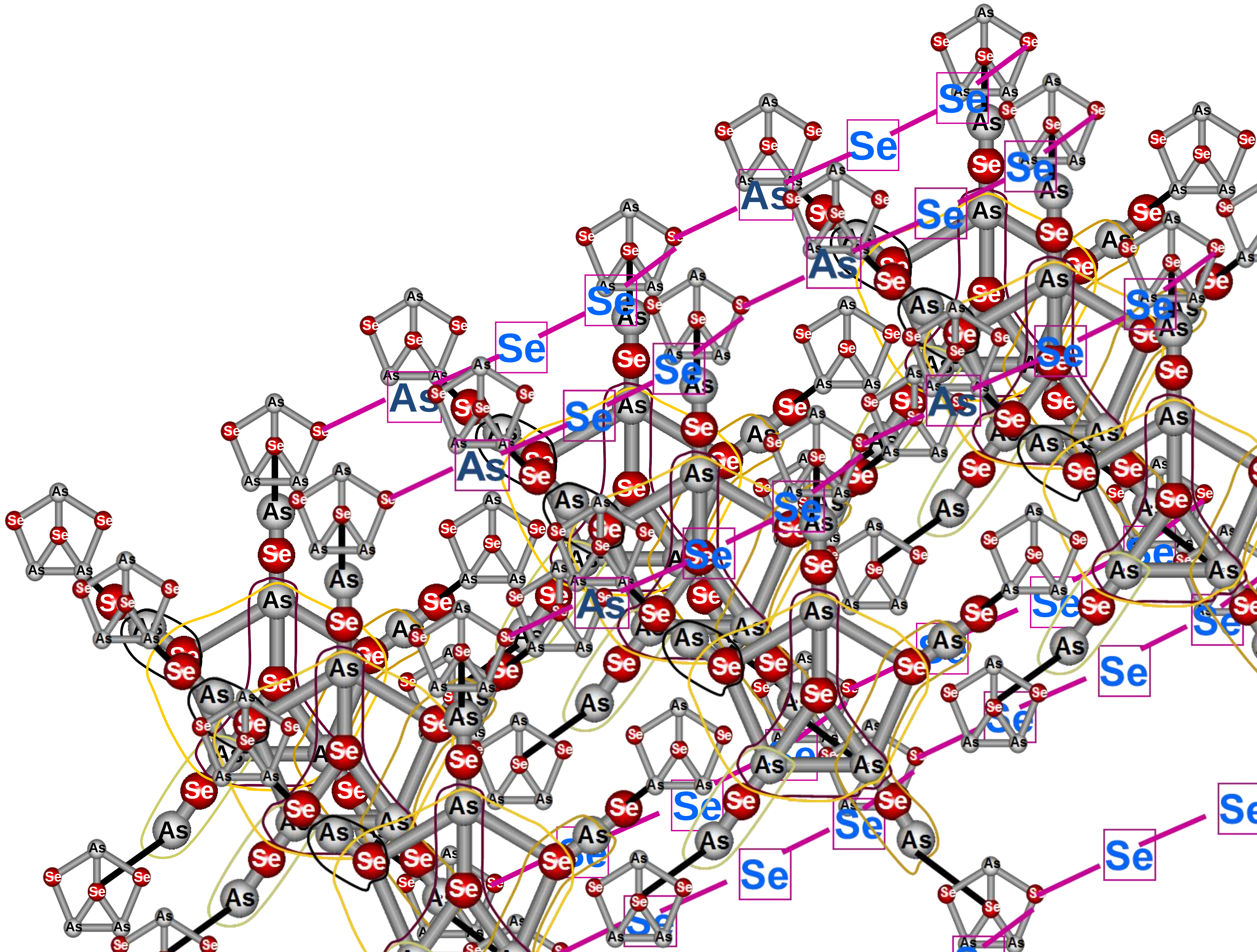

Se
As

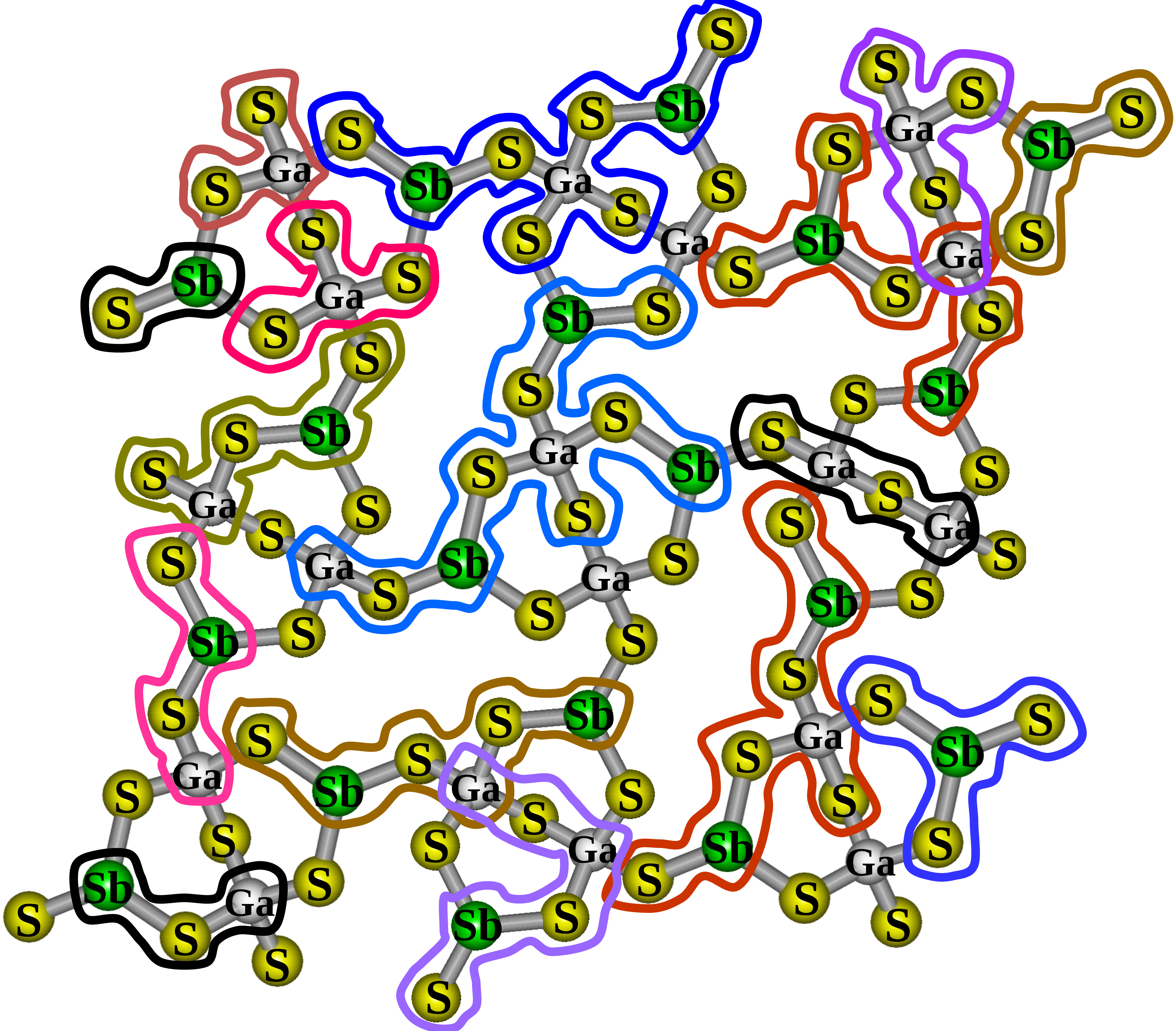

Atomic switch memory $Ge_2Sb_2Te_5$

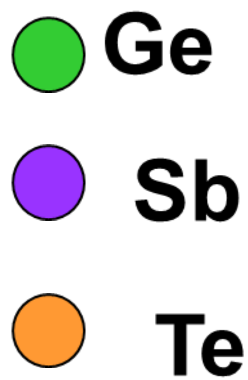

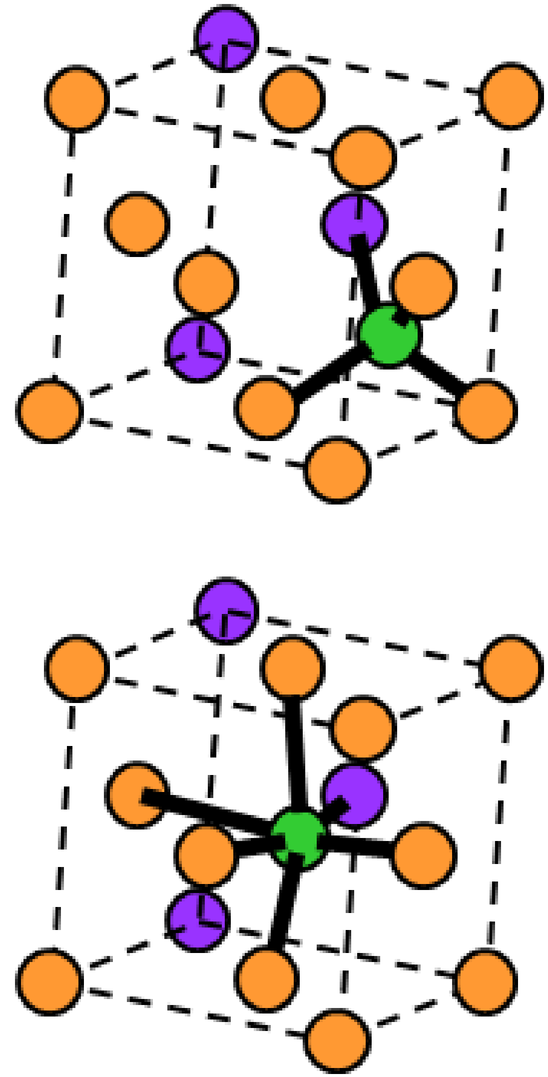

J. Houška, E. M. Peña-Méndez, J. Kolář, J. Přikryl, M. Pavlišta, M. Frumar, T. Wágner a J. Havel. Laser Desorption Time of Flight Mass Spectrometry of atomic switch memory Ge2Sb2Te5 thin films, Rapid Commun. Mass Spectrom, 2014, in print.

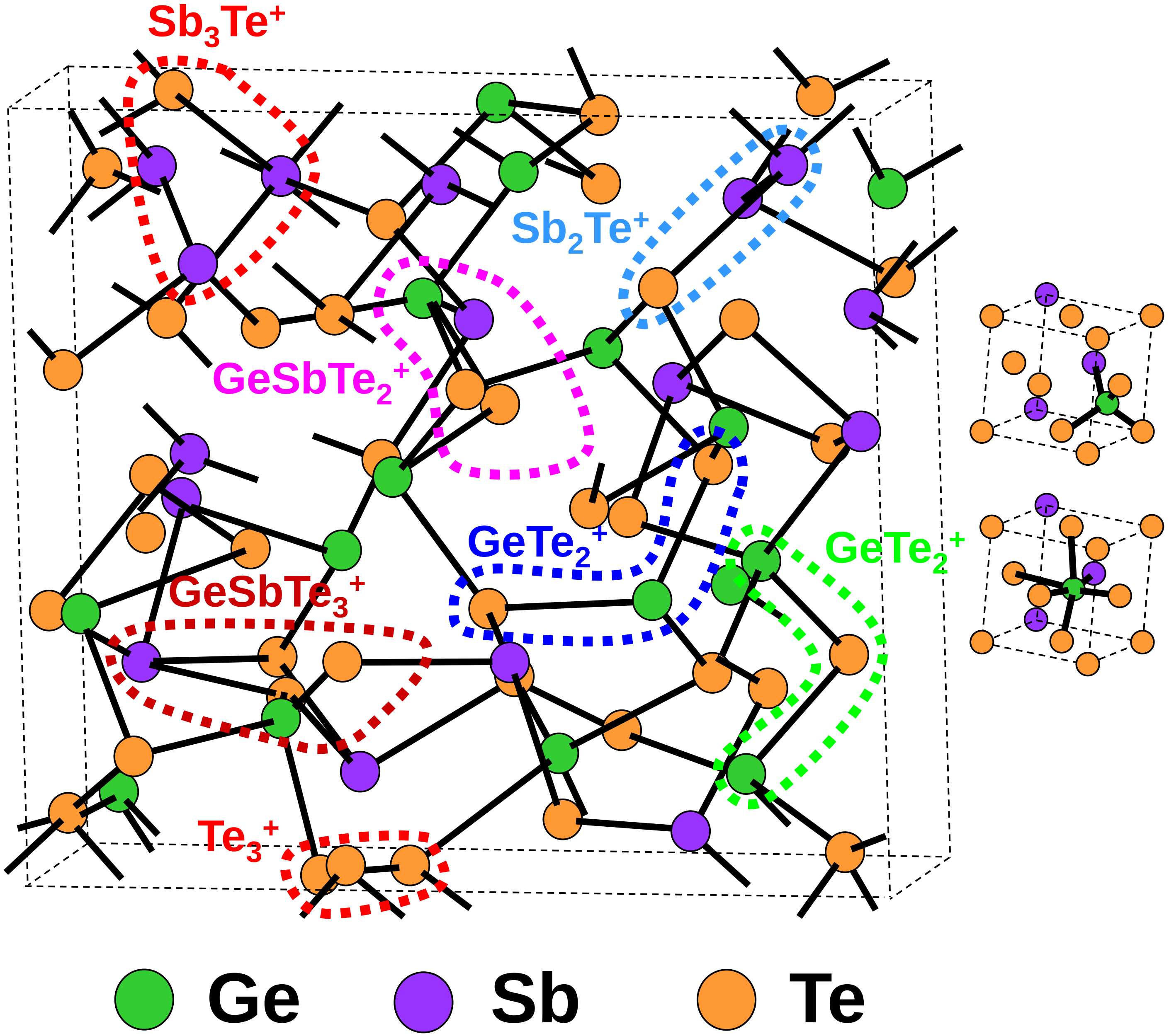

Sb3Te+
Sb2Te+
GeSbTe2+
GeTe2+
GeTe2+
GeSbTe3+
Te3+
Ge
Sb
Te

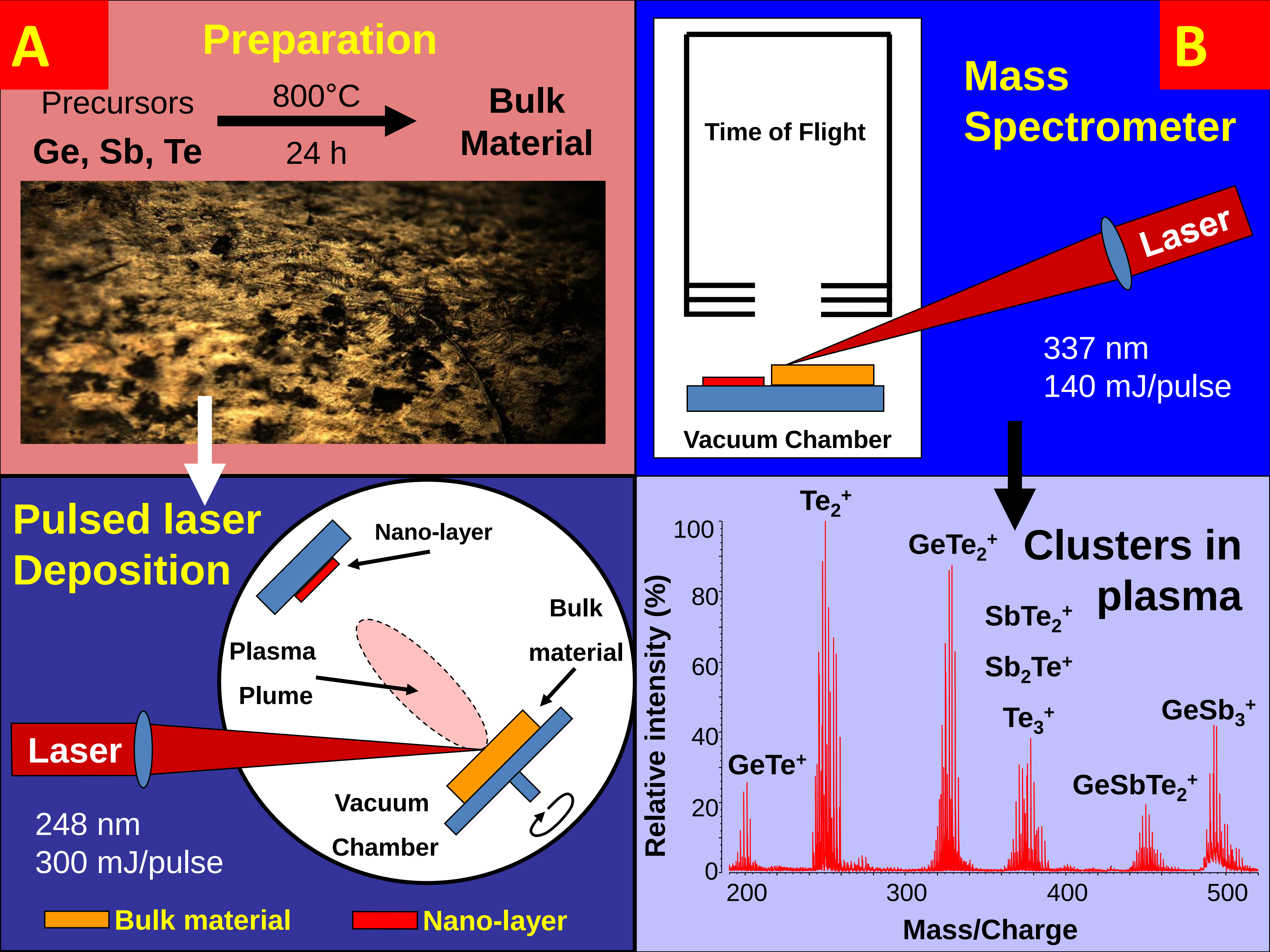
A
Preparation
Precursors
Ge, Sb, Te
800°C
24 h
Bulk
Material
B
Mass
Spectrometer
Time of Flight
Laser
337 nm
140 mJ/pulse
Vacuum Chamber
Pulsed laser
Deposition
Nano-layer
Bulk
material
Plasma
Plume
Laser
Vacuum
Chamber
248 nm
300 mJ/pulse
Bulk material
Nano-layer
Clusters in
plasma
Te_2^+
$GeTe_2^+$
$SbTe_2^+$
Sb_2Te^+
Te_3^+
$GeSb_3^+$
$GeTe^+$
$GeSbTe_2^+$
Relative intensity (%)
0
20
40
60
80
100
200
300
400
500
Mass/Charge

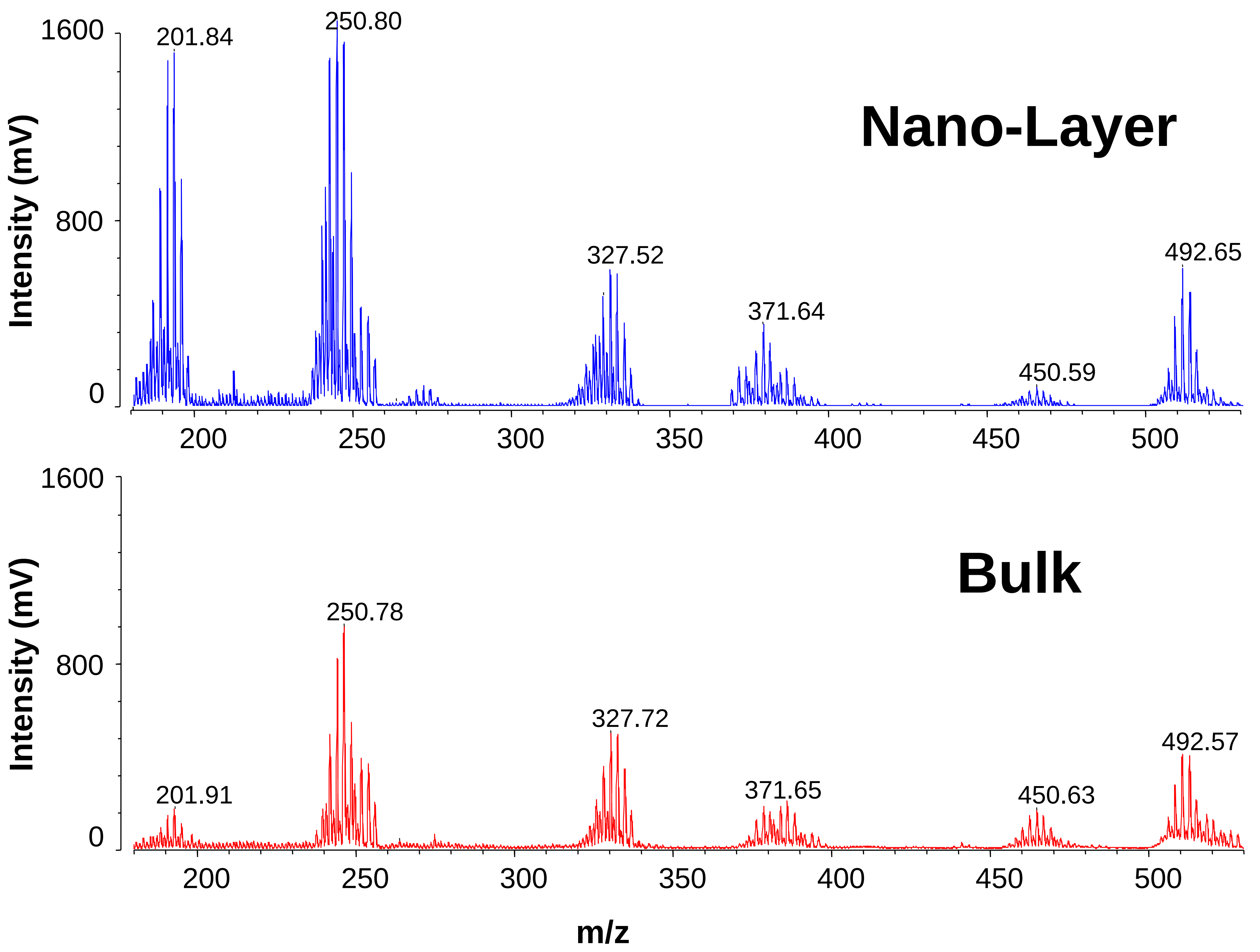

Nano-Layer
Bulk
Intensity (mV)
Intensity (mV)
m/z
1600
800
0
201.84
250.80
327.52
371.64
450.59
492.65
201.91
250.78
327.72
371.65
450.63
492.57
200
250
300
350
400
450
500

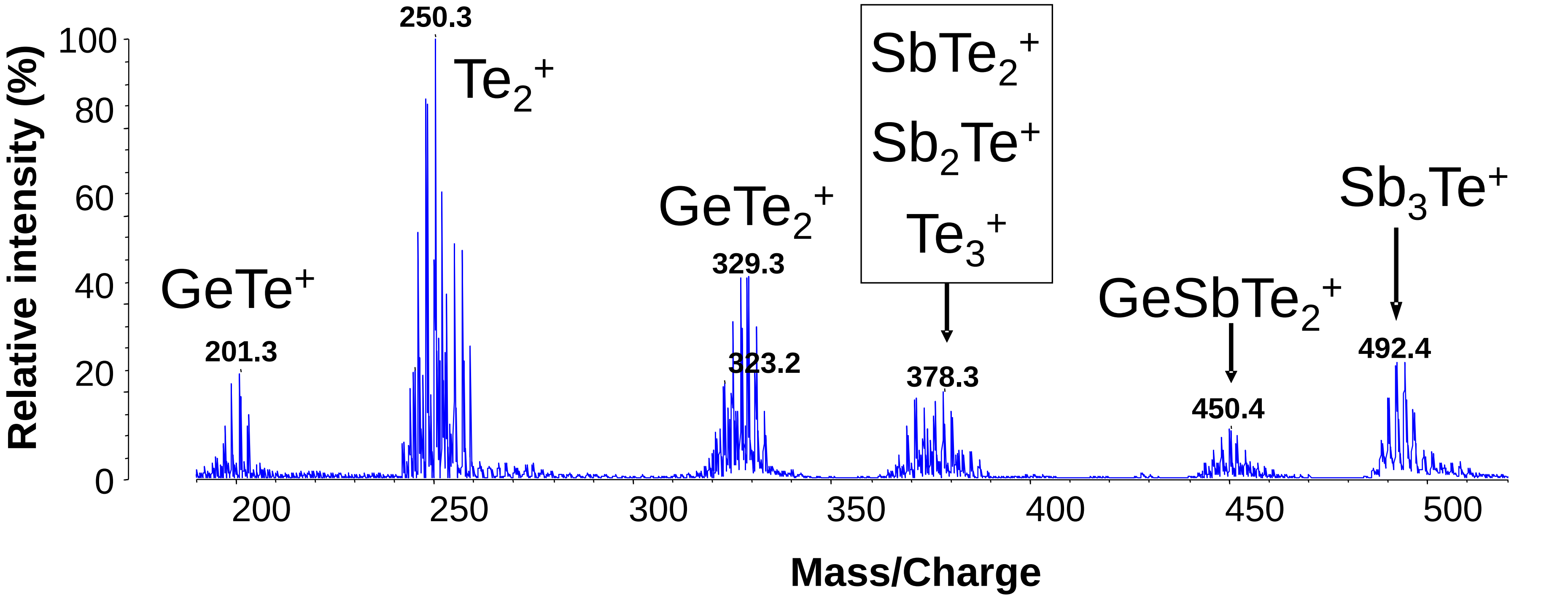

Relative intensity (%)
100
80
60
40
20
0
200
250
300
350
400
450
500
Mass/Charge
GeTe+
201.3
250.3
Te2+
GeTe2+
329.3
323.2
SbTe2+
Sb2Te+
Te3+
378.3
GeSbTe2+
450.4
Sb3Te+
492.4

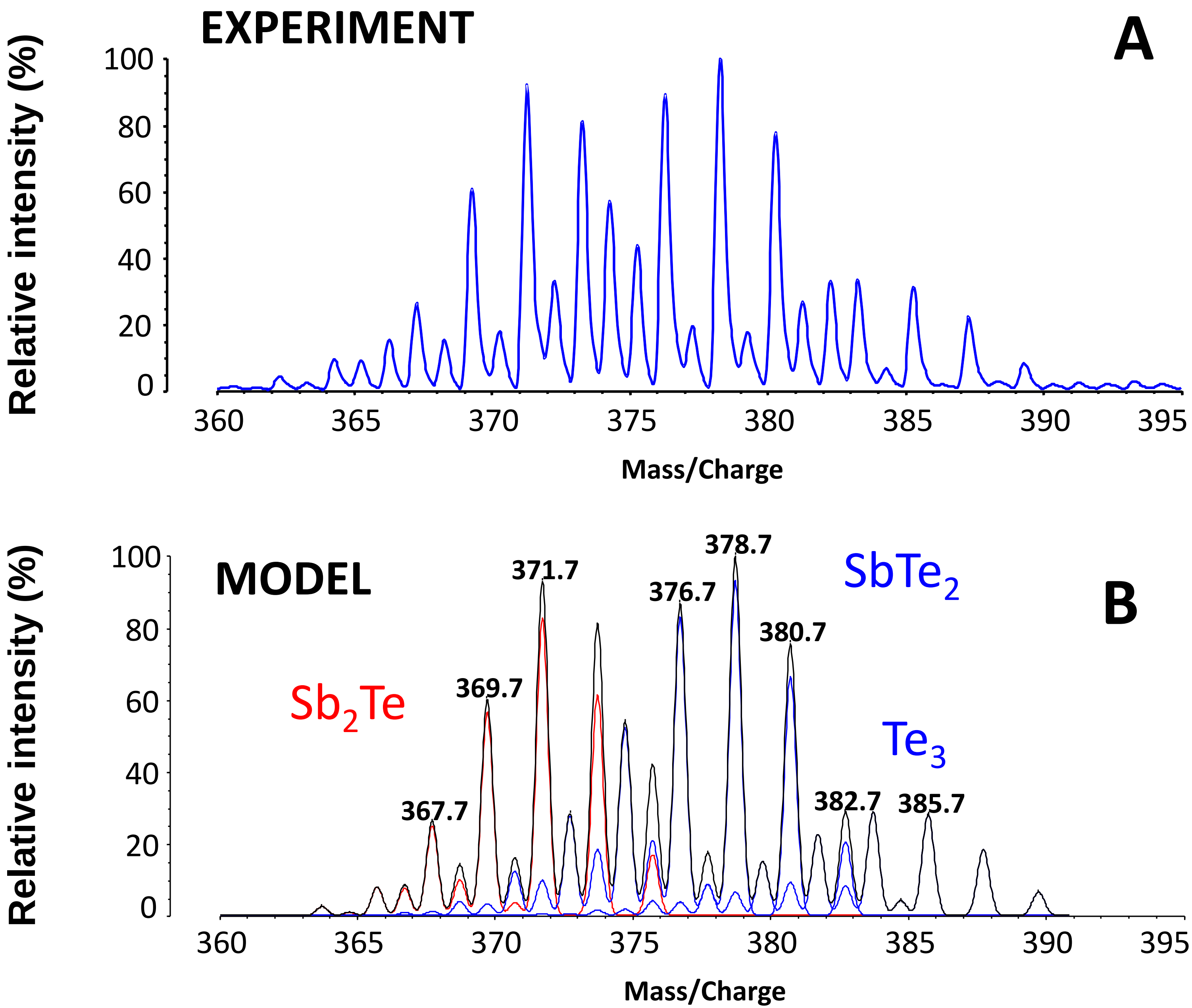

EXPERIMENT
A
Relative intensity (%)
100
80
60
40
20
0
360
365
370
375
380
385
390
395
Mass/Charge
MODEL
B
Relative intensity (%)
100
80
60
40
20
0
Sb$_2$Te
SbTe$_2$
Te$_3$
367.7
369.7
371.7
376.7
378.7
380.7
382.7
385.7
360
365
370
375
380
385
390
395
Mass/Charge

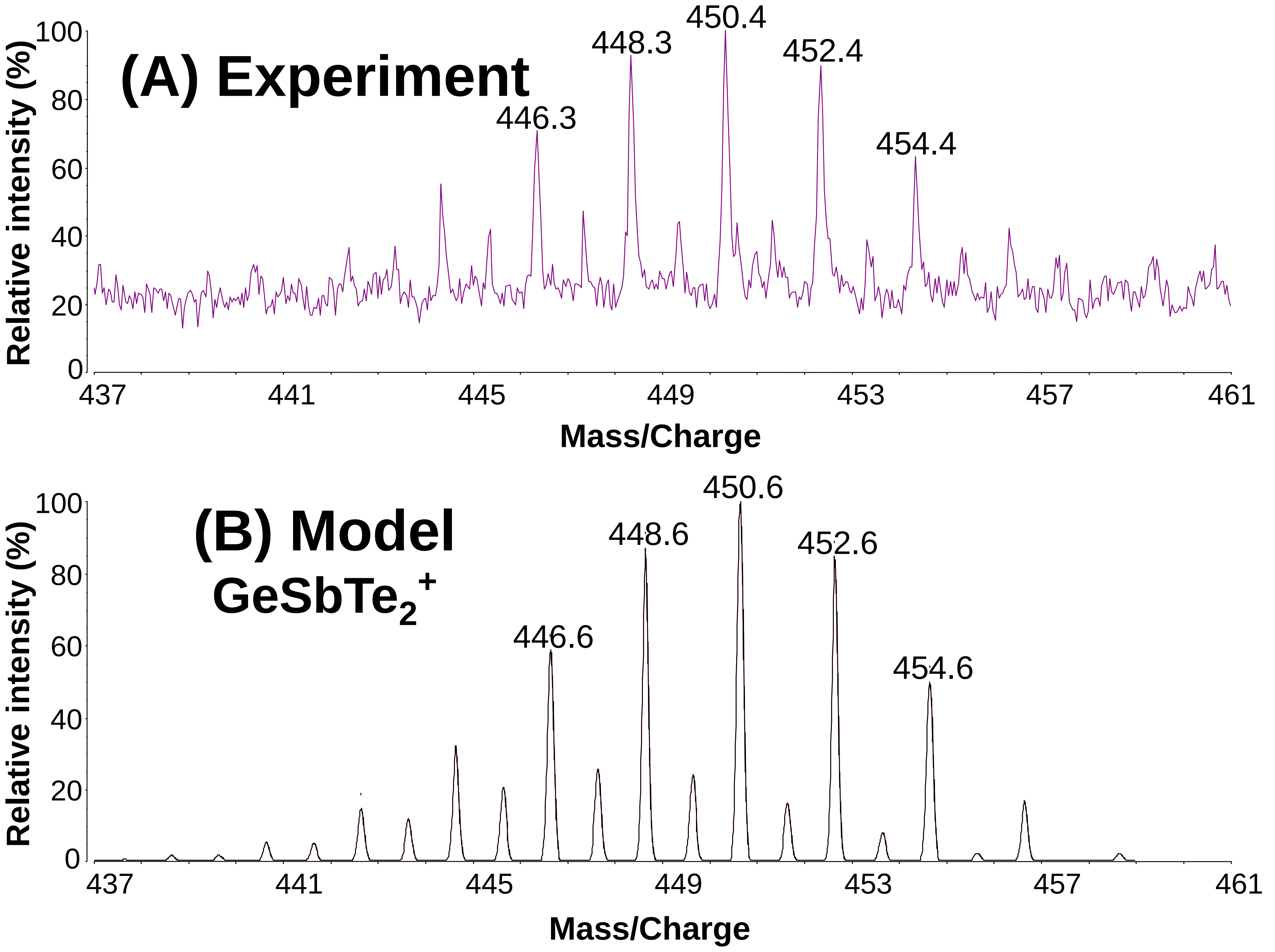
(A) Experiment
446.3
448.3
450.4
452.4
454.4
Relative intensity (%)
0
20
40
60
80
100
437
441
445
449
453
457
461
Mass/Charge
(B) Model
$GeSbTe_2^+$
446.6
448.6
450.6
452.6
454.6
Relative intensity (%)
0
20
40
60
80
100
437
441
445
449
453
457
461
Mass/Charge

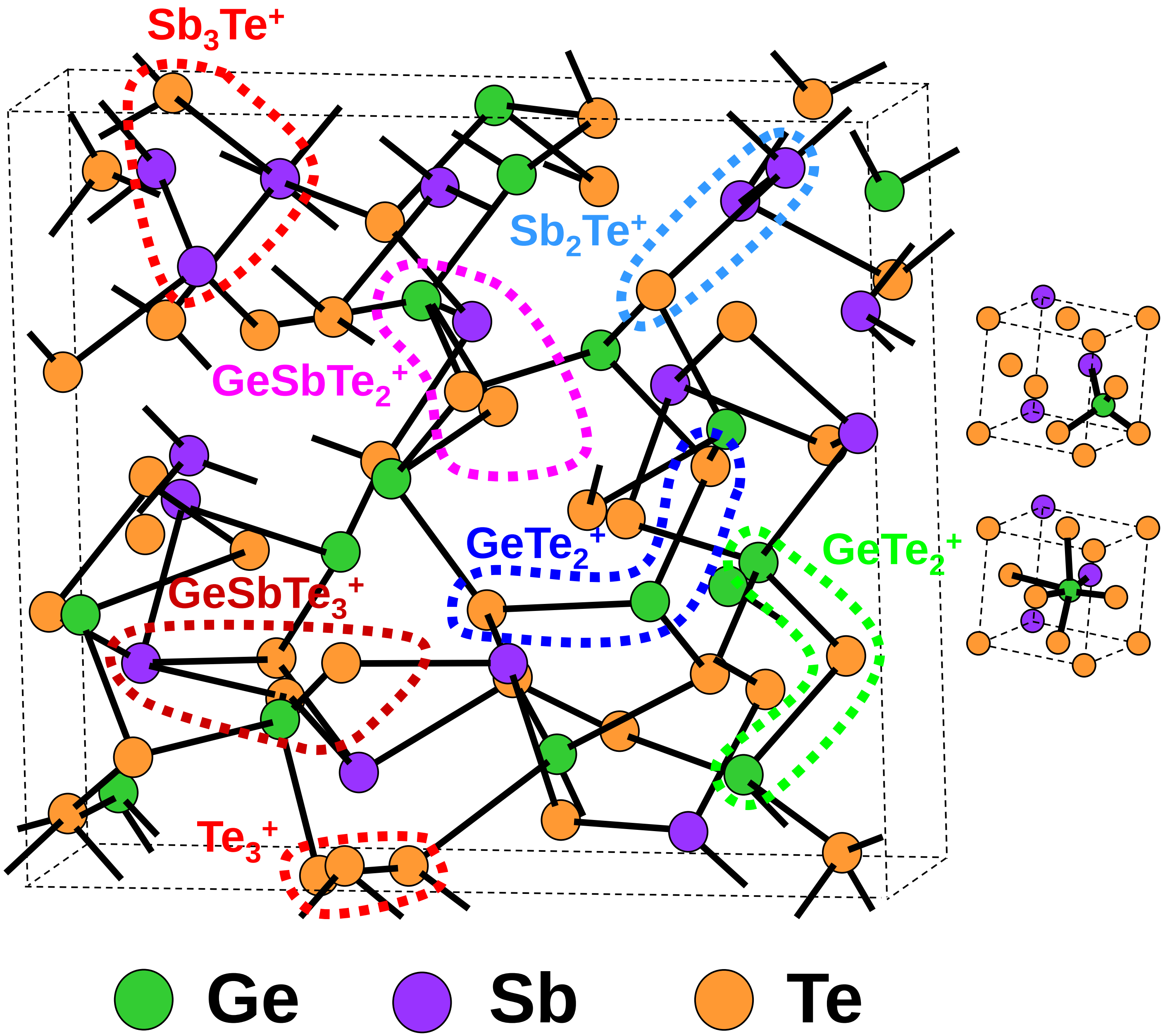

Sb3Te+
Sb2Te+
GeSbTe2+
GeTe2+
GeTe2+
GeSbTe3+
Te3+
Ge
Sb
Te

Publications

1. S. D. Pangavhane, J. Houška, T. Wágner, M. Pavlišta, J. Janča, Josef Havel. Laser ablation of **ternary As-S-Se glasses** and time of flight mass spectrometric study Rapid Commun. Mass Spectrom. 2010, 24: 95.
2. S. D. Pangavhane, P. Němec, T. Wágner, J. Janča, J. Havel. Laser desorption Ionization Time-of-flight mass spectrometric study of binary **As-Se glasses** Rapid Commun. Mass Spectrom. 2010; 24: 2000.
3. Guillermo Ramírez-Galicia, E. M. Peña-Méndez, S. D. Pangavhane, M. Alberti, Josef Havel. **Ab initio structure modeling of AsS_n^+** (n = 1-7) cluster ions Polyhedron 2010; 29: 1567.
4. S. D. Pangavhane, Lucie Hebedová, Milan Alberti, J. Havel. Laser ablation synthesis of new **phosphorus nitride clusters** from α-P_3N_5. Laser desorption ionization and MALDI time of flight mass spectrometry Rapid Commun. Mass Spectrom 2011; 25: 917.
5. S. D. Pangavhane, P. Němec, V. Nazabal, Alain Moreac, Pál Jóvári, J. Havel. Laser desorption ionization time-of-flight mass spectrometric study of erbium doped **Ga-Ge-Sb-S glasses** Rapid Commun. Mass Spectrom. In print, 2014.
6. J. Houška, E. M. Peña-Méndez, J. Kolář, J. Přikryl, M. Pavlišta, M. Frumar, T. Wágner a J. Havel. Laser Desorption Time of Flight Mass Spectrometry of **atomic switch memory** Ge2Sb2Te5 thin films, *Rapid Commun. Mass Spectrom*, 2014, in print.

What is the structure of chalcogenide glasses

?


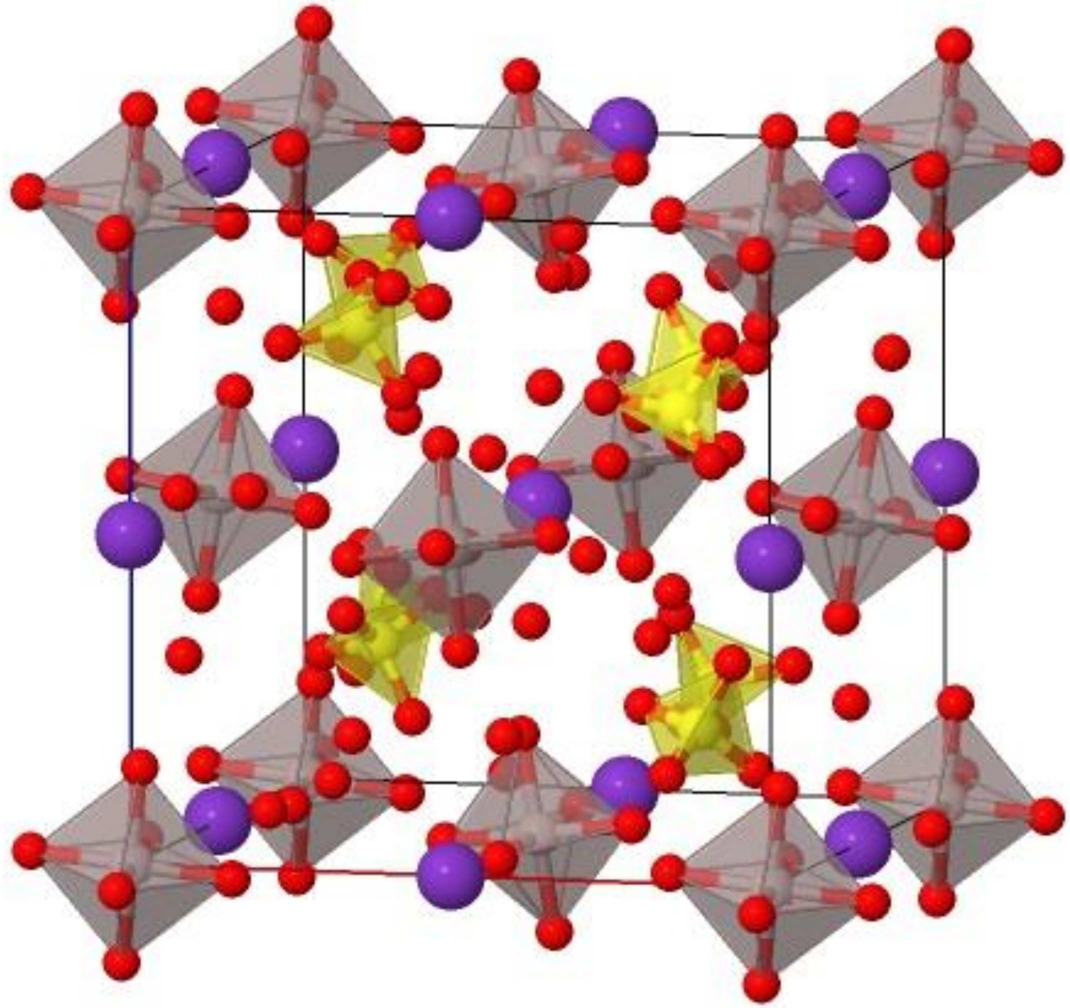
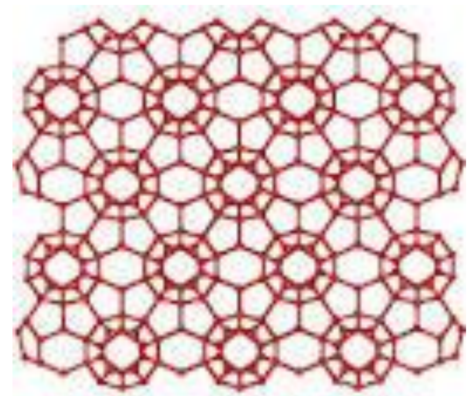

Dan Shechtman

(Hebrew: דן שכטמן;

born January 24, 1941 in Tel Aviv)[1]

Technion – Israel Institute of Technology

The Nobel Prize in Chemistry 2011

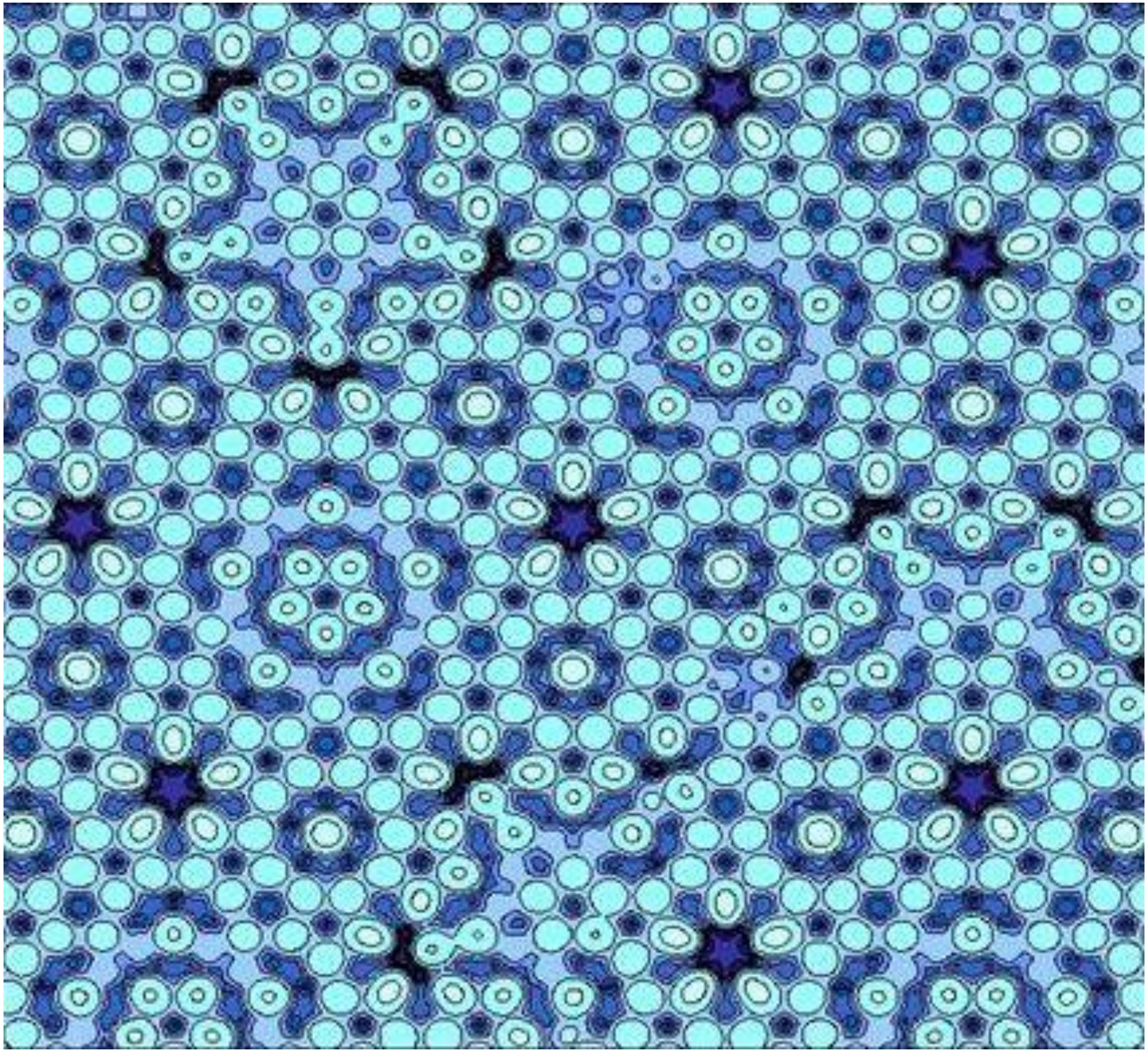

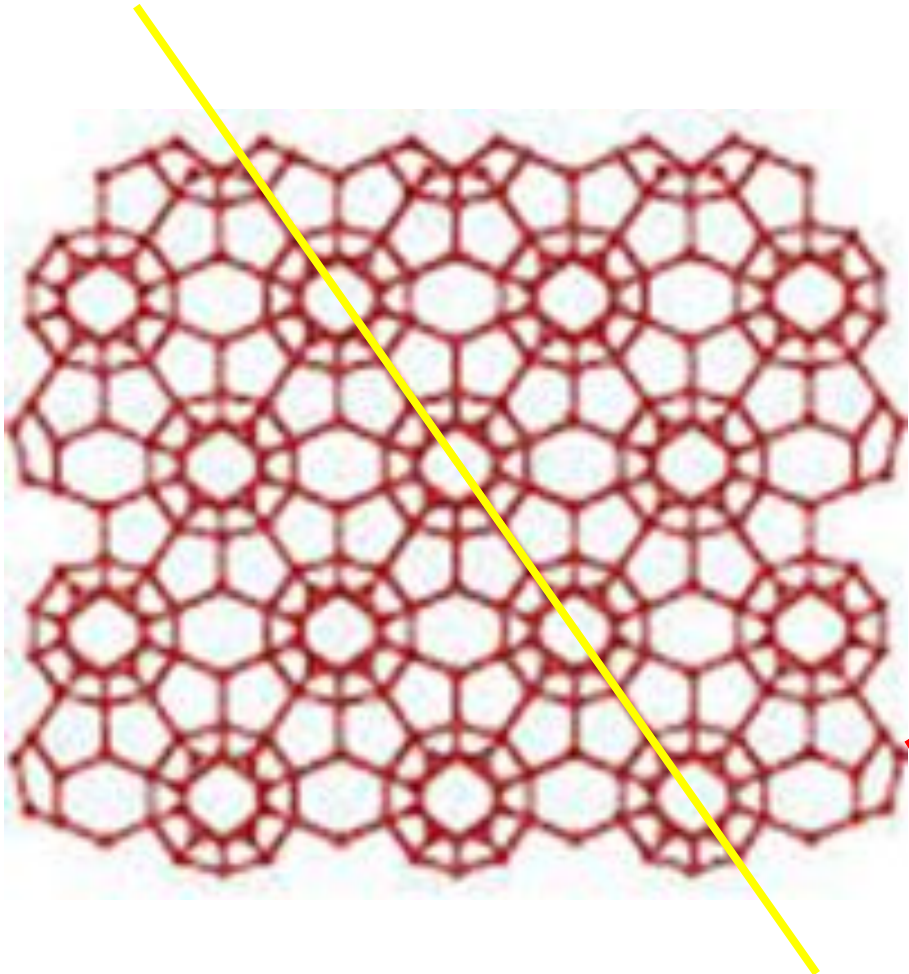

CRYSTALS

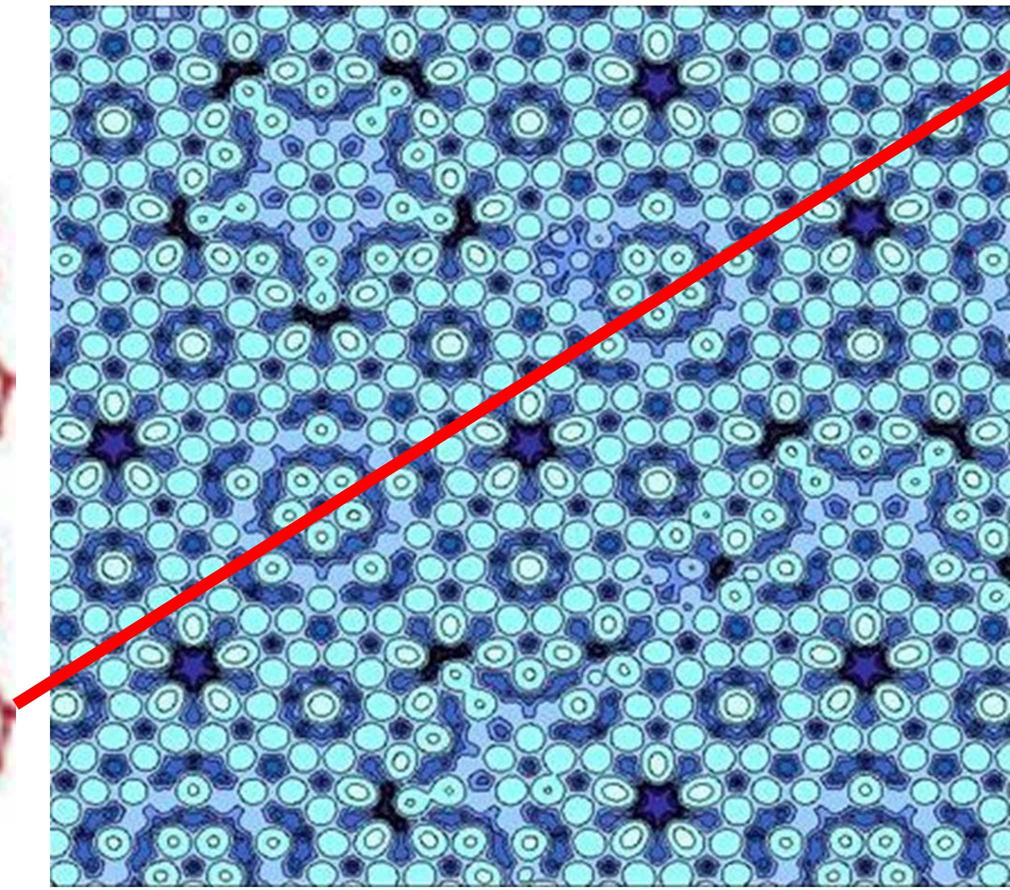

SEMi. CRYSTALS

Are chalcogenide glasses SEMI-CRYSTALS

or

even less organized

CHAOTIC CRYSTALS (Havel´s term)

?

LASER ABLATION SYNTHESIS

LASER ABLATION SYNTHESIS

Gold carbides
Gold arsenides

Gold phosphides

Gold tellurides
Gold selenides

Precursor: mixture of elements or compounds = TOF MS analysis

Gold phosphides Applications

Gold Phosphide is a semiconductor used in

(i) high power, high frequency applications

(ii) laser diodes

(iii) biomedical technology

(iv) fabrication of high purity gold phosphide sputtering targets - useful in semiconductor, chemical vapour deposition (CVD) and physical vapour deposition (PVD) display and optical applications

Gold phosphide sputtering target

Au_6P_3 unit cell

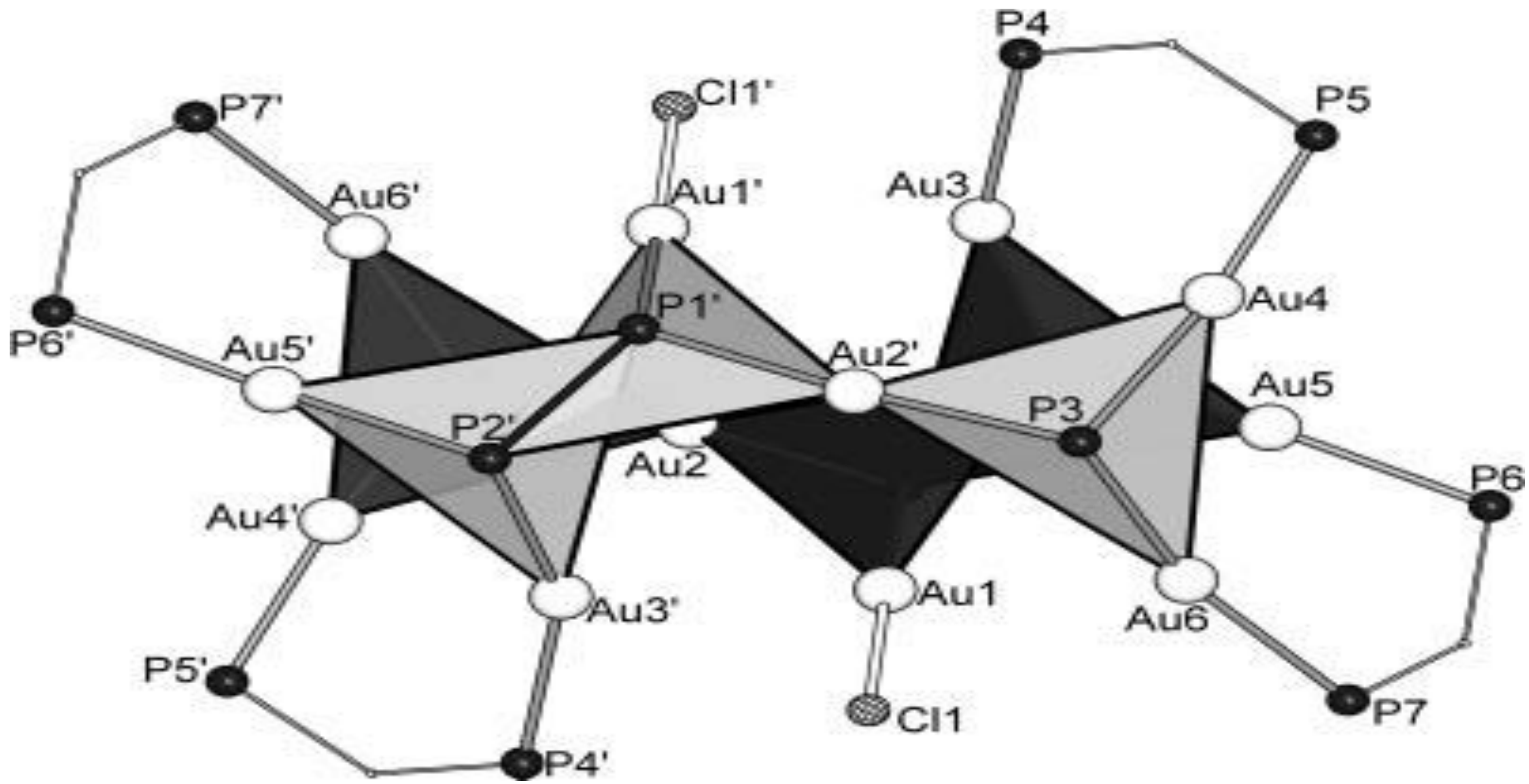

Two phenyl rings bound to each phosphorus are not shown.

P. Sevillano, O. Fuhr, E. Matern, D. Fenske. Synthesis, Crystal structure and Spectroscopic Characterization of $[Au_{12}(PPh)_2(P_2Ph_2)_2(dppm)_4Cl_2]Cl_2$. *Z. Anorg. Allg. Chem.* **2006**, 632, 735-738.

Heterocyclic structures as proposed by X-D. Wen et al. 2009

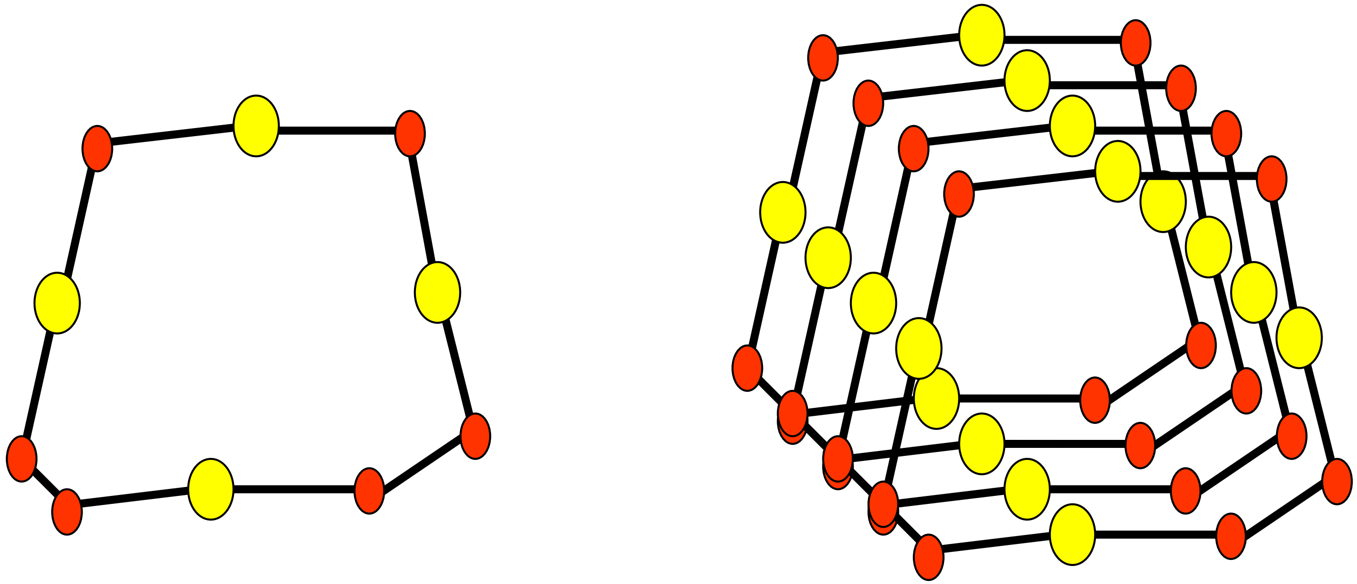

Au$_4$P$_6$ heterocycle

X-D Wen, T. J. Cahill, **R. Hoffmann**. Element Lines: Bonding in the Ternary Gold Polyphosphides, Au$_2$MP$_2$ with M) Pb, Tl, or Hg. *J. Am. Chem. Soc.* **2009**, 131, 2199.

M. Eschen, W. Jeitschko. Au2PbP2, Au2TlP2, and Au2HgP2: Ternary Gold Polyphosphides with Lead, Thallium, and Mercury in the Oxidation State Zero. *J. Solid State Chem.* **2002**, 165, 238.

Gold phosphides

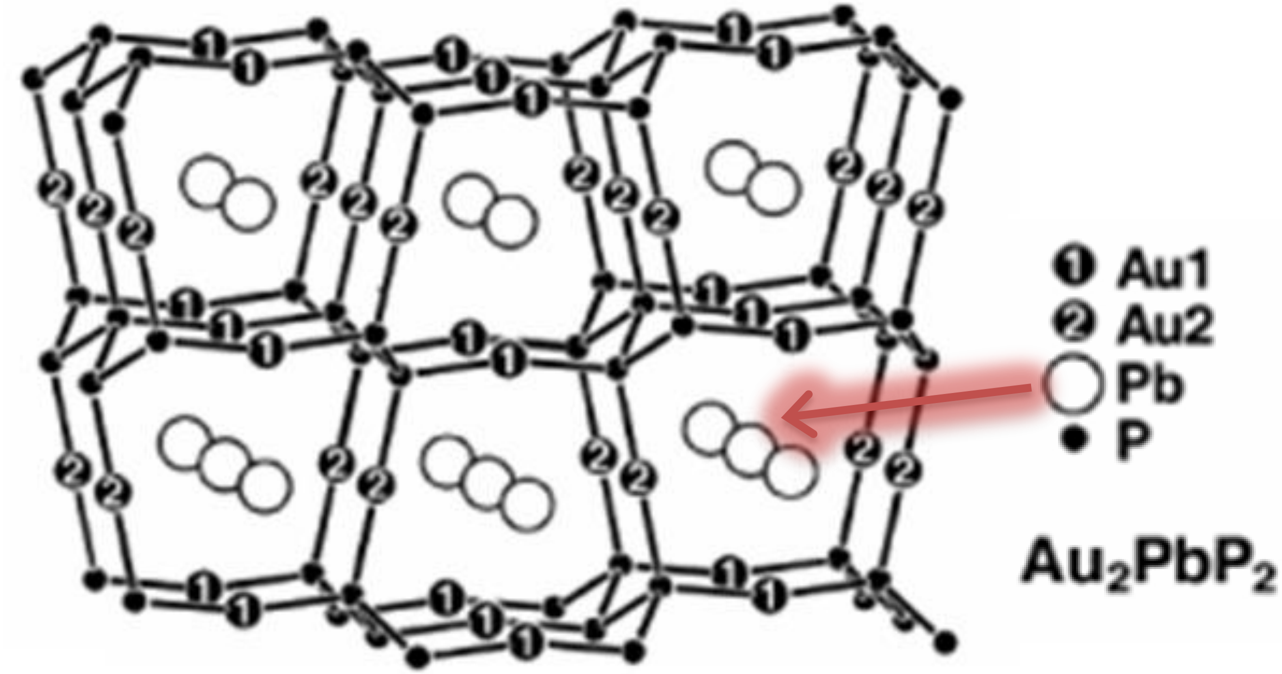

These compounds contain a framework of condensed Au_2P_6 and Au_4P_6 rings forming parallel channels, which are filled by lead, thallium, or mercury atoms.

M. Eschen, W. Jeitschko. Au_2PbP_2, Au_2TlP_2, and Au_2HgP_2: Ternary Gold Polyphosphides with Lead, Thallium, and Mercury in the Oxidation State Zero. *J. Solid State Chem.* **2002,** 165, 238.

X. D. Wen, T.J. Cahill, **R. Hoffmann**. Element Lines: Bonding in the Ternary Gold Polyphosphides, Au_2MP_2 with M= Pb, Tl, or Hg. *J. Am. Chem. Soc.* **2009**, *131*, 2199.


Genius Of Genetics

LASER ABLATION SYNTHESIS

of gold phosphides

from

NANOGOLD and RED PHOSPHORUS

precursors

N.R. Panyala, Havel J, et al. Laser ablation synthesis of new gold phosphides using red phosphorus and nano-gold as precursors. Laser Desorption Ionisation time-of-flight Mass Spectrometry. *Rapid Commun. Mass Spectrom.* 2013

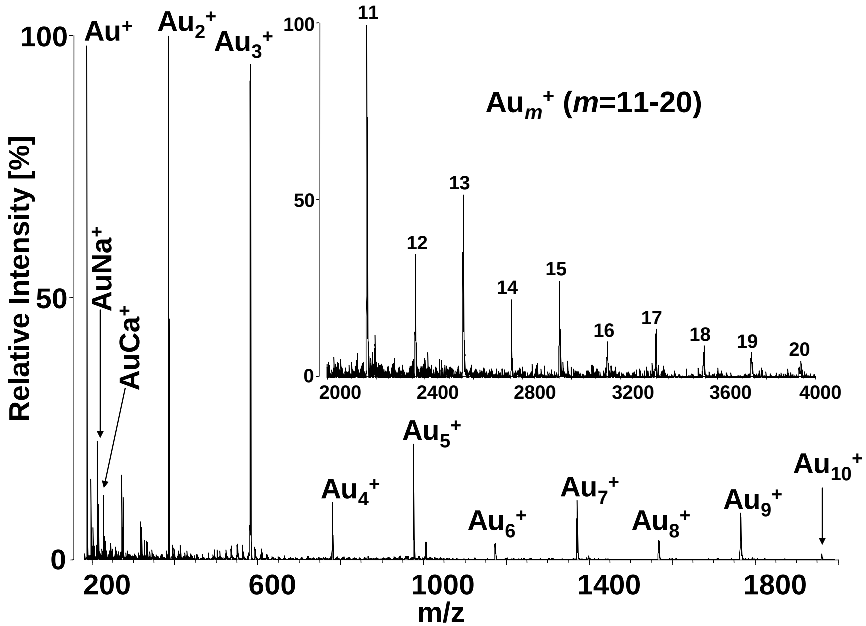

172

N.R. Panyala, et al. *Rapid Commun. Mass Spectrom.* submitted .

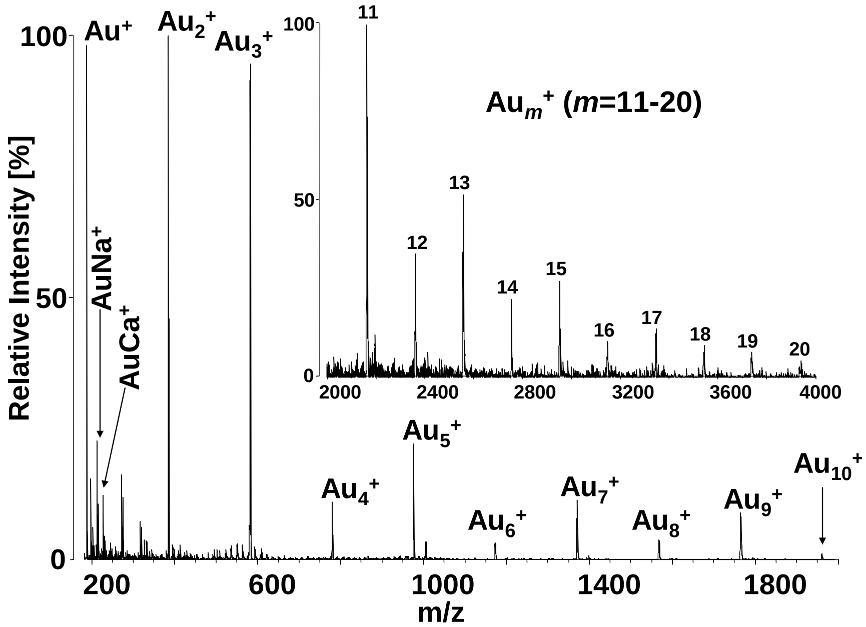
Relative Intensity [%]
m/z
Au+
Au2+
Au3+
AuNa+
AuCa+
Au4+
Au5+
Au6+
Au7+
Au8+
Au9+
Au10+
Aum+ (m=11-20)

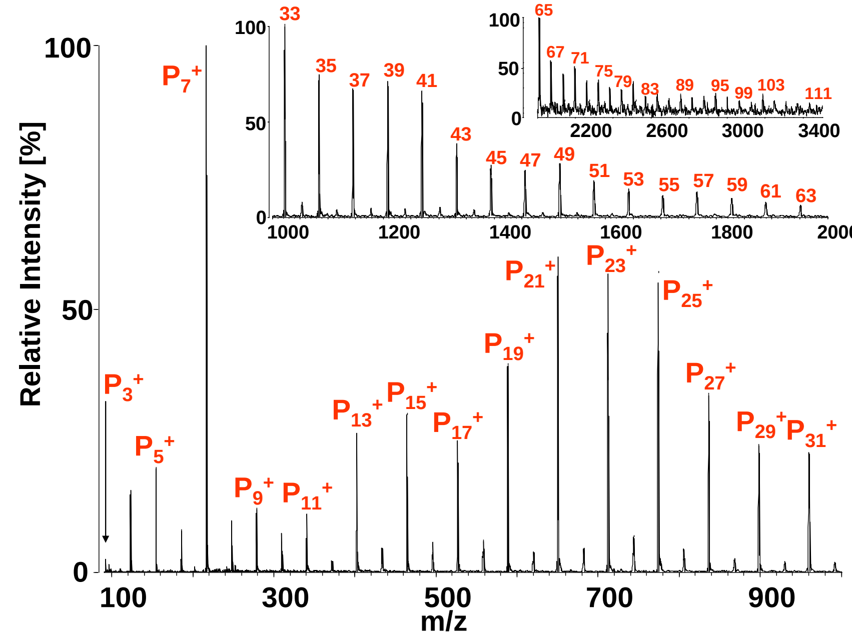
Relative Intensity [%]
m/z
P3+
P5+
P7+
P9+
P11+
P13+
P15+
P17+
P19+
P21+
P23+
P25+
P27+
P29+
P31+

173

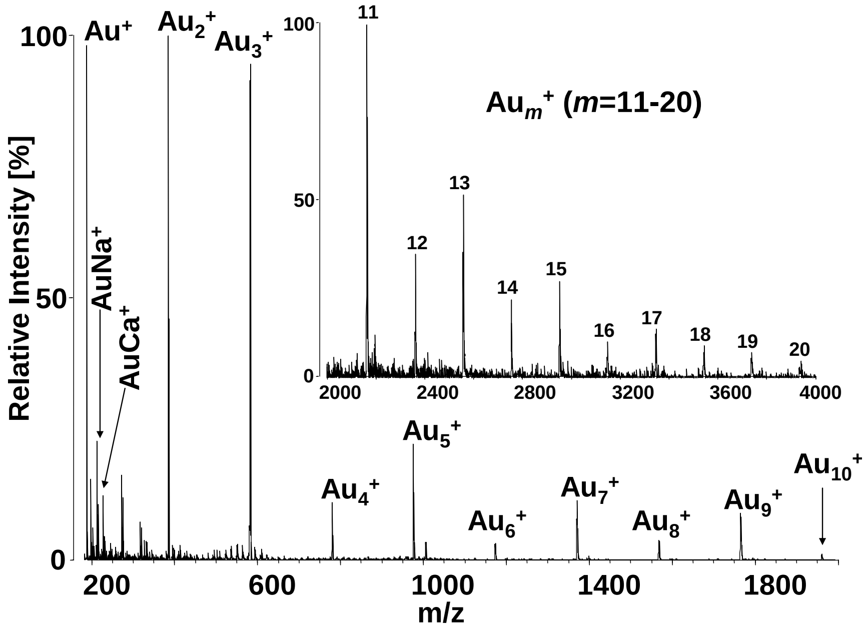

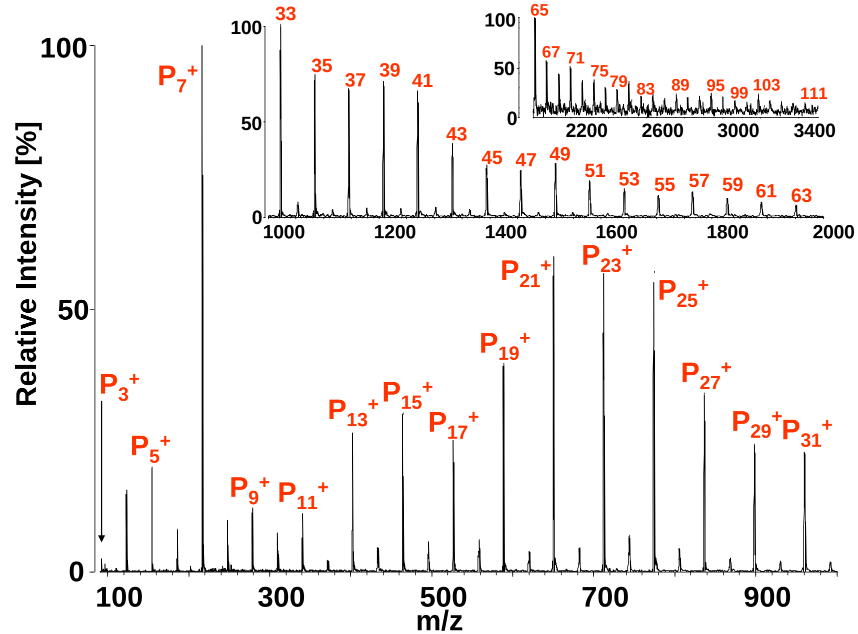

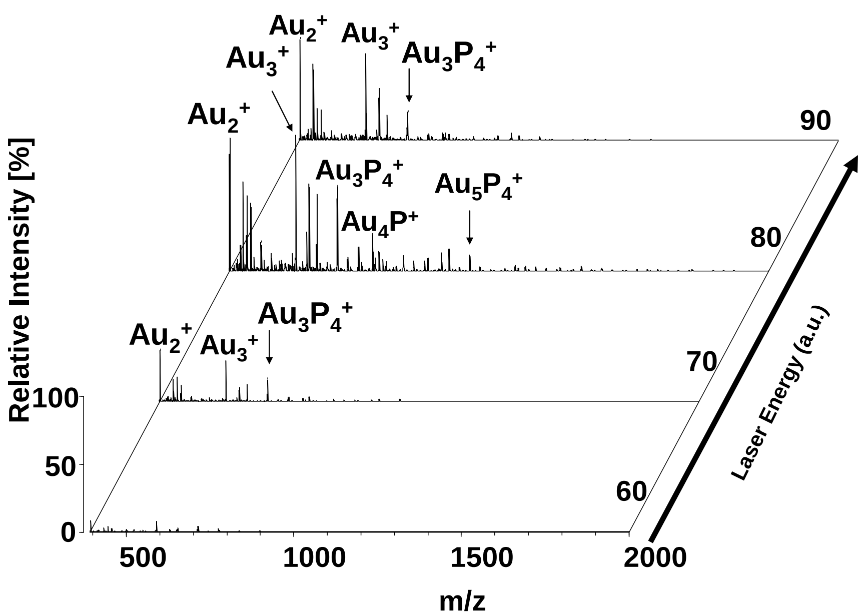

N.R. Panyala, et al. *Rapid Commun. Mass Spectrom.* submitted .

174

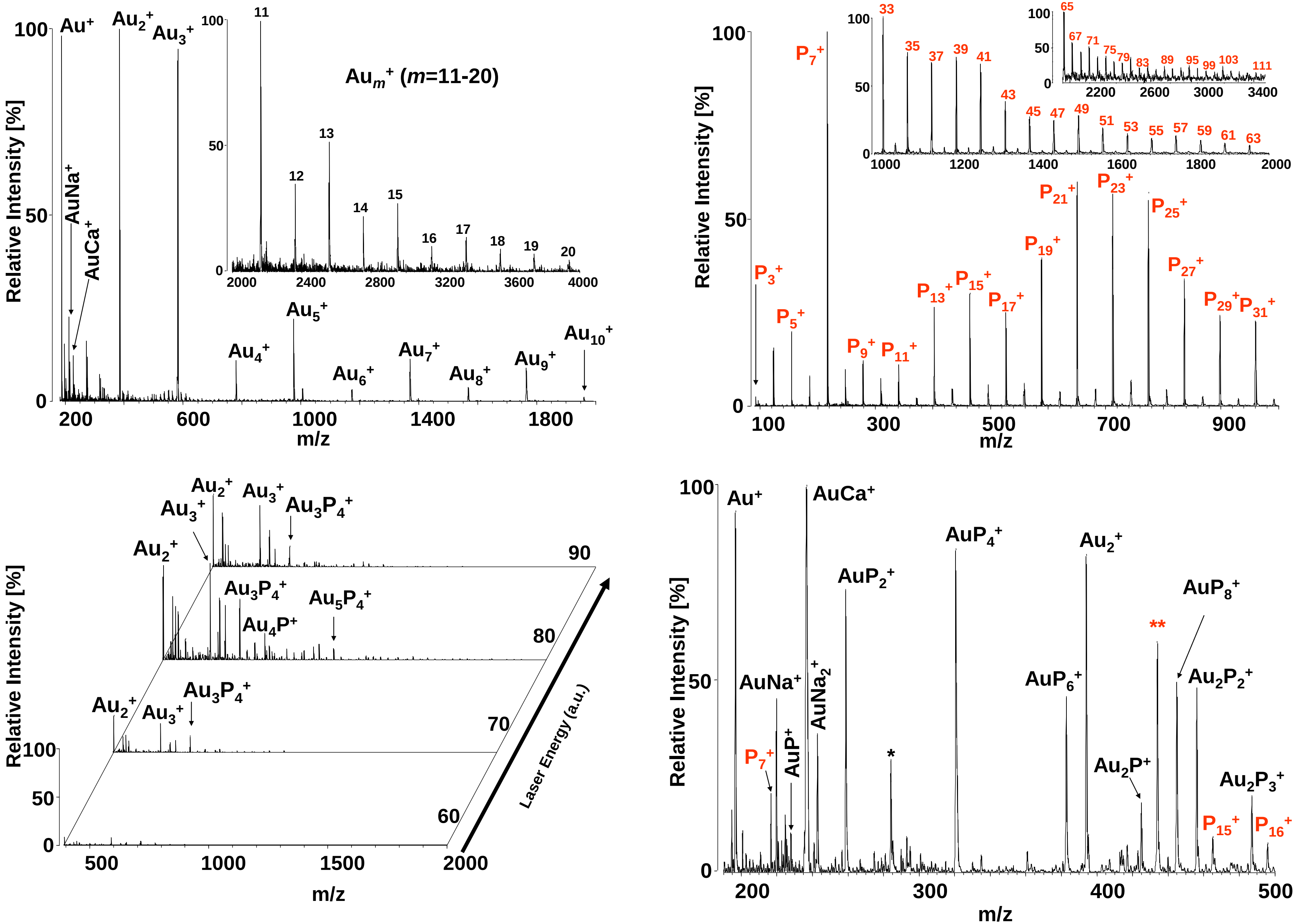

N.R. Panyala, et al. *Rapid Commun. Mass Spectrom.* submitted .

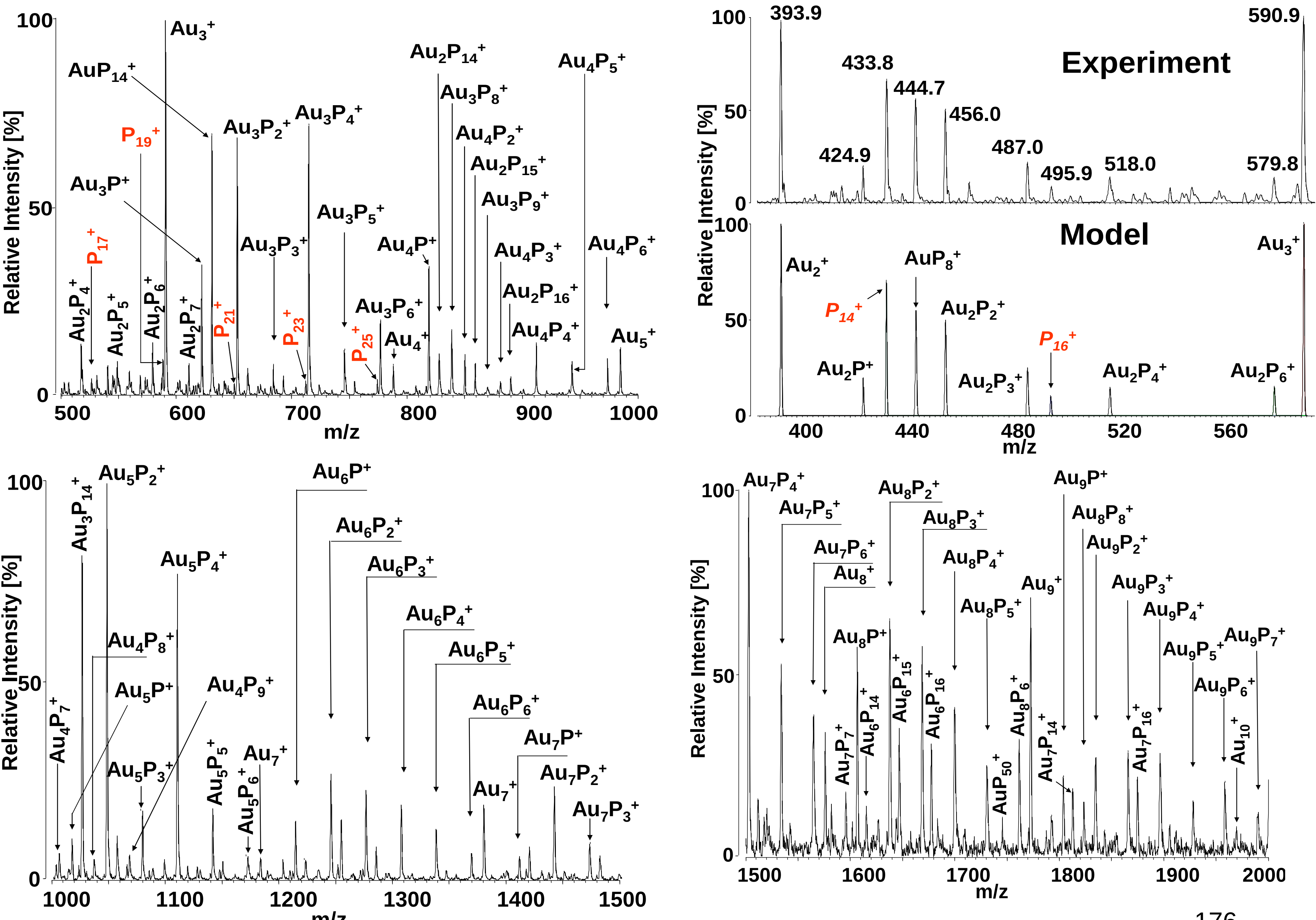

N.R. Panyala, et al. *Rapid Commun. Mass Spectrom.* submitted .

176

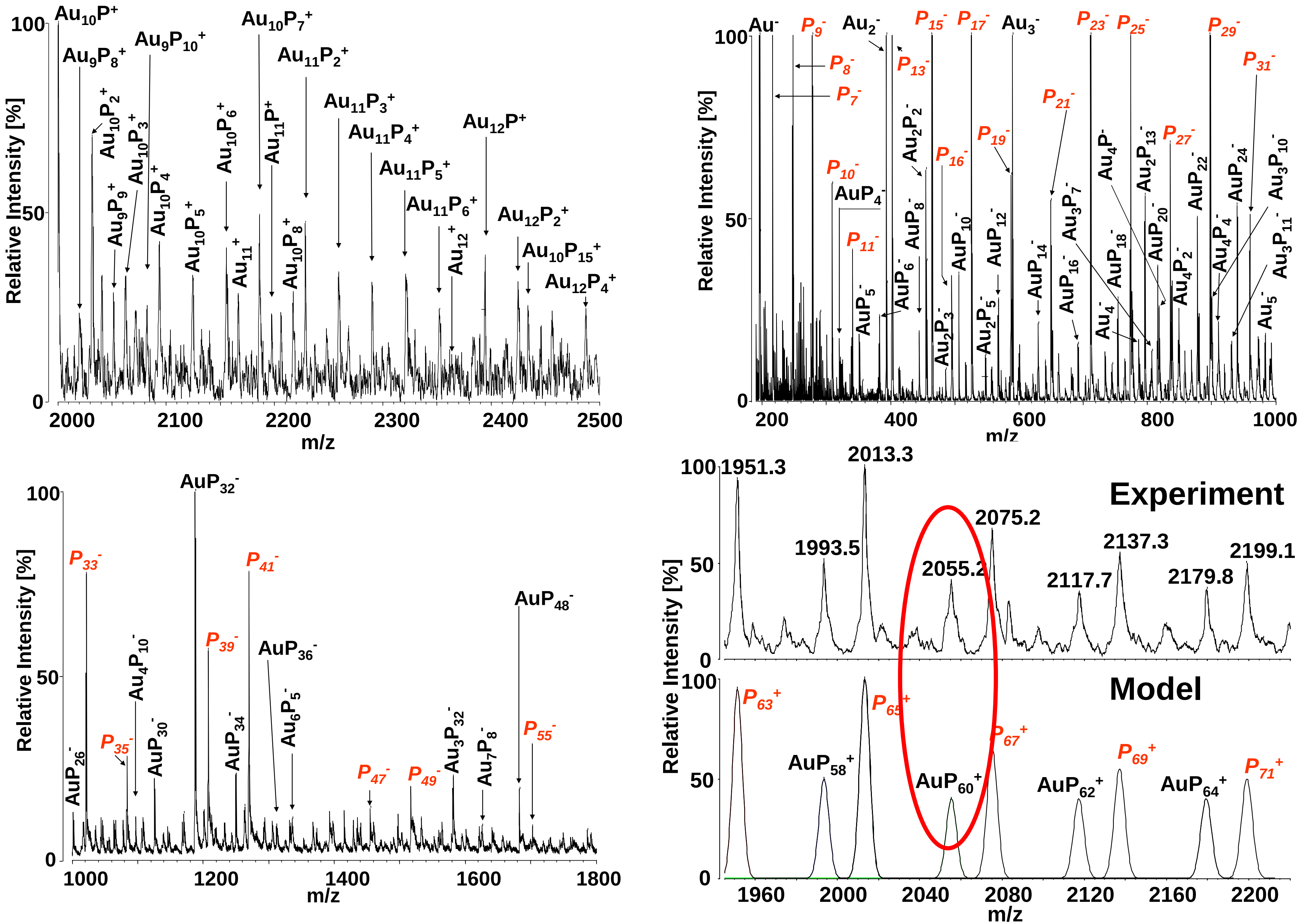

N.R. Panyala, et al. *Rapid Commun. Mass Spectrom.* submitted .

172 Au_mP_n clusters

Table. Overview of clusters detected in plasma plume via laser desorption ionisation of red phosphorus +nanogold mixture

	Au_mP_n clusters observed (excess of gold)
Positive ion mode	
n=0	Au^+ Au_2^+ Au_3^+ Au_4^+ Au_5^+ Au_6^+ Au_7^+ Au_8^+ Au_9^+ Au_{10}^+ Au_{11}^+ Au_{12}^+
m=0	P_2^+ P_3^+ P_4^+ P_5^+ P_6^+ P_7^+ P_{14}^+ P_{15}^+ P_{16}^+ P_{17}^+
m=1	AuP^+ AuP_2^+ AuP_4^+ AuP_6^+ AuP_8^+ AuP_{14}^+ AuP_{50}^+
m=2	Au_2P^+ $Au_2P_2^+$ $Au_2P_3^+$ $Au_2P_4^+$ $Au_2P_5^+$ $Au_2P_6^+$ $Au_2P_7^+$ $Au_2P_{14}^+$ $Au_2P_{15}^+$ $Au_2P_{16}^+$
m=3	Au_3P^+ $Au_3P_2^+$ $Au_3P_3^+$ $Au_3P_4^+$ $Au_3P_5^+$ $Au_3P_6^+$ $Au_3P_8^+$ $Au_3P_9^+$ $Au_3P_{14}^+$
m=4	Au_4P^+ $Au_4P_2^+$ $Au_4P_3^+$ $Au_4P_4^+$ $Au_4P_5^+$ $Au_4P_6^+$ $Au_4P_7^+$ $Au_4P_8^+$ $Au_4P_9^+$ $Au_4P_{14}^+$ $Au_4P_{15}^+$ $Au_4P_{16}^+$
m=5	Au_5P^+ $Au_5P_2^+$ $Au_5P_3^+$ $Au_5P_4^+$ $Au_5P_5^+$ $Au_5P_6^+$ $Au_5P_{14}^{+*}$ $Au_5P_{16}^{+*}$
m=6	Au_6P^+ $Au_6P_2^+$ $Au_6P_3^+$ $Au_6P_4^+$ $Au_6P_5^+$ $Au_6P_6^+$
m=7	Au_7P^+ $Au_7P_2^+$ $Au_7P_3^+$ $Au_7P_4^+$ $Au_7P_5^+$ $Au_7P_6^+$ $Au_7P_7^+$
m=8	Au_8P^+ $Au_8P_2^+$ $Au_8P_3^+$ $Au_8P_4^+$ $Au_8P_5^+$ $Au_8P_6^+$ $Au_8P_8^+$
m=9	Au_9P^+ $Au_9P_2^+$ $Au_9P_3^+$ $Au_9P_4^+$ $Au_9P_5^+$ $Au_9P_6^+$ $Au_9P_7^+$ $Au_9P_8^+$ $Au_9P_9^+$ $Au_9P_{10}^+$
m=10	$Au_{10}P^+$ $Au_{10}P_2^+$ $Au_{10}P_3^+$ $Au_{10}P_4^+$ $Au_{10}P_5^+$ $Au_{10}P_6^+$ $Au_{10}P_7^+$ $Au_{10}P_8^+$ $Au_{10}P_{15}^+$
m=11	$Au_{11}P^+$ $Au_{11}P_2^+$ $Au_{11}P_3^+$ $Au_{11}P_4^+$ $Au_{11}P_5^+$ $Au_{11}P_6^+$
m=12	$Au_{12}P^+$ $Au_{12}P_2^+$ $Au_{12}P_4^+$
	Au_mP_n clusters observed (excess of phosphorus)
Positive ion mode	
n=0	Au^+ Au_2^+ Au_3^+ Au_4^+
m=0	P_3^+ P_4^+ P_5^+ P_6^+ P_7^+ P_9^+ P_{11}^+ P_{13}^+ P_{15}^+ P_{16}^+ P_{17}^+ P_{18}^+ P_{19}^+ P_{20}^+ P_{21}^+ P_{22}^+ P_{23}^+ P_{24}^+ P_{25}^+ P_{26}^+ P_{27}^+ P_{28}^+ P_{29}^+ P_{31}^+ P_{32}^+ P_{33}^+ P_{35}^+ P_{37}^+ P_{39}^+ P_{41}^+ P_{43}^+ P_{45}^+ P_{47}^+ P_{49}^+ P_{51}^+ P_{53}^+ P_{55}^+ P_{57}^+ P_{59}^+ P_{61}^+ P_{63}^+ P_{65}^+ P_{67}^+ P_{69}^+ P_{71}^+ P_{73}^+ P_{75}^+ P_{77}^+ P_{79}^+ P_{81}^+ P_{83}^+ P_{85}^+ P_{87}^+ P_{89}^+ P_{91}^+ P_{93}^+ P_{95}^+
m=1	AuP_2^+ AuP_4^+ AuP_6^+ AuP_8^+ AuP_{10}^+ AuP_{12}^+ AuP_{14}^+ AuP_{16}^+ AuP_{18}^+ AuP_{20}^+ AuP_{22}^+ AuP_{24}^+ AuP_{26}^+ AuP_{28}^+ AuP_{30}^+ AuP_{32}^+ AuP_{34}^+ AuP_{36}^+ AuP_{38}^+ AuP_{40}^+ AuP_{42}^+ AuP_{44}^+ AuP_{46}^+ AuP_{48}^+ AuP_{50}^+ AuP_{52}^+ AuP_{54}^+ AuP_{56}^+ AuP_{58}^+ AuP_{60}^+ AuP_{62}^+ AuP_{64}^+ AuP_{66}^+ AuP_{68}^+ AuP_{70}^+ AuP_{72}^+ AuP_{74}^+ AuP_{76}^+ AuP_{78}^+ AuP_{80}^+ AuP_{82}^+ AuP_{84}^+ AuP_{86}^+ AuP_{88}^+
m=2	$Au_2P_{21}^+$ $Au_2P_{23}^+$ $Au_2P_{25}^+$ $Au_2P_{27}^+$ $Au_2P_{29}^+$ $Au_2P_{31}^+$ $Au_2P_{33}^+$ $Au_2P_{35}^+$ $Au_2P_{37}^+$ $Au_2P_{39}^+$ $Au_2P_{41}^+$ $Au_2P_{43}^+$ $Au_2P_{45}^+$ $Au_2P_{47}^+$ $Au_2P_{49}^+$ $Au_2P_{51}^+$
m=3	$Au_3P_2^+$ $Au_3P_4^+$ $Au_3P_6^+$ $Au_3P_8^+$
m=4	$Au_4P_4^+$ $Au_4P_6^+$
Negative ion mode	
n=0	Au^- Au_2^- Au_3^- Au_4^- Au_5^-
m=0	P_2^{-*} P_3^{-*} P_5^{-*} P_6^{-*} P_7^- P_8^- P_9^- P_{10}^- P_{11}^- P_{13}^- P_{15}^- P_{17}^- P_{18}^- P_{19}^- P_{21}^- P_{23}^- P_{25}^- P_{27}^- P_{29}^- P_{31}^- P_{33}^- P_{35}^- P_{39}^- P_{41}^- P_{47}^- P_{49}^- P_{55}^-
m=1	AuP_4^- AuP_5^- AuP_6^- AuP_8^- AuP_{10}^- AuP_{12}^- AuP_{14}^- AuP_{16}^- AuP_{18}^- AuP_{20}^- AuP_{22}^- AuP_{24}^- AuP_{26}^- AuP_{30}^- AuP_{32}^- AuP_{34}^- AuP_{36}^- AuP_{48}^-
m=2	$Au_2P_2^-$ $Au_2P_3^-$ $Au_2P_4^{-*}$ $Au_2P_5^-$ $Au_2P_8^{-*}$ $Au_2P_{11}^{-*}$ $Au_2P_{13}^-$ $Au_2P_{15}^{-*}$ $Au_2P_{17}^{-*}$

N.R. Panyala, et al. *Rapid Commun. Mass Spectrom.* submitted .

Summary

1. Rich family of several series of Au_mP_n clusters was detected in positive and negative ion modes via laser ablation synthesis.

179

N.R. Panyala, et al. *Rapid Commun. Mass Spectrom.* submitted .

Summary

1. Rich family of several series of Au_mP_n clusters was detected in positive and negative ion modes via laser ablation synthesis.

2. The formation of fullerene like phosphorus containing Au_mP_n (m=1, n=14, 16, 20, 24, 28, 30, 32, 40, 44 and 60) clusters was suggested.

180

N.R. Panyala, et al. *Rapid Commun. Mass Spectrom.* submitted .

Summary

1. Rich family of several series of Au_mP_n clusters was detected in positive and negative ion modes via laser ablation synthesis.

2. The formation of fullerene like phosphorus containing Au_mP_n (*m*=1, *n*=14, 16, 20, 24, 28, 30, 32, 40, 44 and 60) clusters was suggested.

3. Experimental evidence of AuP_{60} cluster formation given for the first time. –possible fullerene?

181

N.R. Panyala, et al. *Rapid Commun. Mass Spectrom.* submitted .

Summary

1. Rich family of several series of Au_mP_n clusters was detected in positive and negative ion modes via laser ablation synthesis.

2. The formation of fullerene like phosphorus containing Au_mP_n (m=1, n=14, 16, 20, 24, 28, 30, 32, 40, 44 and 60) clusters was suggested.

3. Experimental evidence of AuP_{60} cluster formation was proved for the first time.

4. Au_mP_n (m=1, n=10, 14, and 40) clusters formation containing "magic" numbers of phosphorus atoms (n=10, 14, and 40) was detected.

182

N.R. Panyala, et al. *Rapid Commun. Mass Spectrom.* submitted .

Summary

1. Rich family of several series of Au_mP_n clusters was detected in positive and negative ion modes via laser ablation synthesis.

2. The formation of fullerene like phosphorus containing Au_mP_n (m=1, n=14, 16, 20, 24, 28, 30, 32, 40, 44 and 60) clusters was suggested.

3. Experimental evidence of AuP_{60} cluster formation was proved for the first time.

4. Au_mP_n (m=1, n=10, 14, and 40) clusters formation containing "magic" number of phosphorus atoms (n=10, 14, and 40) was detected.

5. Experimental proof of gold-covered phosphorus P_nAu_{12} (n=1, 2, and 4) clusters formation is given.

183

N.R. Panyala, et al. *Rapid Commun. Mass Spectrom.* submitted .

Summary

1. Rich family of several series of Au_mP_n clusters was detected in positive and negative ion modes via laser ablation synthesis.

2. The formation of fullerene like phosphorus containing Au_mP_n (m=1, n=14, 16, 20, 24, 28, 30, 32, 40, 44 and 60) clusters was suggested.

3. Experimental evidence of AuP_{60} cluster formation was proved for the first time.

4. Au_mP_n (m=1, n=10, 14, and 40) clusters formation containing "magic" number of phosphorus atoms (n=10, 14, and 40) was detected.

5. Experimental proof of gold-covered phosphorus P_nAu_{12} (n=1, 2, and 4) clusters formation is given.

6. Phosphorus-rich clusters e.g. AuP_{88}^{+}, AuP_{48}^{-} clusters were detected.

The knowledge about the generation of Au-P clusters might be useful for the inspiration to fabricate new Au-P materials with specific properties.

The elucidation of the structures will require additional experimental and computing work.

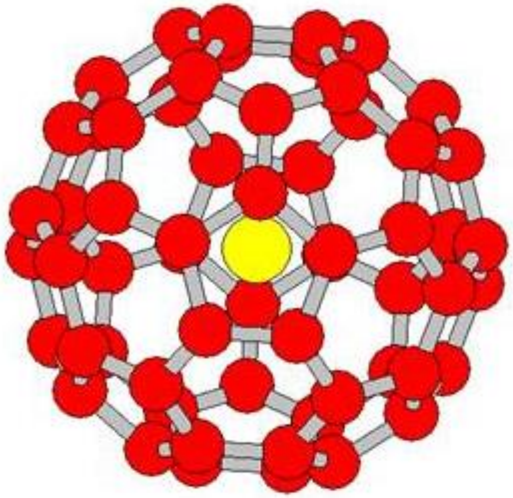

Endohedral Au@P_{60}??

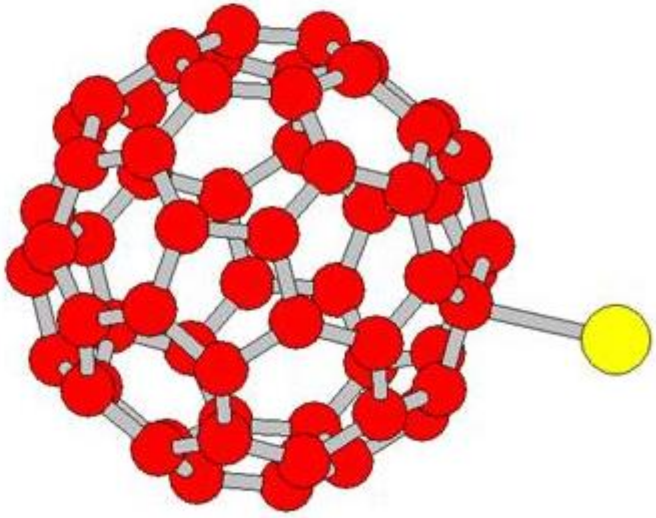

Or Au is bound to P_{60} ??

Cluster-cluster structures ?

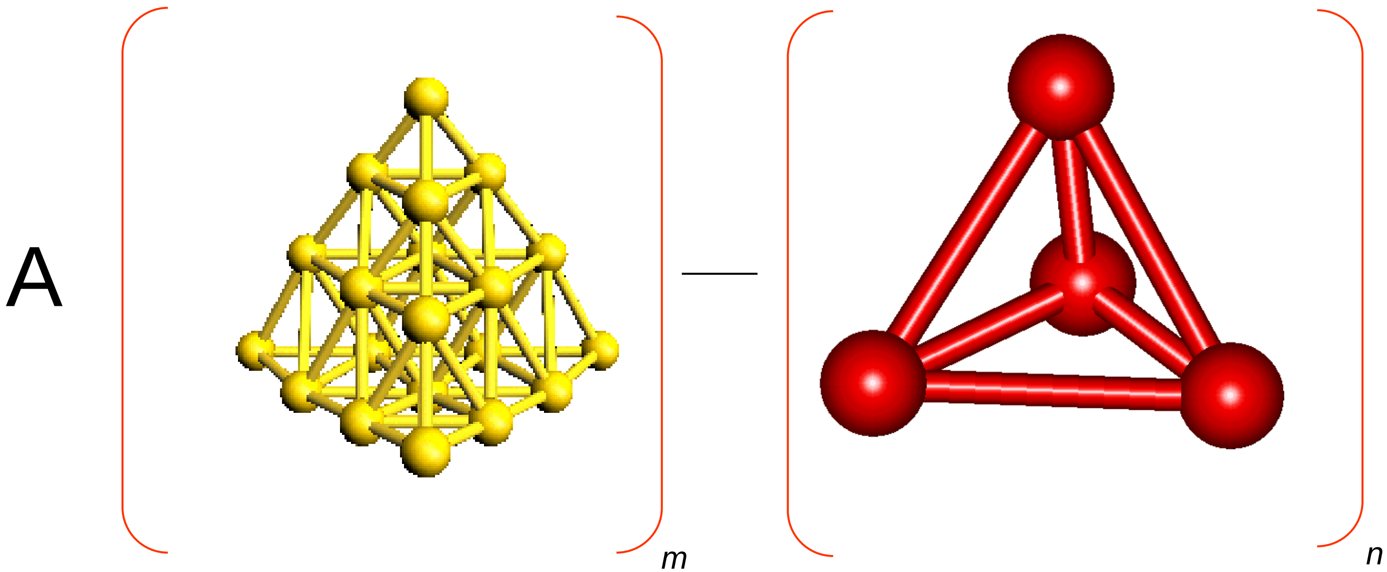

C O N C L U S I O N S

Instrumentation of MALDI, LDI (matrix free) TOF MS can be used for characterization of INORGANIC MATERIALS including NANO MATERIALS or for analysis of surfaces….

In spite of the fact that LDI is partially destructive, some information about the original structure of the materials is obtained

"Puzzle items" of structural fragments can be useful to elucidate the structure of inorganic materials, e.g. of chalcogenide glasses

Combination of LDI TOF MS with non-destructive methods like Raman, NMR etc is needed and highly reccomended

LDI TOF MS based **LASER ABLATION SYNTHESIS** is promising technique for generation of new un-usual clusters and might initiate development of new materials with unusual properties

C O N C L U S I O N S

Instrumentation of MALDI, LDI (matrix free) TOF MS can be used for characterization of INORGANIC MATERIALS including NANO MATERIALS
Or for analysis of surfaces….

In spite of the fact that LDI is partially destructive, some information about the original structure of the materials is obtained

“Puzzle items” of structural fragments can be useful to elucidate the structure of inorganic materials, e.g. of chalcogenide glasses

Combination of LDI TOF MS with non-destructive methods like Raman, NMR etc is needed and highly reccomended

LDI TOF MS based **LASER ABLATION SYNTHESIS** is promising technique for generation of new un-usual clusters and might initiate development of new materials with unusual properties

C O N C L U S I O N S

Instrumentation of MALDI, LDI (matrix free) TOF MS can be used for characterization of INORGANIC MATERIALS including NANO MATERIALS
Or for analysis of surfaces….

In spite of the fact that LDI is partially destructive, some information about the original structure of the materials is obtained

"Puzzle items" of structural fragments can be useful to elucidate the structure of inorganic materials, e.g. of chalcogenide glasses

Combination of LDI TOF MS with non-destructive methods like Raman, NMR etc is needed and highly reccomended

LDI TOF MS based **LASER ABLATION SYNTHESIS** is promising technique for generation of new un-usual clusters and might initiate development of new materials with unusual properties

C O N C L U S I O N S

Instrumentation of MALDI, LDI (matrix free) TOF MS can be used for characterization of INORGANIC MATERIALS including NANO MATERIALS
Or for analysis of surfaces….

In spite of the fact that LDI is partially destructive, some information about the original structure of the materials is obtained

"Puzzle items" of structural fragments can be useful to elucidate the structure of inorganic materials, e.g. of chalcogenide glasses

Combination of LDI TOF MS with non-destructive methods like Raman, NMR etc is needed and highly reccomended

LDI TOF MS based **LASER ABLATION SYNTHESIS** is promising technique for generation of new un-usual clusters and might initiate development of new materials with unusual properties

C O N C L U S I O N S

Instrumentation of MALDI, LDI (matrix free) TOF MS can be used for characterization of INORGANIC MATERIALS including NANO MATERIALS Or for analysis of surfaces….

In spite of the fact that LDI is partially destructive, some information about the original structure of the materials is obtained

“Puzzle items” of structural fragments can be useful to elucidate the structure of inorganic materials, e.g. of chalcogenide glasses

Combination of LDI TOF MS with non-destructive methods like Raman, NMR etc is needed and highly reccomended

LDI TOF MS based **LASER ABLATION SYNTHESIS** is promising technique for generation of new un-usual clusters and might initiate development of new materials with unusual properties

CEPLANT, R&D center for low-cost plasma and nanotechnology surface modifications (CZ.1.05/2.1.00/03.0086) provided by the European Regional Development Fund

Grant Agency of Czech Republic, No. 13-05082S

GAMU, Grant Agency of Masaryk University (MUNI/M/0041/2013).